THE UNIVERSITY OF WAIKATO
Te Whare Wānanga o Waikato
Research Commons

http://researchcommons.waikato.ac.nz/

Research Commons at the University of Waikato

Copyright Statement:

The digital copy of this thesis is protected by the Copyright Act 1994 (New Zealand).

The thesis may be consulted by you, provided you comply with the provisions of the Act and the following conditions of use:

- Any use you make of these documents or images must be for research or private study purposes only, and you may not make them available to any other person.
- Authors control the copyright of their thesis. You will recognise the author's right to be identified as the author of the thesis, and due acknowledgement will be made to the author where appropriate.
- You will obtain the author's permission before publishing any material from the thesis.

Fluxes of Carbon Dioxide and Water Vapour at a Waikato Peat Bog

A thesis
submitted in partial fulfilment
of the requirements for the degree of

Doctor of Philosophy

at the University of Waikato

by

Jeff Smith

The University of Waikato
January 2003

To the memory of Dr. Dave Murray
who sadly passed away 14 January 2003

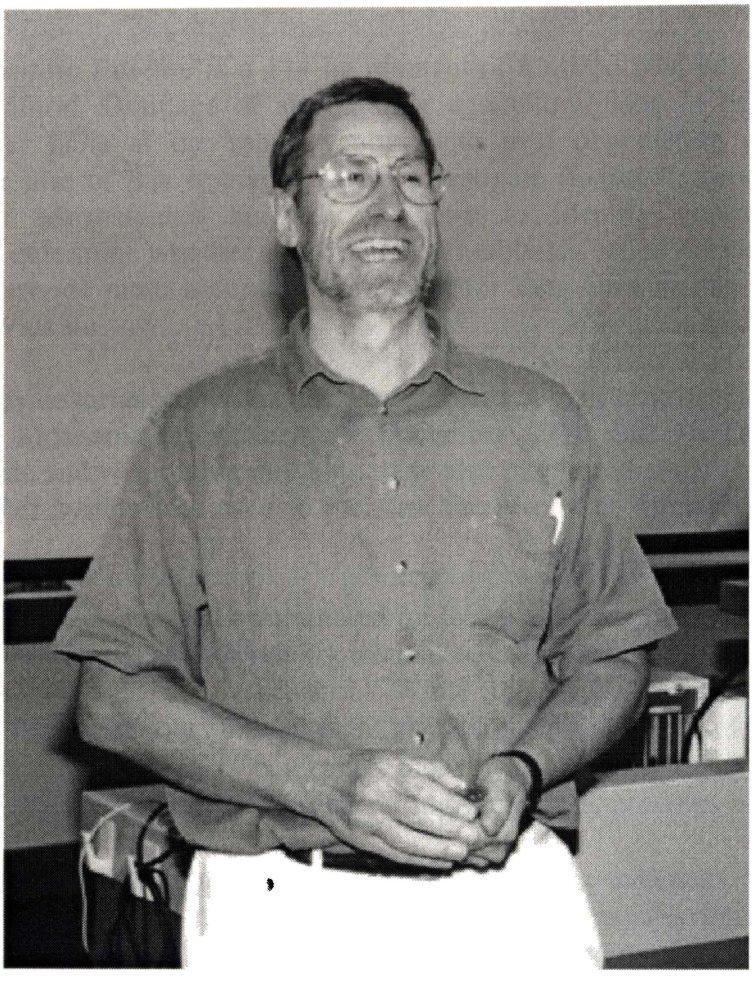

DAVE MURRAY

1942 - 2003

Abstract

New Zealand wetlands are threatened entities and the remaining 15% of pre-European freshwater wetlands are important refuges for plant and animal species, while also providing historical information on past environmental changes. Hydrological regimes ultimately determine wetland ecosystem structure and function, with peat accumulation believed to be promoted by a high water table that minimises aerobic decomposition of peat. The carbon budget is relevant to the successional development of wetlands, as feedback relationships occur between vegetation, soils, hydrology and bog formation. Research on carbon transfer provides knowledge of bog development, along with information for managing wetland resources.

Moanatuatua Scientific Reserve is a 114 ha remnant of a raised peat bog located 18 km southeast of Hamilton. Drainage of surrounding agricultural land is believed to have lowered the water table at the remnant bog, with peat degradation occurring as a consequence. The aim of this research was to investigate fluxes of carbon dioxide and water vapour at Moanatuatua Scientific Reserve to identify controls of carbon sequestration and determine whether a lowered water table has led to net carbon loss. This knowledge will provide more accurate information for long-term management of raised peat bogs in the Waikato.

A closed-path eddy covariance system was used to measure half-hourly fluxes of CO_2 and water vapour at Moanatuatua between 15 December 1998 and 15 December 2000. Meteorological data and water table elevation were also monitored at half-hourly intervals. A portable chamber system was used to measure fluxes of CO_2 from the peat substrate during field visits.

The present precipitation regime is dominated by low magnitude, high frequency events and this ensures that moisture is generally available in the plant canopy so that 64% of precipitation was removed as evaporation. While the dense plant canopy restricts evaporation from the moist peat surface, plant physiological regulation of transpiration is relatively less important and λE is controlled more by availability of radiation than by stomatal controls observed over short periods during summer by previous researchers.

At the diurnal scale, carbon uptake is greatest during summer mornings. The bog was a sink of carbon for almost all of 1999 and 2000, apart from 2–3 months during winter when the wetland was a source of CO_2. Annual sequestration of carbon was 1.85 and 2.10 tC ha^{-1} for 1999 and 2000 respectively: greater than observations at other wetlands around the world. Ecosystem respiration is driven by temperature and GEP was modelled from inputs of PPFD. Reduced magnitude of solar radiation under increasingly cloudy conditions caused by climate change scenarios will have negligible effect on carbon sequestration due to improved radiation use efficiency under these conditions. Compared with annual sequestration for 1999, the magnitude of annual NEP was not reduced in 2000 despite a deeper water table during the latter year. Photosynthetic production may be stimulated by a deeper water table, which would offset increased respiration losses under these conditions. This is encouraging for the sustainability of the wetland habitat, however further research is required to test the hypothesis that sequestered carbon is being stored as peat and not as aboveground biomass.

Acknowledgements

Thanks and appreciation are extended to:

My chief supervisor, mentor and colleague Dr. Dave Campbell. Dave's knowledge, skills and leadership ability are superlative: equalled only by his own energy and propensity to ignore limits and drive through barriers. I also thank Dave for being incredibly human and a friend during some difficult times.

Dr. Louis Schipper (Landcare Research) who was my external supervisor and a brilliant role model. An exceptionally confident, passionate and talented scientist with a profound ability to ask the most pertinent and challenging questions (in a totally non-threatening manner). Dr. Earl Bardsley is also thanked for advice and supervision.

Dr. John Hunt from Landcare Research who liberally gave encouragement, technical advice and knowledge from his experience with eddy covariance equipment and techniques. I enjoyed the synergy and sharing of knowledge. Thanks to Dr. Joost Nieveen (Landcare Research) for friendship and helpful comments on the thesis. Dr. David Whitehead (Landcare Research) is thanked for valuable advice and assistance regarding modelling of photosynthesis and Dr. Frank Kelliher (Landcare Research) for papers, enthusiasm and advice.

Prof. Andy Black from the University of British Columbia for sharing his exceptional experience with eddy covariance research. Prof. John Moncrieff from the University of Edinburgh is thanked for sending reprints and advice about building eddy covariance systems.

Manaaki Whenua Landcare Research who provided funding for the research. Personal funding was also provided by a University of Waikato Doctoral Scholarship and the Broad Memorial Fund administered by the Department of Earth Sciences.

Ian Blair for technical assistance, lugging heavy equipment to the field site and for friendship and some fun surf sessions. Just for a laugh(?!), Phil Hodge also carried some heavy gear to the site. Steve Bergin was a legend for overcoming bureaucratic hurdles, ordering equipment and providing humorous conversation. Liz Brodie provided cheerful IT support. Duncan Miers from the Department of Biological Science generously loaned us the LI-6200 for making respiration measurements.

Fellow students Dr. Ed Brown, Haydon Jones, Jen Purdie, Phil Hodge, Cameron King for esprit de corps and encouragement. The Wallace family kindly allowed access across their farm and the Department of Conservation permitted entry to Moanatuatua Scientific Reserve.

Thanks to Ian and Sandy Smith for financial support and parental encouragement over many years.

Special thanks to my amazing wife Shar, who has loved, encouraged, supported and stuck by me through some incredibly challenging times. Thanks to Skye, Meadow & Zion for being such loving, well-balanced and generally happy children despite doing without for all these years. Thanks to Jesus Christ for being my rock, source of strength and eternal life.

Table of Contents

ABSTRACT iii

ACKNOWLEDGEMENTS iv

TABLE OF CONTENTS v

LIST OF FIGURES viii

LIST OF TABLES x

DEFINITION OF SYMBOLS AND ABBREVIATIONS xi

1 INTRODUCTION 1

1.1 BACKGROUND 1
1.2 WAIKATO PEAT BOGS 2
1.3 RESEARCH AIMS AND OBJECTIVES 3
1.4 THESIS OUTLINE 3

2 THEORETICAL BACKGROUND 5

2.1 INTRODUCTION 5
2.2 BOUNDARY LAYER STRUCTURES 5
2.3 THE TURBULENT SURFACE LAYER 7
2.3.1 Convection *7*
Free convection 7
Forced convection 7
Mixed convection 10
2.3.2 Stationarity and horizontal homogeneity *11*
Stationarity 11
Horizontal homogeneity 11
2.3.3 Fluxes of energy *11*
2.3.4 CO_2 flux *12*
2.3.5 Storage profiles *13*
2.4 MODELS OF EVAPORATION 13
2.4.1 Penman–Monteith model *14*
2.4.2 Limitations of the Penman–Monteith model *15*
2.4.3 Equilibrium model *15*
2.5 MODELS OF CARBON EXCHANGE 16
2.5.1 Photosynthesis and CO_2 exchange *16*
2.5.2 Respiration *17*
2.5.3 Net ecosystem production *18*
2.5.4 Variability of CO_2 exchange *19*

2.5.5 Radiation and water use efficiencies *20*
2.6 WETLAND CO_2 AND WATER VAPOUR EXCHANGE 21
2.6.1 Wetland classification *21*
2.6.2 Peatland evaporation *22*
2.6.3 Carbon sequestration in the wetland environment *23*
2.6.4 Global warming considerations *25*
2.6.5 Dissolved Carbon *26*
2.7 SUMMARY 27
3 FIELD SITE AND METHODOLOGY 28
3.1 MOANATUATUA PEAT BOG 28
3.1.1 Peat Characteristics *28*
3.1.2 Vegetation *31*
3.1.3 Climate *34*
3.1.4 Soil moisture content and water table *36*
3.2 THE EDDY COVARIANCE TECHNIQUE 37
3.3 THE UW EDDY COVARIANCE SYSTEM 38
3.3.1 Hardware *38*
3.3.2 Data acquisition *40*
3.3.3 Post-processing of data *40*
3.4 ERRORS AND CORRECTIONS 42
3.4.1 Change in CO_2 storage *42*
3.4.2 Low friction velocity *46*
3.4.3 Spectral loss *47*
3.4.4 Energy balance closure *49*
3.4.5 Footprint analysis *51*
Interference from mast and hut 51
Flux source area 52
3.5 ADDITIONAL MEASUREMENTS 54
3.5.1 Chamber measurements of respiration *54*
3.5.2 Other measurements of peat properties *56*
3.5.3 Radiation measurements *56*
3.5.4 Other meteorological instrumentation *56*
3.6 SUMMARY 57
4 ENERGY BALANCE AND EVAPORATION 59
4.1 INTRODUCTION 59
4.2 ENERGY PARTITIONING 59
4.2.1 Diurnal energy balance *59*
Summer energy balance partitioning 59
Winter energy balance partitioning 62

4.2.2 Modelling Latent Heat Flux *65*
Models for gap filling 66
Models for annual water balance construction 69
4.3 ANNUAL WATER BALANCE 78
4.3.1 Annual evaporation *79*
4.3.2 Water balance partitioning *79*
4.4 SUMMARY 82

5 THE CARBON BUDGET AT MOANATUATUA 83

5.1 INTRODUCTION 83
5.2 DIURNAL VARIATION 83
5.3 GAP FILLING METHODS TO REPLACE MISSING DATA 87
5.3.1 Respiration model *88*
5.3.2 Modelling missing daytime data *92*
5.3.3 Model validation *94*
5.4 SEASONAL VARIATION 96
5.5 ANNUAL AND INTERANNUAL CARBON EXCHANGE 99
5.5.1 Model extrapolation beyond the two-year measurement period *101*
5.6 SUMMARY 110

6 CONTROLS OF CARBON EXCHANGE 111

6.1 INTRODUCTION 111
6.2 RADIATION USE EFFICIENCY 112
6.2.1 Marginal quantum yield *112*
6.2.2 Effect of clouds on CO_2 exchange *114*
6.3 HYDROLOGICAL INTERACTIONS WITH PEAT PRODUCTION 123
6.3.1 Water Use Efficiency *123*
6.3.2 Sensitivity to water table depth *129*
6.4 IPCC PREDICTIONS OF TEMPERATURE INCREASE 133
6.5 SUMMARY 135

7 CONCLUSIONS 137

7.1 SUMMARY 137
7.2 LIMITATIONS AND ASSUMPTIONS 139
7.3 THE GOOD OIL 140
7.4 RECOMMENDATIONS FOR FUTURE RESEARCH 142

REFERENCES 143

APPENDIX 157

List of figures

FIGURE 2.1 VERTICAL SCALES OF BOUNDARY LAYER STRUCTURES WITHIN THE ATMOSPHERE 6
FIGURE 2.2 DIURNAL DEVELOPMENT OF BOUNDARY LAYER STRUCTURES 6
FIGURE 2.3 PROFILES OF WINDSPEED 8
FIGURE 2.4 VERTICAL WINDSPEED DURING (A) UNSTABLE AND (B) STABLE ATMOSPHERIC CONDITIONS. 10
FIGURE 2.5 ECOSYSTEM CO_2 BALANCE DURING (A) DAY AND (B) NIGHT 18
FIGURE 2.6 PEAT ACCUMULATION (EXPRESSED AS RATE OF GROWTH) VERSUS WATER TABLE DEPTH (Z_0) 25
FIGURE 3.1 LOCATION OF MOANATUATUA PEAT FORMATION 29
FIGURE 3.2 MAP OF MOANATUATUA SCIENTIFIC RESERVE 29
FIGURE 3.3 AERIAL PHOTOGRAPH OF MOANATUATUA PEAT BOG 30
FIGURE 3.4 *SPORODANTHUS FERRUGINEUS* IS ONE OF TWO RESTIAD SPECIES AT MOANATUATUA 32
FIGURE 3.5 THE SPRAWLING WIRE RUSH *EMPODISMA MINUS* 32
FIGURE 3.6 INTERANNUAL COURSE OF DAILY: R_N, PRECIPITATION, D, T AND T_S 35
FIGURE 3.7 DAILY MEANS OF WATER TABLE DEPTH, PRECIPITATION AND SOIL MOISTURE CONTENT (θ_v). 37
FIGURE 3.8 THE EDDY COVARIANCE (EC) SITE SHOWING MAST, SAMPLE TUBE AND HUT. 39
FIGURE 3.9 EDDY COVARIANCE MAST INSTRUMENTATION AT 3.5 M HEIGHT 39
FIGURE 3.10 MEAN WINDSPEED AND NEE WITH CORRECTIONS FOR CHANGE IN STORAGE 44
FIGURE 3.11 NOCTURNAL NEE(STORAGE CORRECTED) VS. U^* FOR 1 OCTOBER, 1999 – 1 APRIL, 2000. 47
FIGURE 3.12 POWER SPECTRAL CORRECTIONS FOR CO_2 48
FIGURE 3.13 ENERGY BALANCE CLOSURE WITH LINEAR REGRESSION 50
FIGURE 3.14 ENERGY BALANCE CLOSURE RATIO ($(\lambda E + H)/(R_N - G - J)$) VERSUS WIND DIRECTION 52
FIGURE 3.15 FLUX FOOTPRINT FOR TWO HALF HOURLY PERIODS WITH UNSTABLE AND STABLE CONDITIONS. 53
FIGURE 3.16 FREQUENCY HISTOGRAMS OF FLUX FOOTPRINT UNDER UNSTABLE AND STABLE CONDITIONS 54
FIGURE 3.17 PVC COLLAR FOR CHAMBER MEASUREMENTS OF RESPIRATION FROM THE PEAT SURFACE. 55
FIGURE 4.1 ENERGY BALANCE COMPONENTS, T, D AND β FOR WET AND DRY CANOPY DAYS 60
FIGURE 4.2 LEAF WETNESS INDEX FOR 19 NOVEMBER 1999 60
FIGURE 4.3 DIURNAL COURSE OF ENERGY BALANCE, T, D AND β FOR SUMMER AND WINTER DAY 63
FIGURE 4.4 MONTHLY ENSEMBLE AVERAGES OF ½-HOURLY ENERGY BALANCE COMPONENTS, T, D AND β 64
FIGURE 4.5 MEASURED AND ESTIMATED EVAPORATION 19–25 NOVEMBER 1999 68
FIGURE 4.6 ANTECEDENT PRECIPITATION INDEX (API) AND LEAF WETNESS (LWS) DATA, 18–28 NOV. 1999 70
FIGURE 4.7 MEASURED AND ESTIMATED E, 19 –25 NOVEMBER 1999. API IDENTIFIES CANOPY WETNESS 71
FIGURE 4.8 MEASURED VERSUS MODELLED EVAPORATION: 15 DECEMBER 1998 – 15 DECEMBER 2000. 73
FIGURE 4.9 DIURNAL MEASURED AND MODELLED EVAPORATION FOR CLEAR SKY DAY WITH DRY CANOPY 75
FIGURE 4.10 ENSEMBLE MEAN DAYLIGHT R_A AND R_C DURING WINTER AND SUMMER 75
FIGURE 4.11 FREQUENCY DISTRIBUTION OF HALF-HOURLY BOWEN RATIO (β) 76
FIGURE 4.12 CUMULATIVE MEASURED AND MODELLED EVAPORATION: 10 JULY 1999 – 10 JULY 2000 78
FIGURE 4.13 INTERANNUAL COURSE OF R_N, D AND E, 15 DECEMBER 1998 – 15 DECEMBER 2000. 80

FIGURE 4.14 INTERANNUAL WATER BALANCE FOR MOANATUATUA PEAT BOG 81
FIGURE 5.1 DIURNAL VARIATION OF NEE, PPFD, T_{AIR}, T_S AND D: 1 DECEMBER 1999 – 6 DECEMBER 1999. ... 84
FIGURE 5.2 DIURNAL COURSE OF ENSEMBLE AVERAGE NEE FOR SUMMER AND WINTER 86
FIGURE 5.3 VALID HALF-HOURLY NEE (1998 – 2000) SHOWING GAPS IN DATASET. 88
FIGURE 5.4 ECOSYSTEM RESPIRATION (R_E) VS PEAT TEMPERATURE (T_S): 11 JULY 1999 – 11 JULY 2000. 89
FIGURE 5.5 RESPIRATION FROM PEAT (R_S) VS PEAT TEMPERATURE AT 8 CM DEPTH (T_S) 90
FIGURE 5.6 ECOSYSTEM RESPIRATION (R_E) VS DEPTH TO WATER TABLE: 11 JULY 1999 – 11 JULY 2000 91
FIGURE 5.7 GEP VS. PPFD FOR DAYTIME DATA COLLECTED BETWEEN 11 JULY 1999 AND 11 JULY 2000 93
FIGURE 5.8 MODELLED VS MEASURED R_E FOR 15 DECEMBER 1998 - 15 DECEMBER 2000 95
FIGURE 5.9 MODELLED VS MEASURED NEE FOR 15 DECEMBER 1998 - 15 DECEMBER 2000 95
FIGURE 5.10 SEASONAL VARIATION OF DAILY MEAN NEE: 15 DECEMBER 1998 – 15 DECEMBER 2000 97
FIGURE 5.11 MONTHLY VARIATION OF CO_2 FLUX : JANUARY 1999 – NOVEMBER 2000 98
FIGURE 5.12 CUMULATIVE NEE FOR 1999 AND 2000 100
FIGURE 5.13 45-DAY RUNNING MEANS OF PPFD AND PEAT TEMPERATURE AT 8 CM DEPTH (T_S). 101
FIGURE 5.14 $K\downarrow$ VERSUS PPFD BETWEEN 15 DECEMBER 1998 AND 15 DECEMBER 2000 102
FIGURE 5.15 CUMULATIVE PLOT OF HALF-HOURLY PPFD FOR TWO YEARS AT MOANATUATUA 103
FIGURE 5.16 PEAT TEMPERATURE (T_S) AT MOANATUATUA VS. T_S AT KOPOUATAI 103
FIGURE 5.17 CUMULATIVE NEE FROM 15 DECEMBER 1998 TO 15 DECEMBER 2000 104
FIGURE 5.18 MODELLED NEE AT MOANATUATUA WETLAND 15 DECEMBER 1996 – 15 DECEMBER 2000 106
FIGURE 5.19 30-DAY MOVING AVERAGES OF T_S AT KOPOUATAI AND PPFD AT MOANATUATUA 107
FIGURE 5.20 MODELLED ANNUAL CARBON BALANCE: 15 DECEMBER 1996 TO 15 DECEMBER 1998 108
FIGURE 6.1 DETERMINATION OF TRANSMISSIVITY COEFFICIENT: K_M AND $K\downarrow$ FOR CLEAR SKY DAYS 115
FIGURE 6.2 CLOUDINESS INDEX FOR A MOSTLY CLEAR SKY DAY AND A CLOUDY DAY 116
FIGURE 6.3 NEE VS. PPFD UNDER CLEAR SKY AND CLOUDY CONDITIONS 117
FIGURE 6.4 RUE UNDER CLOUDY AND CLEAR SKY CONDITIONS DURING SUMMER AND WINTER 119
FIGURE 6.5 BOX AND WHISKERS PLOTS: RUE DURING SUMMER AND WINTER 119
FIGURE 6.6 BOX AND WHISKERS PLOTS: AIR & PEAT TEMPERATURE, θ AND D FOR SUMMER AND WINTER 120
FIGURE 6.7 RADIATION USE EFFICIENCY AS A FUNCTION OF D UNDER CLEAR SKY CONDITIONS 122
FIGURE 6.8 DIURNAL VARIATION OF NEP, λE, WUE AND D ON A CLEAR SKY DAY WITH DRY CANOPY 124
FIGURE 6.9 RELATIONSHIP BETWEEN WUE AND D BETWEEN DECEMBER 1998 AND DECEMBER 2000. 125
FIGURE 6.10 LEAF WETNESS INDEX FOR 23 MARCH, 2000 126
FIGURE 6.11 RELATIONSHIP BETWEEN WUE AND D, FOR DRY-CANOPY AND WET-CANOPY 127
FIGURE 6.12 RELATIONSHIP BETWEEN WUE_{DRY} AND D FOR MARCH AND APRIL 2000. 127
FIGURE 6.13 RUNNING MEAN OF WUE PLOTTED WITH DEPTH TO WATER TABLE.. 128
FIGURE 6.14 GEP VS PPFD FOR: (A) SPRING DATA AND (B) AUTUMN 131
FIGURE 6.15 MODELLED GEP, R_E AND NEE WITH CLIMATE WARMING SCENARIOS 134

List of tables

TABLE 3.1 $F_{\Delta S}$ AS A COMPONENT OF CO_2 FLUXES 45
TABLE 4.1 MODELS USED TO ESTIMATE EVAPORATION AT MOANATUATUA 67
TABLE 4.2 ANNUAL WATER BALANCE COMPONENTS 81
TABLE 5.1 INPUT PARAMETERS USED IN EQUATION 5.2 FOR MODELLING GEP 94
TABLE 5.2 SUM OF MEASURED AND MODELLED CARBON FLUXES 96
TABLE 5.3 MODELLED AND MEASURED CARBON ACCUMULATION OVER TWO YEARS 105
TABLE 5.4 ESTIMATES OF ANNUAL CARBON ACCUMULATION 15 DECEMBER 1996 – 15 DECEMBER 2000 106
TABLE 5.5 COMPARISONS OF PEAT TEMPERATURE (°C) MEASURED AT KOPOUATAI: TUKEY'S METHOD. 108
TABLE 5.6 ANALYSIS OF VARIANCE TABLE FOR MEAN ANNUAL PPFD, 1997–2000. 108
TABLE 5.7 ANNUAL CARBON SEQUESTRATION COMPARED WITH OTHER ECOSYSTEMS 109
TABLE 6.1 MARGINAL QUANTUM YIELD (α_Q) FOR A RANGE OF ECOSYSTEM TYPES 113
TABLE 6.2 ANNUAL PRECIPITATION AND DEPTH TO WATER TABLE 129

Definition of symbols and abbreviations

Roman Alphabet		Units
A_d	advection of sensible or latent heat flux	W m^{-2}
A_{max}	max. rate of GEP at saturating irradiance	μmol m^{-2} s^{-1}
A_n	photosynthesis	μmol m^{-2} s^{-1}
API	antecedent precipitation index	
c	CO_2 concentration	μmol CO_2 mol^{-1} air
c_p	specific heat of air at constant pressure	kJ kg^{-1} °C
C_{ind}	cloudiness index = $K\downarrow/K_m$	
d	zero plane displacement height	m
D	saturation vapour pressure deficit	kPa
EC	eddy covariance	
E_0	Penman open water evaporation	mm
E_{eq}	equilibrium evaporation	mm
E_{PT}	equilibrium-based evaporation using α coefficient	mm
E_{PM}	Penman-Monteith modelled evaporation	mm
F_c	CO_2 flux prior to correction for $F_{\Delta S}$	μmol m^{-2} s^{-1}
F_{cEddy}	$F_{\Delta S}$–corrected CO_2 flux using EC–height CO_2 conc.s	μmol m^{-2} s^{-1}
F_{cProf}	$F_{\Delta S}$–corrected CO_2 flux using profile system	μmol m^{-2} s^{-1}
$F_{\Delta S}$	flux associated with change in CO_2 storage	
G	ground heat flux density	W m^{-2}
GEP	gross ecosystem production	μmol m^{-2} s^{-1}
h	average canopy vegetation height	m
H	sensible heat flux density	W m^{-2}
J	storage of heat energy within the canopy	W m^{-2}
k	von Karman's constant (0.4)	
$K\downarrow$	incoming short-wave radiation	W m^{-2}
K_m	$K\downarrow$ modelled from extra-terrestrial solar radiation	W m^{-2}
L	Obukhov length	
LAI	leaf area index	m^2 m^{-2}
LWS	leaf wetness sensor	
NEE	net ecosystem exchange	μmol m^{-2} s^{-1} (tC ha^{-1} yr^{-1})

NEP	net ecosystem production (= –NEE)	μmol m^{-2} s^{-1} (tC ha^{-1} yr^{-1})
P	precipitation	mm
PAR	photosynthetically active radiation	W m^{-2}
PPFD	photosynthetic photon flux density	μmol m^{-2} s^{-1}
P_s	energy used for photosynthesis	W m^{-2}
Q_w	lateral groundwater discharge	mm
r_a	bulk aerodynamic resistance	s m^{-1}
r_{aM}	aerodynamic resistance to momentum transfer	s m^{-1}
r_c	canopy resistance	s m^{-1}
R_{10}	respiration rate at 10 °C	μmol m^{-2} s-1
R_d	dark respiration of CO_2 from plants	μmol m^{-2} s^{-1}
R_e	ecosystem respiration	μmol m^{-2} s^{-1}
R_m	microbial (heterotrophic) respiration	μmol m^{-2} s^{-1}
R_n	net radiation flux density	W m^{-2}
R_r	(autotrophic) respiration from plant roots	μmol m^{-2} s^{-1}
R_s	respiration from peat	μmol m^{-2} s^{-1}
RUE	radiation use efficiency	μmol CO_2 μmol $PPFD^{-1}$
s	scalar concentration	
s	slope of saturation vapour pressure vs. temperature curve	kPa $°C^{-1}$
S_y	specific yield of peat	mm mm^{-1}
T_{air}	air temperature	°C
T_s	peat temperature measured at Moanatuatua EC site	°C
T_{sKop}	peat temperature measured at Kopouatai bog	°C
u	horizontal windspeed	m s^{-1}
u^*	friction velocity	m s^{-1}
V	molar volume of air	m^3 mol^{-1}
w	vertical windspeed	m s^{-1}
WUE	water use efficiency	mg CO_2 g H_2O^{-1}
x_{80}	distance where 80% flux measurements are sourced	m
x_{max}	distance to which flux measurements are maximised	m
z	windspeed and EC measurement height	m
Z_0	roughness length of the canopy	m

Greek Alphabet		Units
α	Priestley–Taylor coefficient	
α	level of statistical significance (rejection region)	
α_q	marginal quantum yield	μmol CO_2 μmol^{-1} photons
β	Bowen ratio	
ΔS_c	change in CO_2 storage within plant canopy	μmol m^{-2} s^{-1}
ΔS_w	change in storage of groundwater	mm
ΔW	change in water table elevation	mm
γ	psychrometric constant	kPa °C^{-1}
λ	latent heat of vaporisation of water	J kg^{-1} °C
λE	latent heat flux density	W m^{-2}
θ	convexity of GEP vs PPFD hyperbolic model	
θ_v	volumetric peat moisture content	m^3 m^{-3}
ρ	density of air	g m^{-3}
ρ_{can}	canopy material dry density	g m^{-3}
ρ_c	density of CO_2	g m^{-3}
ρ_v	water vapour density	g m^{-3}
σ	standard deviation	

1 Introduction

1.1 Background

New Zealand wetlands are threatened entities and the remaining 15% of pre-European freshwater wetlands are important refuges for plant and animal species (Taylor et al., 1997), while also providing historical information on past environmental changes (e.g. McGlone et al., 1997; Newnham et al., 1995). Surviving wetlands are fragmented and threatened by drainage, burning, mining and the activities of surrounding landuse practices (Taylor et al., 1997).

Wetlands are defined by their hydrology (Ingram, 1983) with water regimes ultimately determining wetland ecosystem structure and function (Mitsch and Gosselink, 1993). An understanding of hydrological processes is therefore a prerequisite to effective wetland restoration and management.

The carbon budget is also relevant to the successional development of wetlands, as feedback relationships occur between vegetation, soils, hydrology and bog formation. Research on carbon transfer in wetland systems provides knowledge of bog development, along with data and criteria useful for protecting, restoring and monitoring wetland resources. Northern Hemisphere wetlands are also significant in the global warming debate, containing about one third of the world's store of carbon in soil (Gorham, 1991).

Stored carbon in wetlands is vulnerable to climate change and these ecosystems may be major carbon sources and/or sinks which regulate atmospheric greenhouse gases (Griffis et al., 2000; Lloyd, 1998; Oechel et al., 1993; Turunen and Tolonen, 1996). A warmer and drier climate may increase carbon loss from wetlands to the atmosphere via enhanced respiration losses (Oechel et al., 1993) or decreased photosynthetic production in *Sphagnum* bogs (Rouse et al., 2002).

The water table is believed to be a particularly important control on wetland carbon budgets, with peat accumulation promoted by a high water table that minimises aerobic decomposition of peat (Clymo et al., 1998). This hypothesis is supported by peatland research where water table lowering has resulted in decreased carbon accumulation or wetlands switching from a sink to a source (e.g. Armentano and Menges, 1986; Oechel et al., 1993; Oechel et al., 1998; Roulet et al., 1998).

1.2 Waikato peat bogs

New Zealand raised peat bogs of the Waikato region differ from Northern Hemisphere peat bogs because their peat-forming vegetation is dominated by vascular plants belonging to the Restionaceae family. The most common restiad found at Waikato peat bogs is *Empodisma minus* (Hook.f.) Johnson & Cutler: a sprawling jointed wire rush that conserves water via a combination of physiological control of transpiration and minimisation of evaporation from the peat substrate by the mulching effect of the dense *E. minus* canopy (Campbell and Williamson, 1997).

The larger erect jointed rush *Sporodanthus ferrugineus* de Lange Heenan et B.D.Clarkson is a threatened species found only at Waikato raised bogs (de Lange et al., 1999) and the bog type in which it grows is a threatened ecosystem (Clarkson et al., 1999). Moanatuatua Scientific Reserve, located 18 km southeast of Hamilton city, is one of only two peat bogs where *S. ferrugineus* survives. Moanatuatua peat formation was once 7500 ha in size but has mostly been drained and converted to pasture while a 114 ha remnant bog is set aside as a Scientific Reserve and managed by the Department of Conservation (Clarkson et al., 1999). Moanatuatua Scientific Reserve has 1–2 m deep drains around the perimeter and lowering of the water table is believed to have caused peat degradation at the bog (Shearer, 1997).

1.3 Research aims and objectives

There is a paucity of knowledge about carbon exchange processes at peat bogs and this research will investigate these processes. The magnitude of carbon budgets from diurnal to interannual time scales will also be determined. The research will identify controls of carbon sequestration and investigate whether a lowered water table has led to net carbon loss. Controls of evaporation will be investigated from diurnal–annual time scales, allowing partitioning of annual water balance components.

This knowledge will provide more accurate information for long-term management of raised peat bogs in the Waikato.

The objectives of this research are to:

- investigate controls on evaporation from diurnal–annual timescales and test models currently used for water balance studies;
- investigate controls and regulation of net ecosystem production including identification of switches between sink and source from diurnal to annual time scales;
- develop simple models of CO_2 exchange for determination of annual carbon balances at Moanatuatua using standard meteorological data as inputs;
- determine whether the wetland is a net source or sink of CO_2 and predict the likely consequences of climate change.

1.4 Thesis outline

Chapter 2 summarises some of the literature on exchanges of heat, water vapour and carbon dioxide between the earth's surface and atmosphere. Literature describing the implications of these processes for wetlands is given special consideration. Chapter 3 describes the field site and research methods.

Chapter 4 describes and compares energy balance results from a two year measurement period with those previously obtained over shorter summer periods at Waikato raised bogs. Annual water balances over the two year period are also determined in Chapter 4. Variability of CO_2 exchange from diurnal to interannual time scales is investigated in Chapter 5, followed by identification of simple models for determination of annual carbon balances using standard meteorological data as inputs.

While Chapter 5 is a descriptive one, Chapter 6 attempts to explain the processes that control rates of carbon accumulation and examines the implications of climate change for carbon exchange at Moanatuatua. Conclusions and recommendations for future research are presented in Chapter 7, along with a list of assumptions and limitations of the research.

2 Theoretical Background

2.1 Introduction

The purpose of this chapter is to summarise contemporary knowledge of the exchanges of momentum, heat, water vapour and carbon dioxide between the atmosphere and the Earth's surface. In particular, carbon budgets in the context of wetlands are considered, including alternative pathways that carbon may depart from wetlands.

2.2 Boundary Layer Structures

At daily time scales, the influence of the Earth's surface on the atmosphere is restricted to the lower 1–2 km of the atmosphere (Oke, 1990). Known as the planetary boundary layer (PBL), this zone may also be referred to as the atmospheric boundary layer or simply the boundary layer (Figure 2.1). The height of the PBL is greatest during the day, when heating of the Earth's surface by the sun produces convection in the atmosphere (Figure 2.2). The convective boundary layer (CBL) exists during the daytime and has a capping inversion that defines the upper boundary (Kaimal and Finnigan, 1994)(Figure 2.2).

At night the ground cools and turbulent mixing is suppressed, forming an inversion layer that may be less than 100 m in height that defines the stable boundary layer (SBL, Figure 2.2). Confounding the rhythmic tempo of PBL height cycling with solar radiation, synoptic scale weather systems may introduce variable windspeed and cloud cover that disrupt the diurnal rhythm of PBL characteristics (Oke, 1990).

Convection and surface roughness concentrate turbulence in the lowest 50–100 m of the atmosphere, known as the turbulent surface layer (Oke, 1990) or simply the surface layer (Kaimal and Finnigan, 1994). At night this surface layer may shrink to a depth of a few metres. At the base of the boundary layer and extending up to three times the height of surface roughness elements, a roughness sublayer is where surface features directly influence turbulence (Kaimal and Finnigan, 1994).

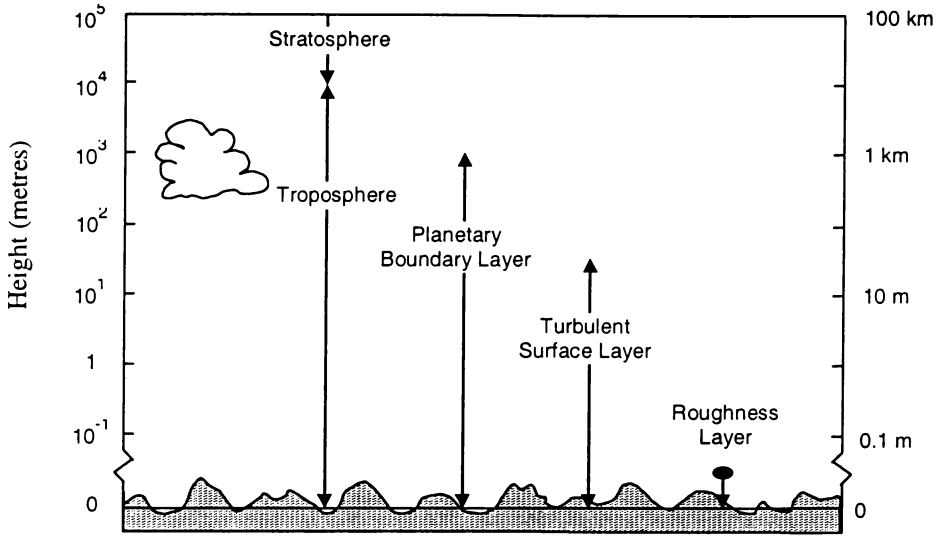

Figure 2.1 Vertical scales of boundary layer structures within the atmosphere (from Oke, 1990).

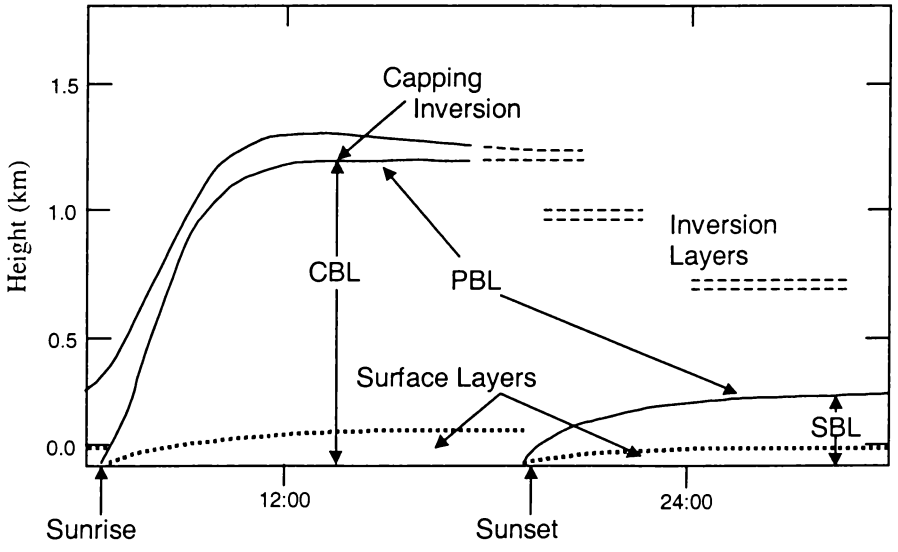

Figure 2.2 Diurnal development of boundary layer structures produced by heating and cooling of the Earth's surface (from Kaimal and Finnigan, 1994).

2.3 The Turbulent Surface Layer

2.3.1 Convection

Within the turbulent surface layer, convection is the vertical transfer of air with associated transport of energy and mass and may exist as free, forced or mixed convection. Each of these is described below.

Free convection

When the sun's rays heat the Earth's surface, the air immediately above the ground is warmed (Kaimal and Finnigan, 1994). Due to density differences, this warm air rises and sets free convection in motion. However the rising air cools as it moves upward because air pressure decreases with height in the atmosphere.

If the rate of atmospheric temperature decrease with height is such that the temperature of the rising air parcel is always greater than the surrounding air, free convection will continue and the atmosphere is said to be unstable (Oke, 1990). Conversely, as it rises in the atmosphere, if the rate of cooling of an air parcel is greater than the rate of decrease in surrounding air temperature, the air parcel will become colder than the surrounding air and will sink. This condition describes a stable atmosphere.

If the rate of temperature change of the rising air parcel equals the rate of temperature change of the atmospheric profile, the air parcel will neither rise nor sink and the atmosphere has neutral stability. Cloudy and windy conditions are conducive to neutral stability (Oke, 1990).

Forced convection

Convection occurs under neutral conditions through turbulence created by frictional drag imposed on wind as it flows over the Earth's surface (Oke, 1990). Close to the ground, windspeed is reduced and if thermal effects are absent the vertical profile of windspeed will depend upon surface roughness (Figure 2.3a).

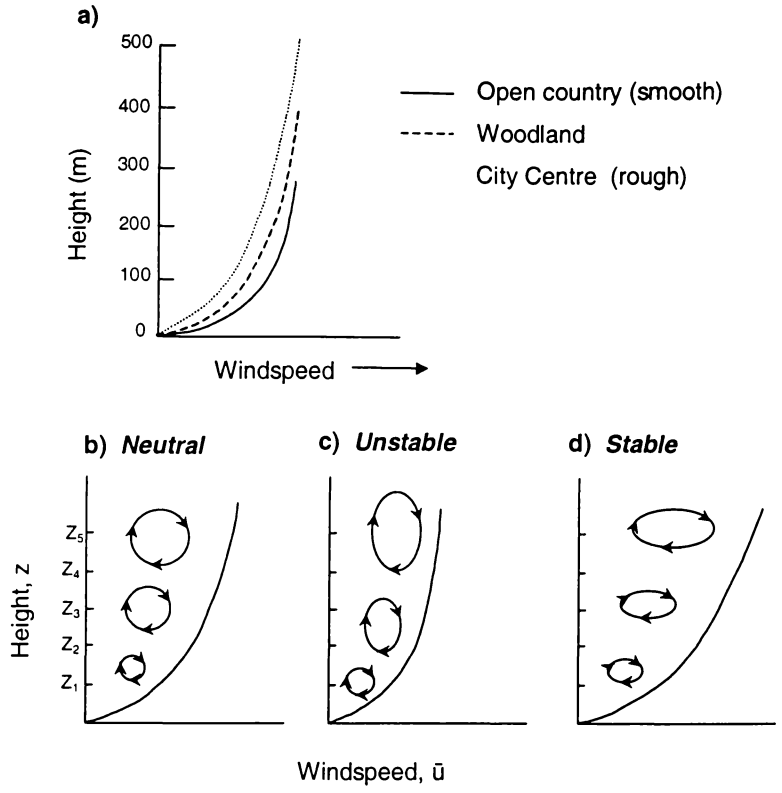

Figure 2.3 Vertical profiles of windspeed showing: **(a)** the effect of frictional drag on the windspeed profile for various degrees of surface roughness, and **(b)** to **(d)** profile and eddy shapes when affected by atmospheric stability (from Thom, 1975).

The flux of momentum, or wind stress upon a surface, is expressed as force/area and may be indexed by the friction velocity, u^*, which varies according to windspeed and the nature of the surface (Kaimal and Finnigan, 1994). Extrapolating the mean windspeed down the logarithmic profile as in Figure 2.3a, the roughness length, z_0, is the height at which windspeed becomes zero and is a measure of the aerodynamic roughness of a surface (Oke, 1990).

Following Thom (1975), the friction velocity may be defined as

$$u^* = ku / \ln[(z - d)/ z_0] \qquad \textbf{2.1}$$

where k = 0.4 is von Karman's constant, u is horizontal windspeed measured at height z, and $d \approx 0.67h$ is the zero plane displacement for average canopy height h (Oke, 1990).

The turbulence created by forced convection is in the form of eddies (Figure 2.3) and under neutral conditions is the mechanism for vertical transport of momentum, heat, moisture and CO_2 between the turbulent surface layer and the Earth's surface. Measurements of windspeed and scalar quantities may be decomposed into long-term mean and shorter period fluctuating values (Moncrieff et al., 1997b), the latter being a result of turbulent eddies. For example, expressions for density of air, (ρ) vertical windspeed (w) and scalar (s) concentrations may be written

$$w = \overline{w} + w' \qquad \textbf{2.2}$$

$$\rho = \overline{\rho} + \rho' \qquad \textbf{2.3}$$

$$s = \overline{s} + s' \qquad \textbf{2.4}$$

where overbars indicate mean values and primes are fluctuations about the mean (Moncrieff et al., 1997b).

As noted by Baldocchi et al. (1988), the instantaneous quantity of material moving through a horizontal plane of unit area per unit of time may be expressed as ρws. To estimate the flux of a scalar (F) in a turbulent atmosphere, a temporal average of this product is required (Baldocchi et al., 1988) so that

$$F = \overline{(\overline{\rho} + \rho')(\overline{w} + w')(\overline{s} + s')} \qquad \textbf{2.5}$$

Equation 2.5 may be expanded and, assuming horizontally homogeneous terrain, Reynolds' averaging procedures may be applied as demonstrated by Baldocchi et al. (1988) so that the following non-zero component remains

$$F = \rho \overline{w's'} \qquad \textbf{2.6}$$

where the overbar indicates the Reynolds average or covariance. Equation 2.6 forms the basis of the eddy covariance method for measuring fluxes.

Mixed convection

Under conditions of neutral stability, eddies approximate a circular shape and increase in diameter with height (Figure 2.3b). However free and forced convection often occur contemporaneously and the atmosphere is then said to be experiencing mixed convection (Oke, 1990). With mixed convection, eddies become extended in an unstable atmosphere (Figure 2.3c) and vertically compressed during periods of stability (Figure 2.3d) when vertical movement is dampened.

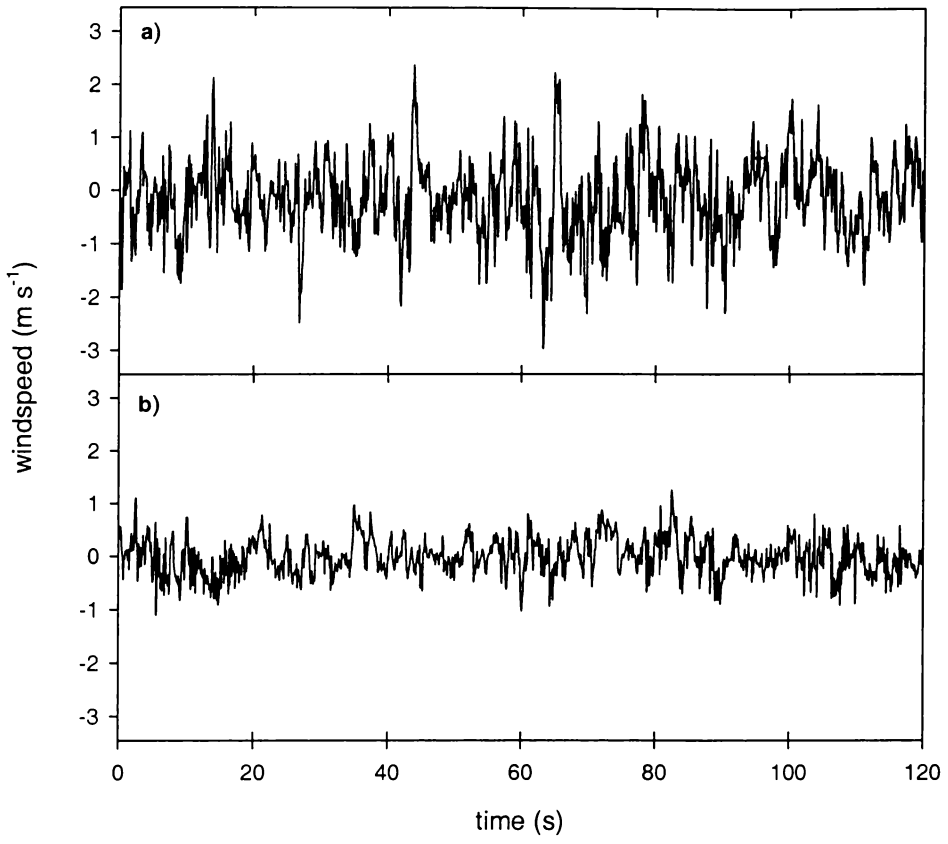

Figure 2.4 Vertical windspeed measured at 10 Hz frequency and height of 3.5 m at Moanatuatua bog during **(a)** unstable and **(b)** stable atmospheric conditions, both with horizontal windspeed of ≈ 2.5 m s^{-1}.

Figure 2.4 illustrates the effects of stability on vertical windspeeds. During unstable conditions (Figure 2.4a), free convection combines with forced convection to produce greater fluctuations in vertical windspeed than during stable conditions (Figure 2.4b) when there is no free convection. Because horizontal windspeed was equivalent for both plots ($\bar{u} \approx 2.5$ m s^{-1}), the differences between the two traces is due to contrasting stability and not variation of forced convection. It is apparent from Figure 2.4 that a stable atmosphere,

which typically occurs at night, is less conducive to vertical transport and mixing than is the unstable boundary layer.

2.3.2 Stationarity and horizontal homogeneity

Two assumptions of turbulent behaviour that are required to validate Equation 2.6 are stationarity and horizontal homogeneity.

Stationarity

Reynolds' decomposition of Equations 2.2 – 2.4 relies upon stationarity (Moncrieff et al., 1997a): the requirement that the properties of flow do not change over the averaging time. For example mean vertical windspeed, $\overline{w}$, must equal zero over an averaging period however this assumption may not always be met especially over tall vegetation such as forests (Lee, 1998). During stable conditions and low wind speeds at night, assumptions of stationarity may not be valid (Black et al., 1996; Lee, 1998).

Horizontal homogeneity

Micrometeorological techniques require horizontal homogeneity of flow conditions and for this the surface must be horizontally homogeneous (Moncrieff et al., 1997a). This assumption ensures that advective phenomena, such as the leading edge effect (Oke, 1990), do not confound measurements of vertical transfer in the turbulent surface layer. As a rule of thumb, the surface layer should be fully adjusted to the properties of a surface when horizontal homogeneity exists for a length greater than 100 times the height of measurement (Baldocchi et al., 1988).

2.3.3 Fluxes of energy

The surface energy balance may be written

$$R_n = G + H + \lambda E + P_s + J + A_d \qquad \textbf{2.7}$$

where R_n is the net radiation flux density; G is ground heat flux density, H is sensible heat flux density; λE is latent heat flux density, P_s is the flux density of energy used for photosynthesis, J is the storage flux of heat within the air space below measurement

height, and A_d is the advection flux of sensible or latent heat (Massman et al., 1990). Generally, P_s is an insignificant component of the energy balance and may be ignored (Massman et al., 1990). The advective term, A_d, may also be ignored over flat homogeneous terrain and the generalised energy balance becomes:

$$R_n = G + H + \lambda E + J \qquad \textbf{2.8}$$

Equation 2.6, the general eddy flux equation, may be used to express the sensible heat flux as

$$H = \rho c_p \overline{w'T'} \qquad \textbf{2.9}$$

where c_p is the specific heat of air at constant pressure and T' is fluctuation in air temperature. The latent heat flux (λE) may be represented by introducing the latent heat of vaporisation, λ, and fluctuations of water vapour density (ρ_v') into Equation 2.6 thus

$$\lambda E = \lambda \overline{w'\rho_v'} \qquad \textbf{2.10}$$

Other components of the energy balance in Equation 2.8 are not convective processes. The net radiation is a consequence of radiative transfer of energy and ground heat flux (G) is achieved by conduction; that is, the collision of rapidly moving molecules within the soil substrate (Oke, 1990).

2.3.4 CO_2 flux

Convective transport of carbon dioxide in the turbulent surface layer may be expressed by formulating Equation 2.6 as

$$F_c = \overline{w'\rho_c'} \qquad \textbf{2.11}$$

where F_c is the CO_2 flux density and ρ_c is density of CO_2 in air (Oke, 1990).

Alternatively, Equation 2.11 may be rewritten to accommodate CO_2 as a mixing ratio (c, μmol CO_2 mol^{-1} air) (Hollinger et al., 1999):

$$F_c = \frac{\overline{w'c'}}{V} \qquad \textbf{2.12}$$

where V is molar volume of air at ambient temperature and pressure.

2.3.5 Storage profiles

An underlying assumption of Equations 2.9–2.12 is that change in atmospheric scalar content is negligible relative to the flux of the scalar (Xu et al., 1999), however at times such as around sunrise or sunset, rate of change in CO_2 storage may be significant. This is especially true for ecosystems such as forests where small CO_2 and water vapour fluxes coincide with a large canopy air space (Xu et al., 1999).

While change in storage of CO_2 approximates zero over periods greater than or equal to one day (Hollinger et al., 1999) it may be necessary to include this phenomenon when considering diurnal variation in F_c. Likewise, Equation 2.9 may require correction for change in storage of sensible heat (Xu et al., 1999).

2.4 Models of Evaporation

The evaporation rate (E) may be derived from the energy flux λE through division by the latent heat of vaporisation (λ). The process of evaporation requires a source of water, energy to vaporise the water, a gradient of vapour concentration and turbulence to transport the water vapour (Oke, 1990). Models of evaporation use input variables of these factors as they are appropriate to particular environments. A widely used, physically based model of evaporation is the Penman–Monteith equation (Monteith, 1965).

2.4.1 Penman–Monteith model

To provide applicability to vegetated surfaces, Monteith (1965) introduced a canopy resistance term (r_c) to the Penman (1948) combination model of evaporation over saturated surfaces. While Penman's (1948) model used an energy term and a term describing the dryness of the air and aerodynamic resistance to transport (Oke, 1990), the Penman-Monteith equation is

$$\lambda E = \frac{s(R_n - G) + \rho c_p D / r_a}{s + \gamma(1 + r_c / r_a)} \qquad \textbf{2.13}$$

where s is the slope of the saturation vapour pressure versus temperature curve, γ is the psychrometric constant, D is the saturation vapour pressure deficit, r_a is aerodynamic resistance and r_c is canopy resistance to water vapour transfer.

Thom (1975) estimated r_a using

$$r_a = \frac{1.6}{ku_*} + r_{aM} \qquad \textbf{2.14}$$

where $r_{aM} = u/u^{*2}$ is aerodynamic resistance to momentum transfer from measurement height to the canopy. The first term on the right of Equation 2.14 is the so-called "excess resistance" which is necessary because the resistance to momentum transfer is less than the aerodynamic resistance to heat and water vapour transfer (Thom, 1975).

While r_c may be calculated as r_{st}/LAI, where r_{st} is leaf stomatal resistance and LAI is leaf area index, in practice it is difficult to measure r_{st} and the Penman–Monteith equation is often inverted to analyse the behaviour of r_c. For example, Thom's (1975) rearrangement of the Penman–Monteith equation has been used (e.g. Campbell and Williamson, 1997; Kelliher et al., 1993; Kelliher et al., 1998)

$$r_c = \frac{(1+\beta)\rho c_p D}{\gamma(R_n - G)} + \frac{r_a s \beta}{\gamma} - r_a \qquad \textbf{2.15}$$

where $\beta = H/\lambda E$ is the Bowen ratio.

2.4.2 Limitations of the Penman–Monteith model

One problem with the one-dimensional Penman–Monteith model occurs when sources of latent and sensible heat vary spatially. Treating the canopy as a single big leaf may produce anomalous estimates of canopy resistance when, for example, a sparse crop exists on moist bare soil (Monteith and Unsworth, 1990). Models such as that developed by Shuttleworth and Wallace (1985) have attempted a two-component dual source approach to combination modelling, where a term is added to account for soil surface resistance.

Dual source models that partition energy into plant and soil components have been used with some success for terrestrial ecosystems (e.g. Kustas, 1990; Massman and Ham, 1994; Qiu et al., 1999; Shuttleworth and Wallace, 1985), including wetlands (Burba et al., 1999; Kim and Verma, 1996). However determining model inputs is often challenging and may preclude the use of multi-source models (Baldocchi and Meyers, 1998).

Similar problems with the Penman–Monteith model can occur when evaporation of intercepted water confounds energy partitioning via the temporary addition of a separate source with varying quantity of available water (e.g. Campbell and Williamson, 1997). This problem was overcome by Asdak et al. (1998) using a rearranged Penman–Monteith equation, requiring measurement of throughfall and stemflow to calculate canopy interception.

2.4.3 Equilibrium model

A commonly used energy–based model of evaporation is that of Priestley and Taylor (1972):

$$\lambda E_{\mathrm{PT}} = \alpha \frac{s}{s+\gamma}(R_{\mathrm{n}} - G) \qquad \textbf{2.16}$$

where α =1.26 is a suggested coefficient used to adjust the equilibrium rate of evaporation (E_{eq}, defined by the remaining terms on the right of Equation 2.16) to match empirical results of evaporation rates from wet sites (Priestley and Taylor, 1972). Thompson et al.

(1999) note that E_{PT} is a better index than models of open water evaporation (E_0) because it is less dependant on local energy partitioning and it is commonly used to demonstrate the level of influence of net radiation as a driver of evaporation. For modelling evaporation at Moanatuatua, α =0.80 and α =0.58 have been used for wet canopy and dry canopy conditions respectively (Grimshaw, 2000).

2.5 Models of Carbon Exchange

2.5.1 Photosynthesis and CO_2 exchange

Plant growth is achieved when uptake of CO_2 through the process of photosynthesis exceeds respiration losses of CO_2. Photosynthesis occurs when CO_2, water vapour and light energy are used by plants to produce carbohydrates (CH_2O) and oxygen (O_2) (Oke, 1990). Stomata open during the daytime to allow CO_2 exchange with the atmosphere, and water vapour is lost through the open pores as transpiration. The exchange of water vapour is important to allow transport of nutrients through the plant and to regulate energy load on leaves (Oke, 1990).

Photosynthesis is regulated by plant water demand and availability, along with biochemical controls that are primarily driven by solar radiation and moderated by temperature, ambient CO_2 concentration and nutrient availability (Scheidegger et al., 2000). The waveband between 0.40–0.70 μm of the solar spectrum is used by plants for photosynthesis and is accordingly known as photosynthetically active radiation or PAR (Oke, 1990). Energy available for photosynthesis is often expressed as photosynthetic photon flux density or PPFD, expressed in units of μmol m^{-2} s^{-1}.

Baldocchi et al. (1987) found that photosynthesis at a well-watered deciduous forest site was determined by PPFD and that factors including vapour pressure deficit, air temperature and stomatal resistance were irrelevant. However stomatal regulation of photosynthesis is not always unimportant. Allen and Pearcy (2000) report that photosynthesis by tropical shrubs under dynamic light conditions was limited by stomatal closure over the dry season and during wet season afternoons.

In general for photosynthesis, other than the main driving variable of PPFD, seasonal effects may be significant for annual crops and when leaf area index varies dramatically such as in deciduous forests. Vapour deficits or soil water shortages may reduce photosynthesis or increase scatter in datasets. Leaf nitrogen content may also be a limiting factor although there is a need for data to verify this indirect relationship. Temperature may affect photosynthesis although some studies suggest effects are not significant (Ruimy et al., 1995). For periods of a day or more, a first order assumption for appropriate ecosystems is that photosynthesis is primarily driven by PPFD (Schmid et al., 2000).

2.5.2 Respiration

Respiration generates energy for plant metabolism and photosynthesis (Baldocchi and Meyers, 1998) and is the process where carbohydrates and oxygen are used to produce combustion energy and by–products of CO_2 and water vapour (Oke, 1990). Respiration may occur in soil, R_s, or as dark respiration, R_d, the latter occurring in above–ground plant tissue and is mainly a function of leaf temperature (Aurela et al., 1998).

Efflux of CO_2 from soil occurs from respiration by plant roots and microbes, with the main controls of respiration rates being soil temperature and soil moisture content (Davidson et al., 1998; Lloyd and Taylor, 1994). Other factors that may be less significant in controlling CO_2 production and transport include the C/N ratio of decomposing organic matter, quantity and type of microbial flora, pH value, oxygen content and diffusivity of the soil (Davidson et al., 1998; Fang and Moncrieff, 1999).

Lloyd and Taylor (1994) developed an Arrhenius type empirical equation that is commonly used to obtain plausible estimates of R_s from measurements of soil temperature

$$R_s = R_{10} e^{308.56\left(\frac{1}{56.02} - \frac{1}{T_k - 227.13}\right)} \qquad \textbf{2.17}$$

where R_{10} is the respiration rate at 10°C and T_k is peat temperature (K).

2.5.3 Net ecosystem production

Figure 2.5 illustrates the various components of CO_2 exchange between ecosystems and the atmosphere. After adapting equations from Ruimy et al. (1995) to maintain consistency with the symbols used in Figure 2.5, Equations 2.18 and 2.19 describe CO_2 fluxes during daylight ($F_{c(d)}$) and night time ($F_{c(n)}$) respectively

$$F_{c(d)} = A_n - (R_s + R_d) + F_{\Delta S} \qquad \textbf{2.18}$$

$$F_{c(n)} = -(R_s + R_d) + F_{\Delta S} \qquad \textbf{2.19}$$

where parameters are defined in Figure 2.5. $F_{\Delta S}$ is the flux of CO_2 associated with change in storage within the plant canopy, which may be especially important during early morning periods if CO_2 stored within the canopy overnight is released when temperature inversions collapse (Hollinger et al., 1999). Because it averages to zero, change in CO_2 storage may be safely ignored when estimating CO_2 flux over 24 hours or more (Greco and Baldocchi, 1996), however over shorter periods $F_{\Delta S}$ contributions may be important. This is especially relevant when modelling relationships between CO_2 flux and environmental variables such as PPFD (Hollinger et al., 1999).

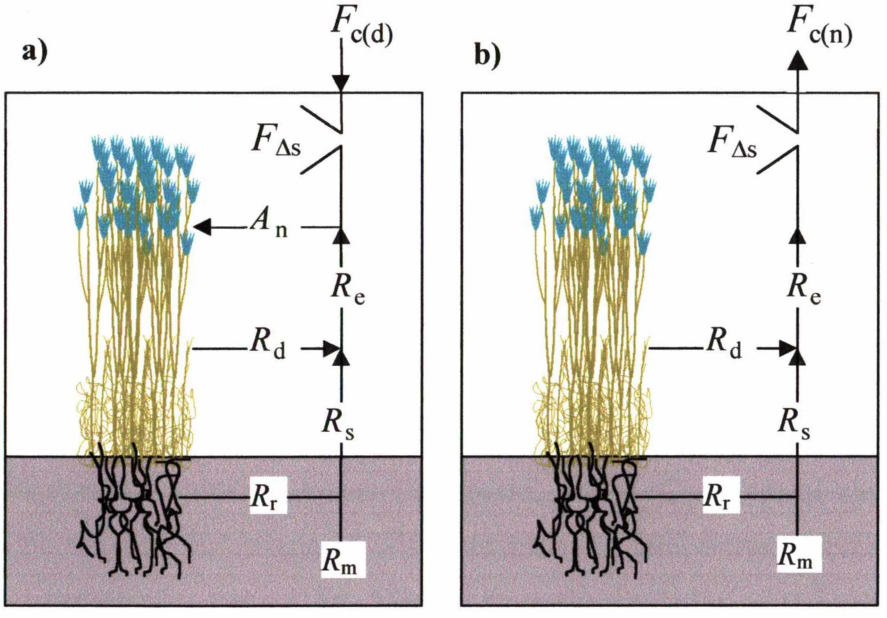

Figure 2.5 Ecosystem CO_2 balance during **(a)** day and **(b)** night. $F_{c(d)}$ is daytime net ecosystem flux; $F_{c(n)}$ is net ecosystem flux at night; $F_{\Delta S}$ is change in CO_2 storage within the plant canopy; A_n is photosynthesis; R_d is dark respiration; R_r is root respiration; R_m is microbial (heterotrophic) respiration; R_s is respiration from the soil; and R_e is total respiration from the ecosystem (adapted from Ruimy et al., 1995).

Integrated over time, the net flux may be used to obtain the net ecosystem production (NEP) which determines the gain or loss of ecosystem carbon and elucidates whether the ecosystem is a source or sink of atmospheric CO_2 (Ruimy et al., 1995). Net primary production (NPP), meanwhile, is plant photosynthesis (A_n) minus respiration losses from plant material ($R_d + R_r$).

Following Schmid et al. (2000), NEP may be defined

$$\mathrm{NEP} = \mathrm{GEP} - R_e = -(F_c + F_{\Delta S}) \qquad \textbf{2.20}$$

where GEP is gross ecosystem production, and R_e is total ecosystem respiration as illustrated in Figure 2.5. Schmid et al. (2000) note that net ecosystem exchange (NEE) is opposite to net ecosystem exchange, NEE = –NEP, and uses micrometeorological sign conventions so that NEE is positive when the flux is upward (away from the ecosystem).

2.5.4 Variability of CO_2 exchange

Comparing diurnal courses of CO_2 flux between wheat (C_3) and corn crops (C_4), Baldocchi (1994) noted that both crops sequestered carbon between 06:30 and 20:00 hr but lost carbon the rest of the day. At night the CO_2 flux density for both crops was controlled by temperature, whereas variation of PPFD explained the variance in daytime CO_2 flux densities.

For the well–watered wheat crop, CO_2 flux density was in phase with the diurnal course of PPFD and peaked at mid–morning. A parabolic diurnal course of CO_2 flux density is characteristic of C_3 species with abundant water. However increased temperatures usually cause a downward ramping of CO_2 flux density between late morning and early afternoon because of increased respiration losses (Baldocchi, 1994). Coincidental saturation or reduction of photosynthesis associated with late morning temperature increase is also common for canopies with a low LAI. Midday stomatal regulation of transpiration may also occur when water is limiting and stomatal closure also reduces the flux density of CO_2 (Baldocchi, 1994).

Even under well-watered conditions, CO_2 flux densities within a corn crop lagged those of the wheat crop and peaked three hours after PPFD peaked (Baldocchi, 1994). This was attributed to biochemical factors of C_4 species that limit photosynthesis of the corn crop and the sparse canopy was also less efficient at absorbing PPFD than the closed wheat stand.

At seasonal to annual time scales, variation of NEP may be explained by variability of any combination of PPFD, precipitation, temperatures, LAI, nutrition and atmospheric CO_2 concentration. At Boreal forests, low temperatures and a dearth of precipitation interact to form a sparse canopy with low LAI and variability of these factors affects photosynthesis and NEP (Baldocchi et al., 2000). Deciduous forests lose carbon during winter senescence and may rapidly gain carbon during the summer growing season (Baldocchi et al., 2001; Schmid et al., 2000).

Water table elevation at wetlands (Joiner et al., 1999; Oechel et al., 1993), snow cover (Fan et al., 1995; Goulden et al., 1998; Lafleur et al., 2001; Wofsy et al., 1993), degree of cloudiness (Fan et al., 1995; Goulden et al., 1996; Lee et al., 1999; Roderick et al., 2001) and drought (Hunt et al., 2002; Wilson and Baldocchi, 2000) are also factors that affect the variance of seasonal–annual carbon budgets at various biomes (Baldocchi et al., 2001).

2.5.5 Radiation and water use efficiencies

Radiation use efficiency, RUE, has been used to describe the effectiveness of ecosystems in using PAR to produce biomass and is the quantity of CO_2 assimilated per unit of solar radiation absorbed (Moncrieff et al., 1997c). Commonly expressed as the ratio of daily CO_2 uptake to PPFD, RUE may be useful for explaining variation of ecosystem production during periods of climatic variation such as cloudy versus clear-sky days and between seasons (Hollinger et al., 1994). Meanwhile canopy quantum efficiency (Moncrieff et al., 1997c) or quantum yield (Hollinger et al., 1994) is defined by the initial slope of the relationship between canopy CO_2 flux and PPFD (0–500 μmol m^{-2} s^{-1}).

Likewise water use efficiency, WUE, is traditionally regarded as the ratio of photosynthetic production to water use via transpiration (Baldocchi et al., 1987). However because photosynthesis and transpiration are difficult to measure at the ecosystem scale,

the ratio of fluxes of CO_2 (NEP) to water vapour (E) provides a useful index of WUE (Baldocchi, 1994; Baldocchi et al., 1985; Moncrieff et al., 1997c).

2.6 Wetland CO_2 and Water Vapour Exchange

2.6.1 Wetland classification

Wetlands are generally distinguished by having the water table at or near the land surface, with unique soil conditions and hydrophytic vegetation (Mitsch and Gosselink, 1993). When the rate of accumulating dead plant material exceeds decomposition rates in a wetland, peat soils are created and these generally contain at least 80% organic material (Clymo, 1983). Wetlands with at least 30 cm depth of peat are defined as peatlands or mires (Lappalainen, 1996) that may be classified further as either fens or bogs; essentially defined by their hydrology (Mitsch and Gosselink, 1993).

Fens are the more fertile of the two peatland types, receiving nutrients from groundwater recharge from surrounding mineral soils, while bogs receive a minimal nutrient input because their exclusive source of water is precipitation (Maltby and Proctor, 1996). While the fertility of fens encourages a rich diversity of plant species, nutrient deficiency and acidity of bogs is such that non-vascular *Sphagnum* moss dominates peat formation in the bog environment (Mitsch and Gosselink, 1993). Peat formation in New Zealand raised bogs is uniquely dominated by vascular vegetation of the *Restionaceae* family (Clarkson et al., 1999).

Along with supply of nutrients, hydrological inputs to wetlands are also important for maintaining the anaerobic zone (catotelm) where microbial decomposition of peat is retarded by the presence of a high water table (Maltby and Proctor, 1996). Rates of peat decay are much lower in the waterlogged catotelm (Clymo, 1983). Therefore to maintain both the catotelm and rates of net peat accumulation, output rates of water are important because water losses must be less than hydrological inputs. Evaporation is an important component of hydrological output in peatlands (Lafleur, 1990b) and has received considerable research attention, especially with studies in the Northern Hemisphere.

2.6.2 Peatland evaporation

Evaporation within wetlands may proceed at a rate equal to or greater than open water evaporation when the water table is at the surface (Lafleur, 1990a). This phenomenon is most often observed in non-transpiring systems with vegetation dominated by *Sphagnum* moss, however evaporation rates are often modified by water table variation in these bogs. This occurs because of low matric potentials and lack of water conducting tissues in *Sphagnum* vegetation which retards capillary rise of water (Ingram, 1983). In this case, the dry biomass creates a ground surface resistance to evaporation (Lafleur, 1990a).

Evaporation from bogs with transpiring vegetation may exhibit highly modified characteristics to those observed in non-vegetated or non-transpiring wetland systems. At a subarctic coastal fen, Lafleur (1990b) found that the presence of vegetation reduced evaporation below the open water rate, possibly because a mat of dead vegetation reduced evaporation to a greater extent than transpiration losses increased it. This reduction in evaporation is thought to be a positive feedback that the vegetation uses to create and maintain the wet environment it thrives in (van Breemen, 1995).

In separate studies, Lafleur (1990b) and Campbell and Williamson (1997) were able to predict evaporation using variations of Penman's model of open water evaporation. In their study of evaporation from the Kopouatai restiad bog in the Waikato, Campbell and Williamson (1997) found evaporation rates were restricted by the combination of a dense vegetation canopy and plant physiological responses. Bowen ratios in the range 3–5 were common during dry canopy conditions in summer. Despite the presence of a water table close to the surface, energy partitioning resembled that observed in arid conditions.

For seasonal to annual time scales, difficulties in applying the Penman–Monteith model saw Campbell and Williamson (1997) offering a crude scheme with coefficients used in combination with Penman's open water evaporation, depending on whether the vegetation canopy was dry or wet.

For dry canopy conditions at both Kopouatai and the modified Moanatuatua bogs, Thompson et al. (1999) observed similar diurnal evaporation characteristics to Campbell and Williamson (1997) with the latent heat flux plateauing in the morning as evaporation rates were believed to be constrained by plant physiological controls. Energy partitioning in Thompson et al.'s (1999) study was also consistent with Campbell and Williamson's

(1997) observations of extreme modification caused by great variation in canopy wetness which prevented physically realistic evaporation modelling.

Thompson et al. (1999) found no significant difference between summer time evaporation rates at Kopouatai and Moanatuatua bogs, despite the water table elevation and soil water contents being lower at Moanatuatua.

Bridgham et al. (1999) found that evaporation from a *Sphagnum* dominated bog in Minnesota (USA) was insensitive to water table fluctuations, while evaporation within a fen was influenced by variable water table elevations. The water table was lowered to depths down to 0.26 m and it was hypothesised that the capillary action of *Sphagnum* at the bog was more effective at drawing water to the surface than was the vascular vegetation at the fen (Bridgham et al., 1999). However Lafleur and Roulet (1992) noted that capillary draw by *Sphagnum* at only 3 cm distance was unable to support evaporative demand.

At a Minnesota fen dominated by *Sphagnum* with sparse vascular plants, Kim and Verma (1996) found water table elevation to be a control on evaporation rates. Evaporation was augmented by transpiration of the vascular vegetation, increasing to Penman's open water rates when the water table reached the rooting zone and vascular plants were not senescent, while evaporation was reduced during senescence and when the water table dropped below the rooting zone (Kim and Verma, 1996).

In contrast, the plant physiological controls and canopy structure at Waikato restiad bogs are thought to be so effective at restricting evaporation and maintaining their wetland environment, that water table elevation has little consequence and the effects of drainage and drought are reduced (Thompson et al., 1999).

2.6.3 Carbon sequestration in the wetland environment

Peat accumulation occurs when rates of atmospheric carbon sequestration exceed release. Clymo et al. (1998) proposed that peat accumulation is promoted by a high water table that minimises aerobic decomposition of peat, so that CO_2 losses are reduced. This hypothesis is supported by peatland research where water table lowering has resulted in decreased carbon accumulation or wetlands switching from a sink to a source of

atmospheric carbon (e.g. Armentano and Menges, 1986; Oechel et al., 1993; Oechel et al., 1998; Roulet et al., 1998).

Sharp (1995) hypothesised that a lowered water table at Moanatuatua bog imposes water stress on the vegetation and is responsible for reduced CO_2 assimilation. This hypothesis may be supported by observations of decreased carbon accumulation in some Northern Hemisphere bogs that was caused by water stress imposing constraints on rates of photosynthesis (Neumann et al., 1994; Shurpali et al., 1995). However Thompson et al. (1999) found no difference between summertime evaporation rates from *Sporodanthus ferrugineus*–dominated vegetation at Moanatuatua and Kopouatai bogs, despite large differences in water table depth and peat moisture content.

Moreover, Nieveen et al. (1998) observed a net release of carbon at a bog where the water table had once been lowered by drainage, but was restored near to the surface 10 years before the study. This suggests that carbon accumulation at peat bogs may not respond as a simple linear function of water table depth. A dynamic non-linear model of peat accumulation developed by Hilbert et al. (2000) recognises that peat production may be inhibited by either very dry or very wet conditions. Plant species composition and NEP may be affected by water table position so that while peat production may be reduced following a lowered water table, it is also possible that peat production may increase.

In Figure 2.6, the line where the rate of growth of peat height (dh_p/dt) is zero illustrates how two equilibria may occur at peat bogs with contrasting water table regimes. Optimal growth occurs at a point in between the two equilibria, so that a lowering of the water table at a deep, wet bog may result in sudden and rapid peat accumulation (Hilbert et al., 2000). This model could explain Nieveen et al.'s (1998) observation because, conceptually, restoration of the water table to the surface may not produce optimal peat development and could result in net loss of carbon if the water table moves beyond the second equilibrium state (Figure 2.6).

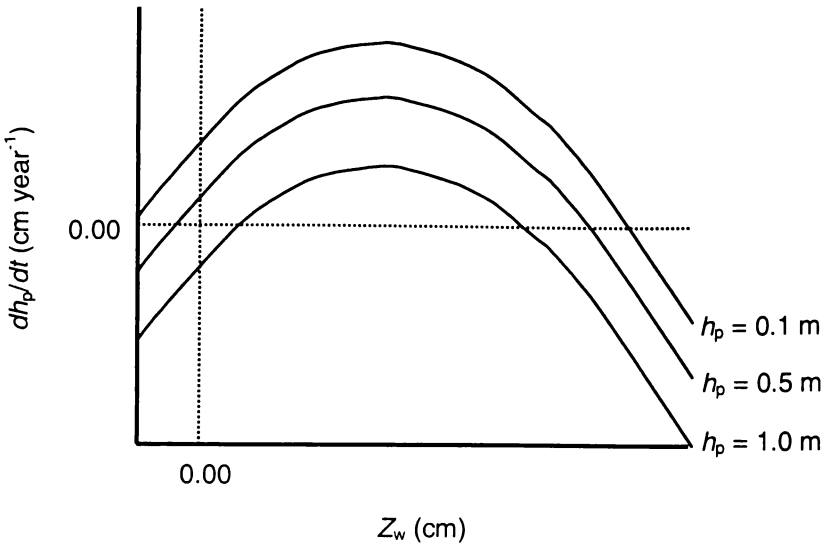

Figure 2.6 Conceptual model of peat accumulation expressed as rate of growth (dh_p/dt) versus water table depth (z_w) for various peat thickness (h_p). For deeper bogs, net growth occurs over a smaller range of water table depths (from Hilbert et al., 2000).

Alm et al. (1999) note that lowered water levels may effect increased carbon accumulation via augmented root production and litterfall at drained peatlands. Verification and development of Hilbert et al.'s (2000) model for particular wetlands may be valuable for ascertaining optimal water table height for bog management and restoration.

2.6.4 Global warming considerations

Given that wetlands are a major carbon sink on the global scale, a positive feedback of wetland degradation on atmospheric CO_2 and greenhouse warming has been proposed (Grulke et al., 1990; Oechel et al., 1993; Oechel et al., 1998). Notwithstanding the hypothesis that wetlands may generally become a source of carbon under a warmer and drier climate (Roulet et al., 1998), it is also possible that wetland systems might move towards the deep dry equilibrium. They may therefore undergo a sudden and rapid increase in carbon storage as optimal growth conditions are approached (Hilbert et al., 2000), becoming a stronger sink of carbon and a negative feedback to greenhouse warming.

While methane fluxes are much smaller than CO_2 emissions from wetlands, CH_4 emitted from bogs may be a significant greenhouse gas because it is twenty one times more radiatively efficient than CO_2 (Roulet et al., 1998). In terms of the carbon budget, however, the loss of peatland carbon through methane production is insignificant (Alm et

al., 1999), estimated at less than one percent of NPP at the subarctic fens of Hudson Bay (Klinger et al., 1994).

CH_4 fluxes are also correlated with water table depth and peat temperature of wetlands, so that a drier or colder wetland is likely to produce less methane than a warm, saturated one (Roulet et al., 1998). Illustrating this, CH_4 emissions at a boreal bog were 11% and about 0.95% of the annual carbon balance from hollows and hummocks respectively, with the water table fluctuating between 0–15 cm at the former microsites and 30–48 cm below hummock microsites (Alm et al., 1999). Meanwhile, measurements at 17 Finnish peatland sites identified annual methane emissions of 8.0 $gCH_4\ m^{-2}$ and 3.9 $gCH_4\ m^{-2}$ at natural and drained ombrogenous bogs respectively (Nykänen et al., 1998).

Along with a decrease in CH_4 production *per se*, methane emissions at drained wetlands are attenuated even further by oxidation in the aerobic zone (acrotelm) (Sundh et al., 1995). At peatlands with lowered water tables, methanotrophic bacteria in the acrotelm can be so effective at oxidising CH_4 to CO_2 that methane concentrations in the upper peat profile are less than atmospheric levels, switching the bog to a methane sink (Martikainen, 1996). While drained fens are more prone to becoming methane sinks (Nykänen et al., 1998), the effect of draining bogs causes significant reductions in methane emissions. Nykänen et al. (1998) found that lowering the water table by 10 cm would induce a 45% reduction in CH_4 emissions from Finnish peat bogs.

The presence of vascular plants may increase the release of methane to the atmosphere and couple CH_4 emissions to NEE, however this is limited to sites that remain wet with the water table near the surface (Waddington et al., 1996). For the purposes of this study, CH_4 emissions may be ignored because the literature suggests methane loss does not represent a significant component of the carbon balance for peat bogs: especially those with a lowered water table.

2.6.5 Dissolved Carbon

An alternative flux of carbon from ecosystems is the discharge of dissolved carbon in hydrological runoff.

Alm et al. (1999) estimated dissolved organic carbon (DOC) leaching of 7 $gC\ m^{-2}\ yr^{-1}$ from a boreal bog, contributing about 8% of the net loss of 90 $gC\ m^{-2}$ for the year of their

study. This is a large estimate in the range of 3.5–8.6 gC m^{-2} yr^{-1} leached carbon measured at various Finnish catchments (Nykänen et al., 1998).

Meanwhile, estimates of dissolved organic carbon (DOC) export from northeastern bogs in the USA range from 5–20 gC m^{-2} yr^{-1}, and a study of three peatlands in Minnesota found rates of DOC export between 8–40 gC m^{-2} yr^{-1} (Urban et al., 1989). Relative to DOC export from catchments with mineral soils, losses of DOC from Minnesota peatlands are large yet represent only 5% of annual NPP (Urban et al., 1989).

During the 1992 and 1993 growing seasons (May–September) at a Swedish peatland, Waddington and Roulet (2000) measured DOC and dissolved inorganic carbon (DIC) to ascertain the export of total dissolved carbon (DOC+DIC). Over the area of the wetland, losses of dissolved carbon were greatest at ridges where the water table was 20–30 cm below the surface. However the total seasonal loss of DOC+DIC from ridges was only 0.7 gC m^{-2}: a small fraction of gross ecosystem production that averaged 231.5 gC m^{-2} (Waddington and Roulet, 2000).

2.7 Summary

This chapter has described the theory of turbulent transfer of energy and CO_2 in the surface layer of the atmosphere. For diurnal evaluations, the role of storage may be important at certain times of the day. General models of evaporation and CO_2 transfer were considered, before describing the implications of these for peatlands. While water table elevation may control evaporation rates within peat bogs, the role of vegetation may be significant by constraining evaporation. Depth to the water table is generally an important control of carbon fluxes within wetlands, however the exact consequences of raising or lowering the water table are uncertain.

For the purposes of this research, methane is likely to be an insignificant component of the carbon balance and shall be ignored. Dissolved carbon egress from peatlands is also generally a negligible component of the annual carbon balance.

3 Field Site and Methodology

3.1 Moanatuatua Peat Bog

Moanatuatua peat bog is located 18 km southeast of Hamilton city (Figure 3.1) and was once 7500 ha in size (Clarkson et al., 1999). The peat formation has mostly been drained and converted to pasture while a 114 ha remnant bog is set aside as a Scientific Reserve and managed by the Department of Conservation. Henceforth referred to as Moanatuatua, the reserve has 1–2 m deep drains around the entire quasi-rectangular perimeter (Figure 3.2). Moanatuatua has a maximum width of approximately 650 length of 2000 m and a row of pine trees (*Pinus radiata*) approximately 15 m in height along the eastern boundary (Figure 3.3).

It has been suggested that perimeter drains are responsible for lowering the water table at Moanatuatua (Clarkson et al., 1999; Shearer, 1997). A more recent investigation of groundwater fluxes suggests that the hydrological impact of the drains extends no further than 20 m into the bog and variations of meteoric recharge and vegetation changes are a greater influence on water table elevation (Grimshaw, 2000). The bog ecosystem is abruptly bounded by farmland (Figure 3.3) that suffers from peat degradation and compaction, so the surface is 1–2 metres lower than the Scientific Reserve (Shearer, 1997).

3.1.1 Peat Characteristics

Peat began forming on top of the fluvial Hinuera formation at Moanatuatua *c.*13–14 000 BP and continued developing at an average rate of 1 mm yr^{-1} (Clarkson et al., 1999; Schipper and McLeod, 2002). During the first 1000 years of bog development, peat accumulated above the influence of groundwater and minerotrophic plant species were replaced by ombrotrophic vegetation as the dominant species (Clarkson et al., 1999).

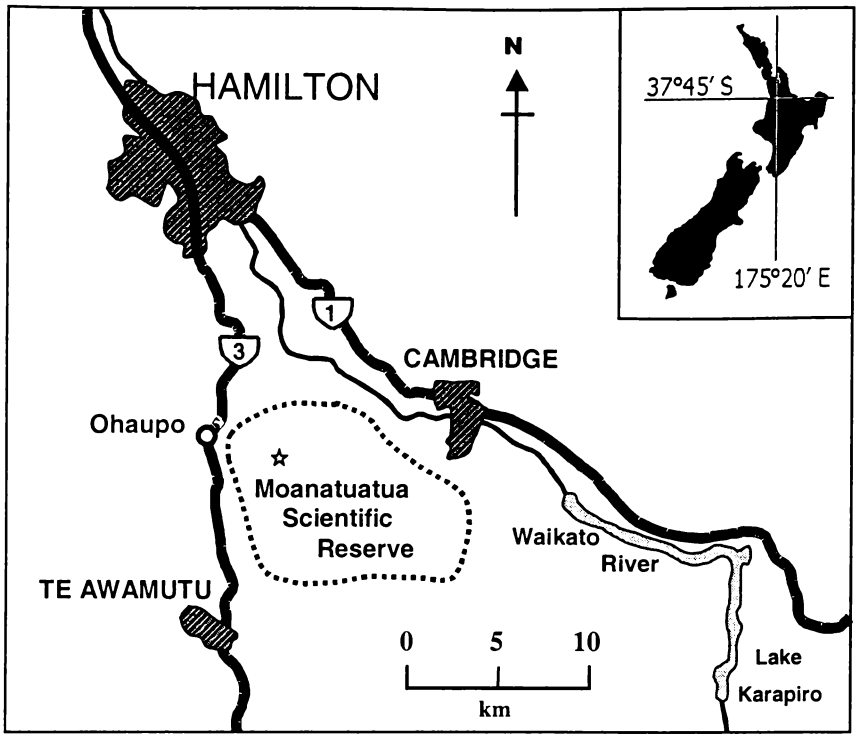

Figure 3.1 Location of Moanatuatua peat formation (dotted line). The peatland has been largely drained and converted to pasture, apart from a 1.14 km^2 remnant set aside as Moanatuatua Scientific Reserve (star symbol). (Adapted from Grimshaw, 2000).

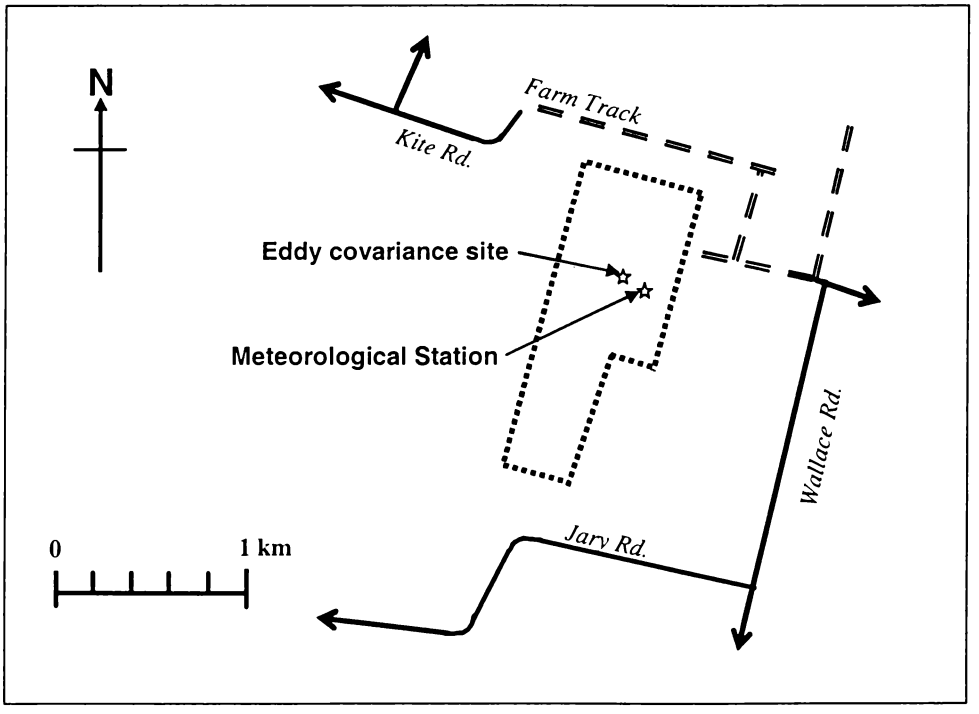

Figure 3.2 Map of Moanatuatua Scientific Reserve (dotted line) showing location of eddy covariance site and meteorological station. (Adapted from Thompson, 1997).

Figure 3.3 Aerial photograph of Moanatuatua peat bog showing abrupt modification to developed agricultural land. Drains exist around the entire perimeter of the bog, with mature *Pinus radiata* visible at margins on the right hand side. (Photograph: Environment Waikato, 1999).

The main peat former is the restiad wire rush *Empodisma minus*, with its dense mat of fine roots possessing water retention and peat forming characteristics similar to *Sphagnum* moss in Northern Hemisphere wetlands (Clarkson et al., 1999). Moanatuatua is 60 m above sea level and has a maximum peat depth of 12 m (Shearer, 1997).

Dry bulk density of peat from a depth of 0.05 m below the surface has been measured by Thompson et al. (1999) and averaged 50 kg m^{-3}. A layer of tephra from the Taupo eruption (*c.* 200AD) is 178 cm below the surface at Moanatuatua but 5 cm below the surface on some surrounding farmland (Shearer, 1997). Schipper and McLeod (2002) ascertained dry bulk density above the Taupo tephra at Moanatuatua is 60 kg m^{-3} compared with 260 kg m^{-3} at surrounding farmland. This difference is attributed to compaction and mineralisation of peat developed for agriculture, while the loss in height is also caused by microbial degradation of the peat to carbon dioxide (Schipper and McLeod, 2002).

Despite modification of surrounding farmland, Moanatuatua peat generally is close to its original condition with low pH (4.4) and poor nutrient status (e.g. total nitrogen 0.6 mg cm^{-3}) characteristic of oligotrophic wetlands (Clarkson et al., 1999). Nutrient characteristics of Moanatuatua peat substrate are similar to those at the pristine Kopouatai bog, apart from an increase of the important nutrient phosphorous at Moanatuatua

(Clarkson et al., 1999). Total phosphorous in the upper 10 cm of the peat profile at Kopouatai was 3.89 $\mu g\ cm^{-3}$, while at Moanatuatua it was significantly greater (α=0.05) at 108 $\mu g\ cm^{-3}$ (Clarkson et al., 1999). This exception of phosphorus augmentation is believed to be a consequence of aerial drift of fertiliser during application to agricultural land adjacent to Moanatuatua (Clarkson et al., 1999).

3.1.2 Vegetation

Restiad bogs are so called because the dominant vegetation at these wetlands belongs to the *Restionaceae* (restiad) family. At Moanatuatua the restiad rushes *Sporodanthus ferrugineus* (Figure 3.4) and *Empodisma minus* (Figure 3.5) are the most prevalent vegetation and the latter is the dominant peat former (Agnew et al., 1993). Both species have evergreen stems with leaves reduced to sheaths at short intervals (Agnew et al., 1993).

S. ferrugineus is unique to Moanatuatua and Kopouatai wetlands (de Lange et al., 1999). Because its habitat is protected by reservation, the species is classified as declining although without this ecosystem protection it would be considered endangered (de Lange et al., 1999). *S. ferrugineus* has a horizontal rhizome at depths to 80 mm, with roots that extend down to 0.6 m below the rhizome, while the stems grow up to 2.8 m tall at Moanatuatua.

Sporodanthus ferrugineus has recently been distinguished from closely related *Sporodanthus traversii*, a species confined to Chatham Islands (de Lange et al., 1999). An important distinction is that following fire, *S. ferrugineus* is re-established only by seed from remnant plants whereas *S. traversii* reestablishes more rapidly via activation of dormant seed. Following fire, *S. ferrugineus* may require 12 years to reestablish fully within a peat bog. A fire in 1972 destroyed 67% of vegetation at Moanatuatua, however reestablishment to a climax community of restiads was facilitated via provision of seed from areas of unburnt vegetation (Clarkson et al., 1999).

Figure 3.4 *Sporodanthus ferrugineus* grows up to 2.8 m tall and is one of two restiad species dominating the vegetation at Moanatuatua. Closeup (left) shows leaves reduced to sheaths along jointed evergreen stems. Photographs: Dave Campbell.

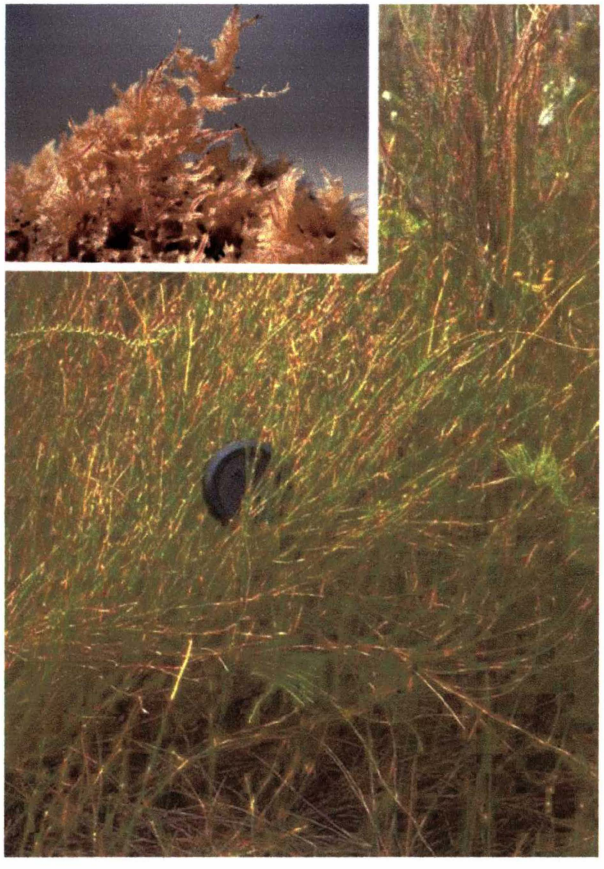

Figure 3.5 The sprawling wire rush *Empodisma minus* is one of two restiad species dominating the vegetation at Moanatuatua. Note the weft of fine root hairs (inset) typical of those responsible for peat formation. Main photograph: Dave Campbell; inset: Bev Clarkson.

While *S. ferrugineus* is an erect rush, the sprawling *E. minus* forms a dense tangled growth up to 0.7 m, although supported amongst *S. ferrugineus* it may reach 1.7 m in height (de Lange et al., 1999). Whereas *S. ferrugineus* is ecologically significant because its existence is limited to threatened ecosystems, *E. minus* is found throughout New Zealand and parts of Australia yet has a highly valued and unique role in establishing and maintaining the peat that forms these ecosystems (Clarkson et al., 1999).

E. minus is also a rhizomatous perennial yet forms a dense network of subaerial roots (Figure 3.5) with base exchange capacity and water retention similar to *Sphagnum spp.* (Agnew et al., 1993). This fine root mass is the dominant peat former at Moanatuatua, contributing almost all the material responsible for development and growth of the bog.

Aboveground *E. minus* dominates the Moanatuatua canopy, with 5.74 kg m^{-2} of densely tangled biomass compared with 2.97 kg m^{-2} of *S. ferrugineus* (Thompson, 1997). Much of the *E. minus* biomass was dead material (3.98 kg m^{-2}), with a thick mulch of *E. minus* stems in the subcanopy layer below 0.5 m height (Thompson, 1997). Leaf area index (LAI) was measured by Thompson (1997) in December 1995 and total LAI of 2.35 was partitioned into *E. minus* and *S. ferrugineus* LAI of 1.55 and 0.8 respectively.

Two important implications of the dense *E. minus* canopy are the propensity to intercept and store significant amounts of precipitation (Campbell and Williamson, 1997), plus the reduction of evaporation by preventing diffusion of water vapour from the moist peat surface and through shading from incident solar radiation (Thompson et al., 1999). Stomatal regulation by *E. minus* is also considered important for reducing transpiration under conditions of high evaporative demand (Thompson et al., 1999). Xerophytic adaptations of *E. minus* allow the species to tolerate drought in arid environments, with features such as perenniality, reduced leaf size and thick cuticle being suited to survival in oligotrophic environments (Sharp, 1995).

Other plant species at Moanatuatua include liverworts, mosses and orchids. While these species are ecologically significant, relative to the restiad species their abundance and biomass are negligible so they are assumed to have an insignificant effect on evaporation and carbon sequestration for this study. An exception may be *Epacris pauciflora* A.Rich, a

vascular shrub species growing to similar height as *S. ferrugineus*. Whereas Thompson (1997) reported that non-restiad plant species represented an insignificant 2% of the biomass at Moanatuatua in 1995, anecdotal evidence suggests that *Epacris pauciflora* has increased in abundance and plant size since then (Campbell, pers. comm.)[1].

3.1.3 Climate

The measurement period for this project was 15 December 1998 to 15 December 2000. Because the project did not occur strictly within calendar years, annual data for 1999 and 2000 refer to 15 December 1998 – 15 December 1999 and 15 December 1999 – 15 December 2000 respectively.

Daily maximum net radiation (R_n) throughout the project varied between 60 W m^{-2} and 1000 W m^{-2}, with maximum midwinter values of 360 W m^{-2} (Figure 3.6a). Precipitation was calculated as the mean catch of two raingauges at Moanatuatua eddy covariance site and meteorological station (see Figure 3.2 for locations). Annual rainfall was 1046 mm in 1999 and 943 mm in 2000. The former year was closer to 1190 mm mean annual rainfall measured at nearby Cambridge (1970–1999: Grimshaw, 2000) than year 2000, which was drier than average. The study period was characterised by many low intensity precipitation events, with 75% of the total 1989 mm being the aggregation of rainfall on days with less than 20 mm (Figure 3.6b). Greater than 20 mm precipitation was recorded on only 15 days, with the largest event of 71 mm on 17 January 1999.

Figure 3.6b displays daily maximum vapour pressure deficit (D) and a 45 day moving average for the entire study period. Maximum D increased steadily from winter to reach a maximum of 2.5 kPa in late summer. The moving average of daily maximum D shows a steady increase to autumn, followed by a sudden and abrupt decrease to approximately 0.5 kPa in winter (Figure 3.6b). Seasonal trend of D follows that of mean daily air temperature (Figure 3.6c) more so than R_n (Figure 3.6a).

[1] Personal communication with Dr. Dave Campbell, Dept. of Earth Sciences, University of Waikato.

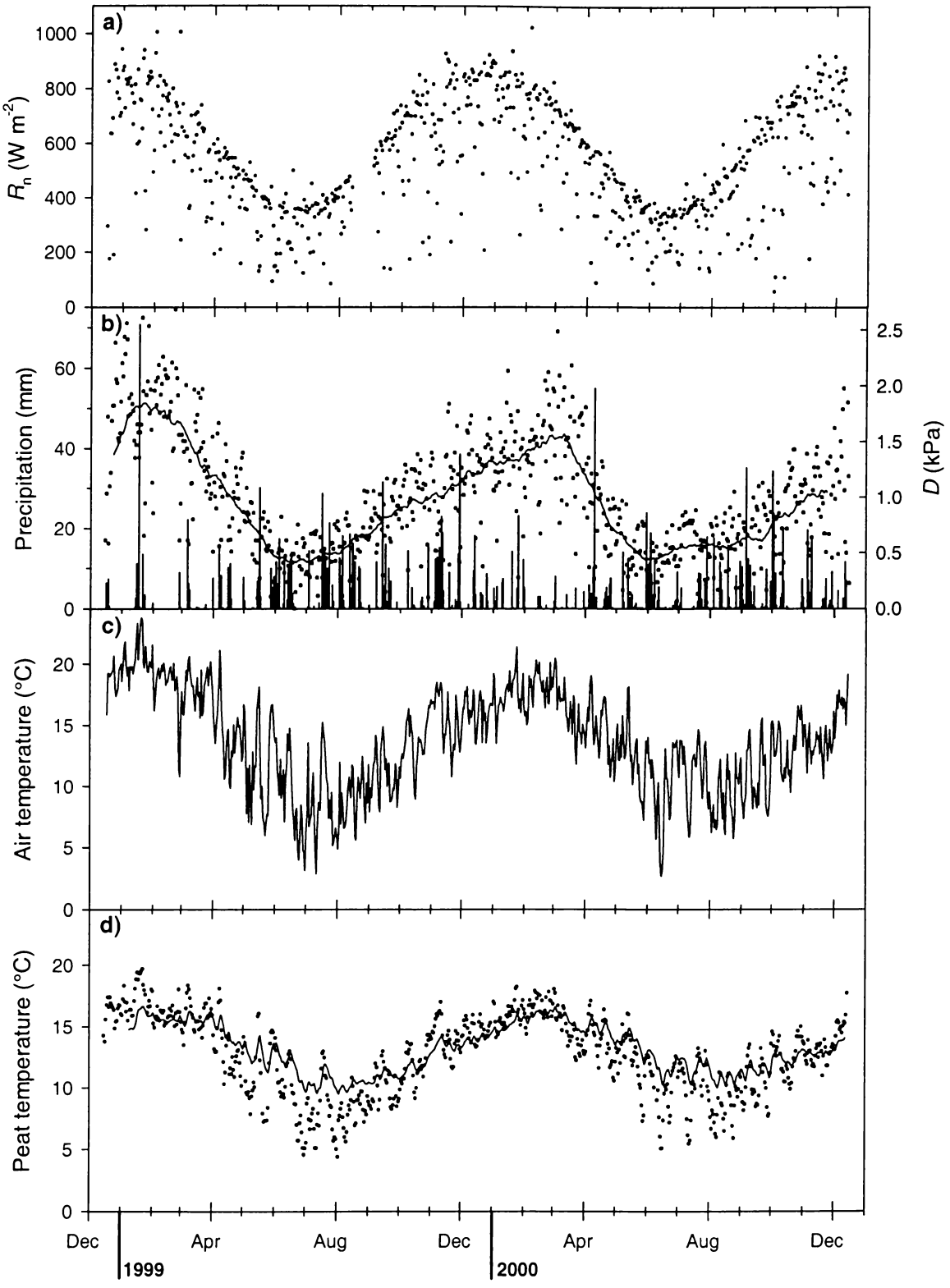

Figure 3.6 Interannual course of: **(a)** daily maximum net radiation (R_n); **(b)** daily total precipitation (bars), daily maximum vapour pressure deficit (D, points) with 45 day moving average (solid line); **(c)** daily mean air temperature; **(d)** daily mean peat temperature at 8 cm depth (points) and 30 cm depth (solid line).

The maximum daily mean air temperature was 24 °C in summer of 1999/2000, with minimum daily mean air temperature of 3°C occurring in both winter periods (Figure 3.6c). Mean annual air temperature was 13.8 °C for 1999 and 13.55 °C for 2000, comparable in both years to 13.6 °C mean annual temperature measured at nearby Cambridge between 1976–1989 (Grimshaw, 2000).

Mean peat temperature measured at 8 cm and 30 cm depth was 12.6 °C and 13.1 °C respectively for the entire study period. Daily mean peat temperature measured at 30 cm depth varied between 10 °C and 16 °C for winter and summer respectively. The daily mean temperature at 8 cm depth was more variable over seasonal periods: between 14–20 °C during summer and 4–12 °C during winter.

3.1.4 Soil moisture content and water table

Over a 30 day period that included several rain events, Campbell et al. (2002) observed little variation of volumetric moisture content (θ_v) in the upper 20 cm of peat at Moanatuatua, while measurements made deeper in the peat profile mimicked behaviour of the water table. Figure 3.7 demonstrates that over longer time periods, θ_v in the upper profile follows the trend of the water table. Mean daily θ_v followed broadly the same trend as depth to water table over the study period, with shallow water table corresponding with high θ_v.

While the ecosystem is a wetland, the upper 10 cm of the peat profile is relatively dry, ranging between 0.04–0.27 m^3 m^{-3}. The water table was also relatively deep for a peat wetland, varying between 325–815 mm below ground with a mean of 580 mm. At the relatively pristine Kopouatai restiad peat bog, 90 km north of Moanatuatua, the water table generally varies between 0–120 mm below the peat surface (Newnham et al., 1995). The maximum depth to water table throughout the project coincided with minimum θ_v in March–April 2000, while the shallowest water table and greatest θ_v was during winter–spring 1999. This also follows the pattern of rainfall, with the plot of cumulative precipitation showing negligible rainfall (34 mm) in Feb-Mar 2000 and significant precipitation (270 mm) in Jul-Aug 1999 (Figure 3.7).

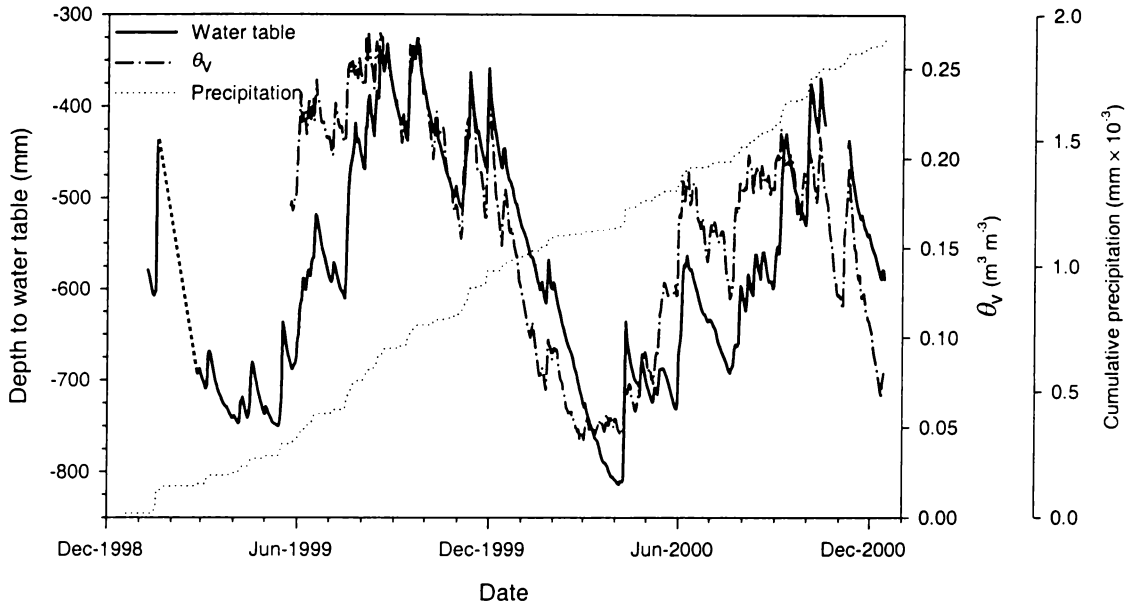

Figure 3.7 Daily means of depth to water table, cumulative precipitation and volumetric soil moisture content (θ_v). Due to instrument failure, water table data from 17 October 2000 – 08 November 2000 are omitted. Missing water table data from 18 January 1999 – 25 February 1999 are interpolated (dotted section) because only 22 mm rainfall occurred during this 37 day period.

3.2 The Eddy Covariance Technique

The eddy covariance method has become a standard for measuring flux densities of sensible heat, water vapour and CO_2 at the local scale (Baldocchi et al., 1996; Grelle and Lindroth, 1996). To ascertain these flux densities using Equations 2.9–2.11, high frequency measurements of air temperature, water vapour and CO_2 concentrations are required, along with vertical windspeed.

Sonic anemometers are employed for high speed measurement of three turbulent windspeed components: two horizontal and one vertical. By measuring the speed of sound, sonic anemometers also allow the calculation of air temperature and the determination of sensible heat flux (Moncrieff et al., 1997b). High frequency measurements of CO_2 and water vapour concentrations are commonly made with a closed path, infrared gas analyser (IRGA). Air is passed along a path separating a source of infrared radiation and a detector, with absorption of infrared radiation used to determine trace gas concentration.

3.3 The UW Eddy Covariance System

3.3.1 Hardware

The University of Waikato (UW) closed-path eddy covariance (EC) system was used to measure fluxes of sensible heat, water vapour and carbon dioxide. The EC site was located so that fetch of 290 m to the eastern border and 360 m to the western border was achieved (Figure 3.2). Greater than 1000 m fetch was achieved to the northern and southern boundaries. With prevailing winds from the westerly quarter, the mast and hut (Figure 3.8) were positioned southeast of the instrumentation to minimise disturbance of fluxes.

A Campbell Scientific Inc. (CSI), (Utah, USA) CSAT3 sonic anemometer measured air temperature and 3-dimensional components of windspeed at 3.5 m measurement height (Figure 3.9). A sample tube intake was also positioned at this height, 0.23 m horizontal distance from the CSAT3. Air was drawn along the 5.5 m, 4 mm ID sample tube (Dekabon, Deane & Co., Glasgow, UK) to a gas analyser (LI-6262, LiCor, NE, USA) located inside a hut (Figure 3.8). An open path krypton hygrometer (KH2O, CSI), used for verification of water vapour fluxes, was also mounted at 3.5 m height with 0.23 m horizontal distance between the measurement path and the CSAT3.

The sample tube was fitted with a 90 μm sintered filter (Swagelok, Crawford Fitting Co., OH, USA) 0.15 m downstream of the intake and a 1 μm PTFE filter (Pall Gelman Laboratory, Ann Arbor, MI, USA) immediately upstream of the LI-6262. To minimise condensation inside the sample tube, a nichrome heating element was wrapped around the sample tube and surrounded with insulating material (Aeroflex). Sample tube heating was controlled by a datalogger (CR10X, CSI). Air was drawn along the sample tube to the gas analyser using two 12VDC pumps (TD-4N & TD-4X2N, Brailsford & Co., Rye, NY, USA), at a rate of approximately 6 l min^{-1}.

A tanked supply of oxygen free nitrogen (OFN) flowed continuously at a rate of 40 cm^3 min^{-1} through the LI-6262 reference cell, providing a reference gas of zero CO_2 and water vapour. Calibrations were automated so that a zero gas (OFN) and span gas (352 ppm CO_2 in air) were consecutively drawn through the sample cell at 0005 hr daily.

Figure 3.8 The eddy covariance (EC) site showing mast, sample tube and hut.

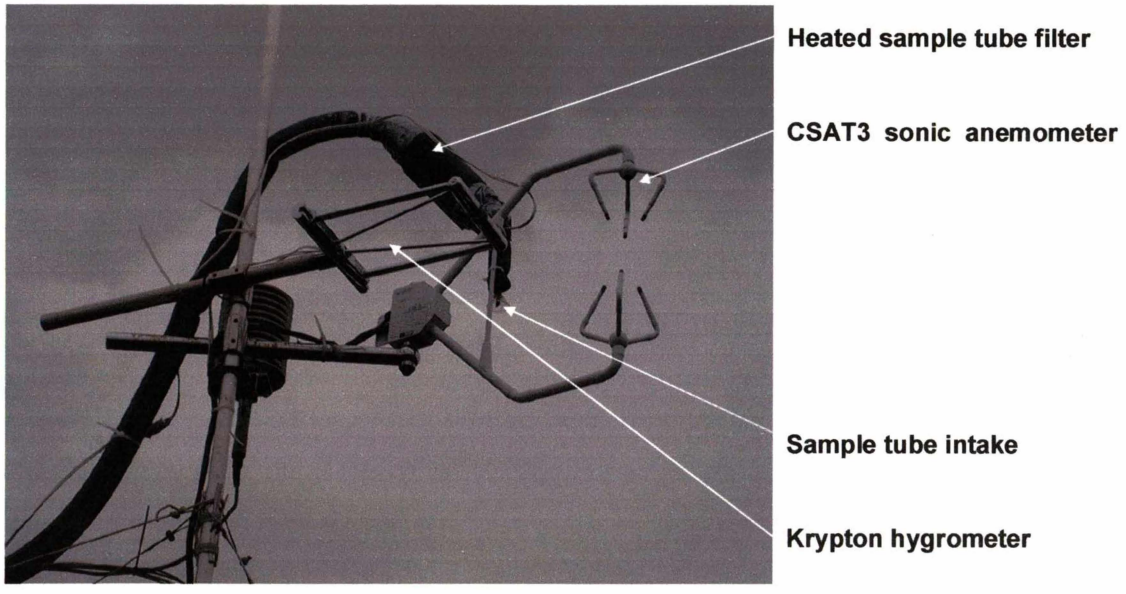

Figure 3.9 Eddy covariance mast instrumentation at 3.5 m height. Air was drawn down a sample tube with intake positioned 0.23 m horizontally from the CSAT3 sonic anemometer. The measurement path of an open path krypton hygrometer was also 0.23 m horizontal distance from the CSAT3.

A CR10X datalogger was dedicated to functions including control of calibrations, power supply and sample-tube heater. Power demand of the system was usually less than 50W and was supplied by ten 80W solar panels.

Details of the EC system design and operation are appended on CDROM.

3.3.2 Data acquisition

Raw mV data from the CSAT3, KH2O and LI-6262 were sampled at 10 Hz by a dedicated CR10X and output as a text file to computer (Toshiba Satellite 320CDS) every minute. The CR10X data acquisition program is appended on CDROM.

A Matlab (The Mathworks Inc., MA, USA) function (DAQ.m, appended on CDROM) read texfiles shortly after being written and appended data to a time-stamped binary file. Binary data files were saved to hard drive every half hour and manually transferred to magnetic tape (Sony 2GB Ditto) during (usually) 3-weekly site visits. Raw data were then archived to CDROM.

3.3.3 Post-processing of data

Mixing ratios of CO_2 and H_2O were calculated from raw mV data using procedures described in the LI-6262 manual (LiCor, 1996). Pressure broadening and dilution corrections of CO_2 due to water vapour were applied so that mV data were corrected for these phenomena. Following Webb et al. (1980), corrections were applied to water vapour measurements from the KH2O to account for variations in air density and oxygen absorption as described in Tanner et al. (1993) and Kelliher et al. (1997).

To account for transit time in the sample tube, time series' of gas concentrations were shifted to maximise the correlation coefficient with the time series of vertical wind velocity. Typical delays were 2.0–2.4 seconds. Coordinate rotations were applied following Baldocchi et al. (1988), to correct covariances for tilt of the sonic anemometer.

Filters were used to reject spurious data identified by 'hard spikes' as described by Schmid et al. (2000). Hard spikes include obviously spurious CSAT3 data identified by absolute value of sonic temperature (T_{sonic}) greater than 60 °C or vertical windspeed (w) greater

than 100 m s^{-1}. For trace gas concentrations, hard spikes were identified by absolute values of CO_2 concentration greater than 1200 μmol mol^{-1} and H_2O concentration greater than 50 g m^{-3}.

'Soft spikes' were identified by large short-lived departures from 30 min means following Schmid et al. (2000). For each variable, a threshold for spikes was identified as a multiple of the standard deviation (σ) using an iterative process beginning with 3.6σ and increasing by 0.3σ for two subsequent passes. For each pass, soft spikes were identified if the fluctuation from the 30 min mean was greater than the threshold value and the duration of the spike was less than four consecutive points (0.3 s for the 10 Hz sampling frequency). After each pass, soft spikes were removed and the mean and standard deviation were recalculated before repeating the process until no more spikes were detected or the maximum of three iterations was achieved (following Schmid et al., 2000).

Covariances between vertical velocity and scalar fluctuations were then calculated and written to a binary database. If less than 67% of raw data remained after filtering, the covariance was treated as missing. While averaging periods of 15 min have been used for eddy covariance research (e.g. Lafleur et al., 2001), the 67% criteria used here ensured that at least 20 min of quality raw data were used for flux calculations.

Latent heat flux (λE, W m^{-2}) was calculated by applying the covariance between vertical wind velocity and atmospheric water vapour content to Equation 2.10. Sensible heat flux (H, W m^{-2}) was determined using Equation 2.9 and applying the covariance between vertical wind velocity and sonic air temperature, with virtual temperature correction following Laubach et al. (1994). The CO_2 eddy flux (F_c, μmol m^{-2} s^{-1}) was calculated by applying to Equation 2.12 the covariance between vertical wind velocity and atmospheric CO_2 content.

Filtering eddy flux data to only include values falling within the following thresholds rejected obviously spurious fluxes:

- $-150<H<1000$ W m^{-2}
- $-150<\lambda E<1000$ W m^{-2}
- $-15<F_c<15$ μmol m^{-2} s^{-1}

3.4 Errors and Corrections

Along with rejecting obviously spurious data, eddy fluxes were corrected for errors due to low friction velocity and spectral loss. Footprint analysis was also required to test for a valid source area of eddy covariance data. CO_2 flux (F_c) was also corrected for change of CO_2 storage below the measurement height, to allow estimation of net ecosystem exchange (NEE). The following sections describe these processes.

3.4.1 Change in CO_2 storage

To evaluate the significance of CO_2 flux associated with change in storage ($F_{\Delta S}$), a profile system was operated during seven Intensive Field Campaign (IFC) periods. The profile system was developed following Xu et al. (1999), to measure concentrations of CO_2 at heights of 0.25 m, 0.50 m, 1.0 m, 1.5 m, and 2.0 m. Air was sequentially drawn from each height using a system of solenoids and a sample pump (TD-4NA, Brailsford & Co., Rye, NY, USA) and a dedicated LI-6262 gas analyser (LiCor, NE, USA) measured concentrations of CO_2 and water vapour.

Following Xu et al. (1999), a large purge pump (model 7010, ASF Thomas, Puckheim, Germany) was used to continuously draw air along the three sample tubes not being measured to minimise the volume of stale air requiring transport through the LI-6262 between measurements for each height. Response times were determined following Xu et al. (1999), and sample times of 7.5 s for each height were achieved so that one cycle of sampling was completed in 30 s. Five cycles were completed so that, for each height, the mean CO_2 concentration over 2.5 min was recorded. CO_2 profiles were measured every half hour during IFC periods.

Following Hollinger et al. (1999), $F_{\Delta S}$ was calculated as

$$F_{\Delta S} = \sum_{i=1}^{n} \frac{\Delta c_{(i)}}{t} z_{(i)} \qquad \textbf{3.1}$$

Where $\Delta c_{(i)}$ is change in CO_2 concentration of the ith canopy layer over a measurement period t, $z_{(i)}$ is the thickness of the layer and n is the number of canopy layers used for computation.

Three of the IFC periods were selected for comparison (Figure 3.10a): IFC3 (24–25 May 2000) had very little wind throughout the day and night; IFC1 (24–25 March 2000) was selected as the IFC period with reasonably high daytime windspeed and the strongest windspeed throughout the night; and IFC6 (7–8 November 2000) had strong winds during the first day of the IFC, but these abated and became weak during the night. Because of their diverse windspeed variations, these three (out of the seven) IFC periods are most likely to demonstrate the significance that change in storage has on CO_2 flux measurements at Moanatuatua.

Three storage correction methods are tested:

1. No correction: F_c is CO_2 flux uncorrected for change in storage.

2. Using profile measurements: F_{cProf} is CO_2 flux corrected for change in storage using Equation 3.1.

3. Using CO_2 concentration measured at EC system sample intake height: F_{cEddy} is CO_2 flux corrected for change in storage using Equation 3.1 for a single (n=1) layer with height z = 3.5 m.

For each of the IFC periods in Figure 3.10b–d, the diurnal course of uncorrected CO_2 flux (F_c) is plotted with corrected fluxes (F_{cProf} and F_{cEddy}). All plots are indistinguishable and this suggests that $F_{\Delta S}$ is a negligible component of CO_2 fluxes at Moanatuatua.

Table 3.1 reveals that the differences between mean (averaged over the IFC period) corrected and uncorrected half hourly CO_2 fluxes are negligible. This is expected because storage within the profile equals zero over periods of a day or more (Hollinger et al., 1999) However $F_{\Delta S}$ is more important for the determination of individual half-hourly fluxes. For example, underestimation of early morning NEE estimates may occur if $F_{\Delta S}$ is ignored and this may introduce errors into models of NEE based on environmental factors such as PPFD.

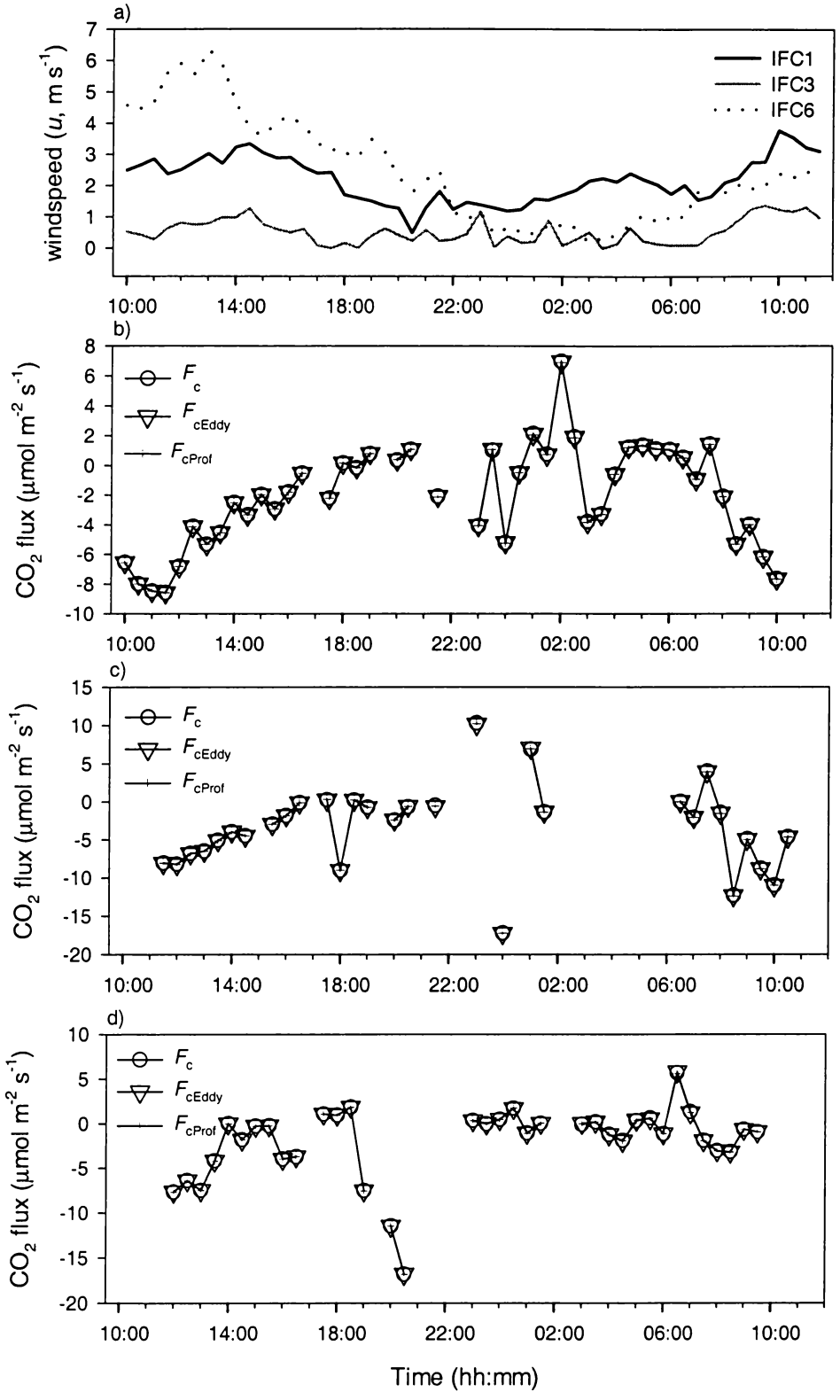

Figure 3.10 **(a)** Half-hourly mean windspeed recorded during the course of IFC periods; and **(b–d)** CO_2 fluxes where F_c is uncorrected eddy flux and F_{cProf} and F_{cEddy} are CO_2 fluxes corrected using profile system and eddy height CO_2 concentrations respectively during measured during **(b)** IFC period 1; **(c)** IFC period 3; and **(d)** IFC period 6.

The maximum contribution of $F_{\Delta S}$ to half-hourly CO_2 fluxes during each IFC is included in Table 3.1. Expressed as a percentage of the applicable corrected half-hourly flux, the maximum contribution of $F_{\Delta S}$ during all IFC periods is 5.7%. Storage corrections may be applied to all eddy fluxes (i.e. not just during IFC periods) using CO_2 concentrations measured with the eddy covariance system. With this procedure, underestimation of $F_{\Delta S}$ comprises a maximum of 2.48% of corrected CO_2 fluxes measured during IFC periods.

Table 3.1 The importance of $F_{\Delta S}$ as a component of CO_2 fluxes during IFC periods. Units are μmol m^{-2} s^{-1}. Max % error is the maximum half-hourly difference F–F_{cProf} expressed as a percentage of F_{cProf}. Spurious data were recorded during IFC5.

IFC	Max F_c–F_{cProf}	Max % error (F_c)	Max F_{cEddy}–F_{cProf}	Max % error (F_{cEddy})	Mean F_c	Mean F_{cProf}	Mean F_{cEddy}
1	0.058	0.84	0.048	0.69	-2.727	-2.734	-2.730
2	0.063	1.22	0.158	0.95	-3.728	-3.730	-3.726
3	0.079	1.14	0.101	1.46	-4.291	-4.297	-4.297
4	0.005	0.04	0.003	0.03	-5.021	-5.021	-5.021
6	0.071	5.70	0.031	2.48	-3.803	-3.809	-3.811
7	0.027	0.48	0.019	0.34	-1.837	-1.837	-1.838

The maximum $F_{\Delta S}$ contribution occurred during IFC6, when daytime windspeeds were relatively high and nocturnal winds were light. Maximum change in CO_2 storage is associated with these conditions because CO_2 concentration increases in the profile when windspeed is light, then a sudden release of CO_2 from storage occurs via morning windspeed increase. The 2.48% contribution of $F_{\Delta S}$ unaccounted for when using the eddy height CO_2 concentration occurred at 0700 hr during IFC6. This error is likely to be in the upper range for the study period because $F_{\Delta S}$ is most significant when very light nocturnal winds are followed by a flush of CO_2 in the early morning (Xu et al., 1999), and this is what happened between 0630–0700 hr during IFC6.

As a percentage, $F_{\Delta S}$ was generally a small contribution to NEE and the magnitude of $F_{\Delta S}$ determined using the profile system between 0630–0700 hr during IFC6 was only 0.16 μmol m^{-2} s^{-1}. This represents a small error compared with 3.81 μmol m^{-2} s^{-1}, which was mean half-hourly F_c for IFC6 (Table 3.1). The average maximum half-hourly $F_{\Delta S}$

contribution for IFC periods is only 1.5% of the corrected half-hourly CO_2 flux, which again suggests that $F_{\Delta S}$ is not significant.

For forests, $F_{\Delta S}$ may contribute more than 50% of total half-hourly CO_2 flux (e.g. Lee et al., 1996), which is probably due to the large canopy space. In these cases it is necessary to continuously gather profile data to determine $F_{\Delta S}$. However Greco and Baldocchi (1996) compared eddy height and profile measurements of CO_2 concentrations and justified the use of the former to determine $F_{\Delta S}$ at a temperate deciduous forest. For a Canadian peat bog, Lafleur et al. (2001) concluded that $F_{\Delta S}$ was a minor component of CO_2 exchange and measurements of CO_2 concentrations at flux measurement height were sufficient to estimate $F_{\Delta S}$.

At Moanatuatua, $F_{\Delta S}$ is very small and measurements of eddy height CO_2 concentrations were appropriately used for determining the $F_{\Delta S}$ correction to CO_2 fluxes.

3.4.2 Low friction velocity

Flux measurements during periods with low friction velocity (u^*) are known to return incomplete accounts of carbon exchange (Hollinger et al., 1999). Eddy covariance researchers often determine a threshold of u^* for each flux averaging period, so that flux data are rejected when u^* is below the rejection value. A generally accepted explanation for this phenomenon is that insufficient mixing and/or preferential flow in the stable atmosphere causes flux underestimation during conditions of low u^* (Lafleur et al., 2001). Typical friction velocity thresholds for forests range between 0.15 m s^{-1} (Hollinger et al., 1999) and 0.20 m s^{-1} (Goulden et al., 1997), while Lafleur et al. (2001) confirmed a rejection u^* threshold for the ombrotrophic Mer Bleue peatland at Ottawa, Canada of 0.1 m s^{-1}.

Hollinger et al. (1999) and Goulden et al. (1997) observed a decrease in nocturnal NEE when u^* was below the rejection threshold, while Lafleur et al. (2001) noted increased variation in NEE at low friction velocity.

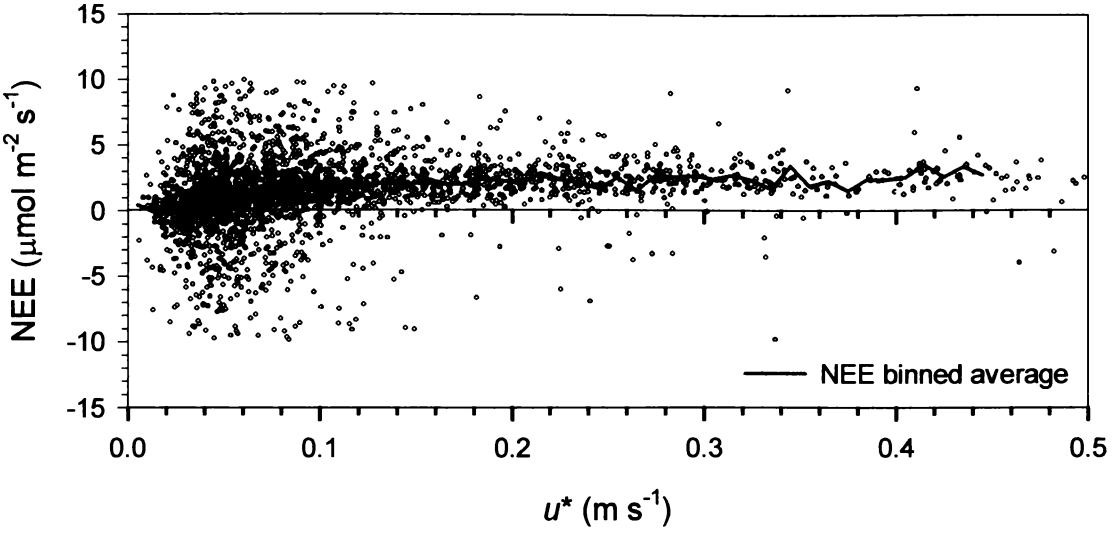

Figure 3.11 Nocturnal net ecosystem exchange (NEE, storage corrected) vs. friction velocity (u^*) for six months 1 October, 1999 – 1 April, 2000. NEE binned average indicates mean NEE averaged through u^* bins of 0.01 m s^{-1} width.

Scattered NEE at low u^* in Figure 3.11 is consistent with the results of Lafleur et al. (2001), while the decrease in binned average NEE resembles the observations of Hollinger et al. (1999) and Goulden et al. (1997). A rejection threshold was therefore chosen so that periods with $u^*<0.10$ m s^{-1} were rejected from further analysis.

3.4.3 Spectral loss

Spectral deficiencies of eddy covariance measurements are important in closed-path systems where the IRGA and sampling tube result in flux underestimation due to damping of high-frequency fluctuations (Moore, 1986). Spectral corrections were determined using the procedure of Goulden et al. (1997) and Hollinger et al. (1999).

A degraded sensible heat flux (H_f) was determined for each 30 minute period by digitally filtering the temperature signal used for calculating the sensible heat flux (H) to match the spectral response of CO_2 and water vapour signals from the LI-6262 (Figure 3.12a). Upward trending values of CO_2 spectra for frequency > 1.5 Hz (Figure 3.12a) are a result of aliasing and do not affect covariances (Hollinger et al., 1999). The ratio of uncorrected to corrected sensible heat flux, H/H_f, defines the empirical transfer function used to correct

the CO_2 and water vapour signals. H/H_f varied diurnally (Figure 3.12b) and when spurious corrections were apparent, monthly averages of the diurnal trend in H/H_f ratio were used to provide CO_2 flux corrections for applicable half-hourly periods.

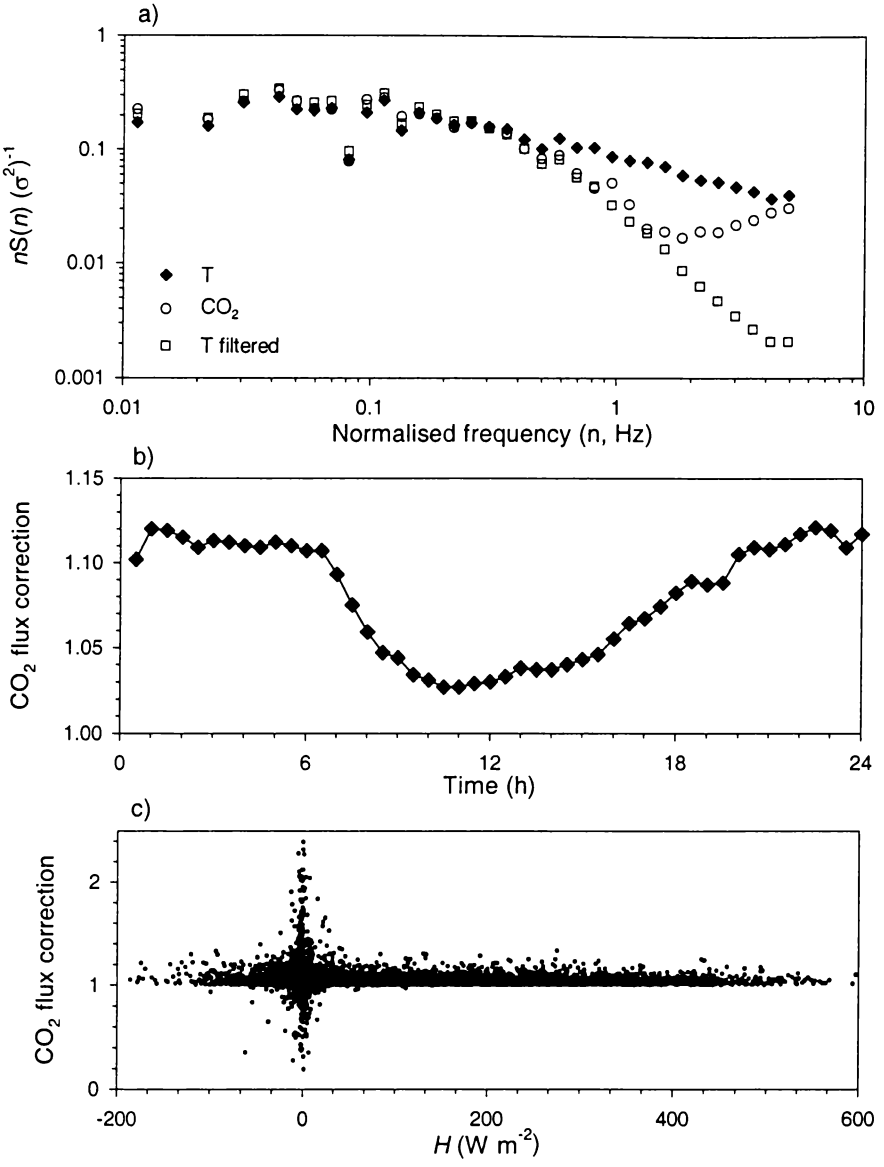

Figure 3.12 **(a)** Power spectra for temperature and CO_2 fluctuations between 1200 and 1230 hr on 6 January 1999. A lag was applied, so that the filtered temperature response approximates the CO_2 response; **(b)** Ensemble average CO_2 spectral corrections (H/H_f), averaged over half-hourly periods throughout the study period; **(c)** CO_2 spectral correction (H/H_f) versus measured sensible heat flux (H).

For CO_2, the H/H_f corrections averaged approximately 3% of uncorrected fluxes for daytime and approximately 12% for nocturnal periods (Figure 3.12b). Associated with reduced windspeeds at night time is a linear decrease of cut-off frequency at which the spectral response of CO_2 and water vapour signals is degraded (Aubinet et al., 2000). This explains the increased H/H_f corrections required for nocturnal data. Cut-off frequencies for water vapour are always lower than for CO_2 (Aubinet et al., 2000) and as a consequence the average H/H_f corrections ranged between 8% for daytime and 22% for nocturnal water vapour flux corrections.

As noted by Hollinger et al. (1999), this technique does not provide stable corrections when $H \rightarrow 0$ W m^{-2} (see Figure 3.12c). Relevant half-hourly H/H_f corrections from monthly ensembles are used to provide spectral corrections for particular half-hourly periods when $-15<H<10$ W m^{-2}.

3.4.4 Energy balance closure

The ability to close the energy balance (closure) is a common test of data quality for eddy covariance systems and may be demonstrated by plotting net radiation against the sum of λE, H, G and J (Moncrieff et al., 1997a), or calculating the closure ratio $\lambda E+H/(R_n-G-J)$.

Lack of energy balance closure is common for eddy covariance research and closure ratios range from 70-100% (Aubinet et al., 2000; Twine et al., 2000). There is no generally accepted solution to poor closure and greater than 70% closure is used as a threshold of acceptance for model validation or calibration (Kustas et al., 1991). For example, Lafleur et al. (1997) could not explain median daily closure of only 75% for a study of 126 days at a northern boreal wetland, yet seasonal trends of energy fluxes and an annual water balance were constructed from these data.

For the closed-path and open-path eddy covariance systems used at Moanatuatua, available energy (R_n-G-J) is plotted against the sum of λE and H in Figure 3.13. Using the LI-6262 for determination of λE, the slope of the regression line in Figure 3.13a was 0.89 with r^2=91%. However the offset of the regression line in Figure 3.13a was –65 W m^{-2}, so that mean closure ratio with 95% confidence interval was 79.1 ±0.5% which is within

the generally accepted range for eddy covariance research, but indicates errors exist in the energy flux terms.

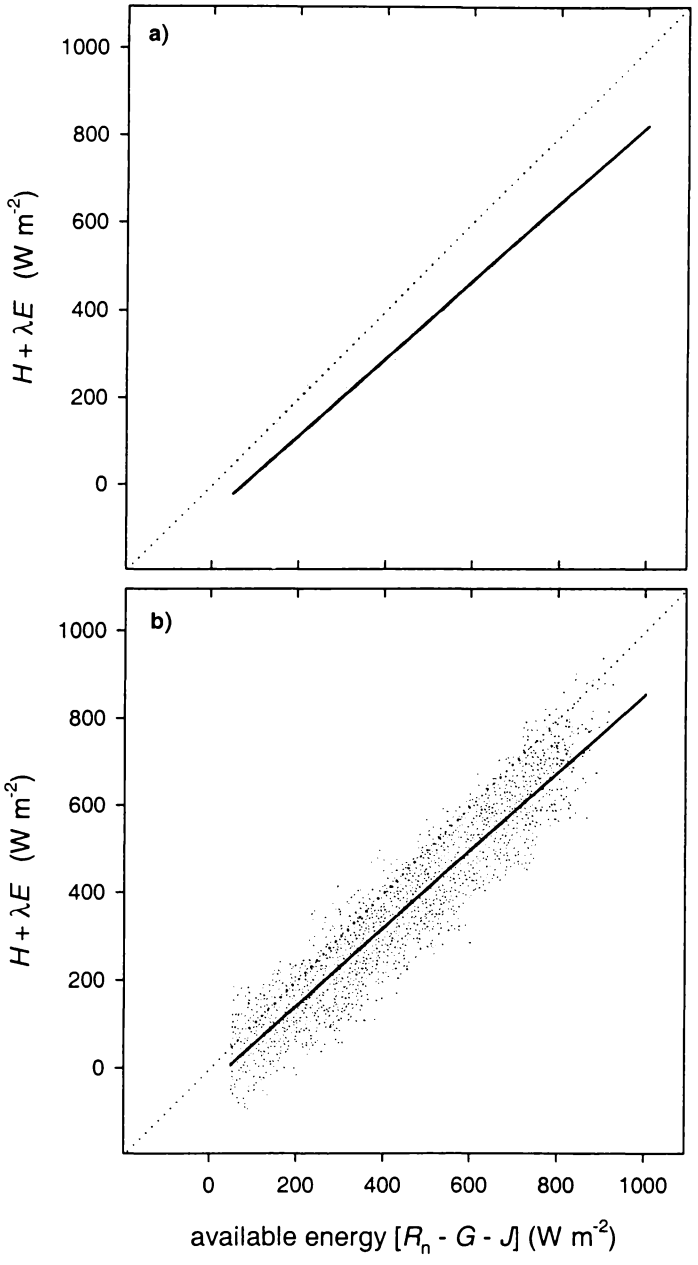

Figure 3.13 Energy balance closure with linear regression (solid line) at Moanatuatua. Data are half-hourly values filtered to exclude small values of net radiation (R_n<50 W m^{-2}). The plots are identical except for the measurement of λE, which was determined using **(a)** LI-6262 closed path gas analyser (y = -65+0.89x, r^2=0.91); and **(b)** open path KH2O (y = -37+0.89x, r^2=0.93). Dotted line is one–one line.

Poor closure may be due to errors exclusive to the closed path system such as miscalculation of signal delay due to transit time in the sample tube, or to mixing and smearing of air within the sample tube causing attenuation of frequency resolution of H_2O measurements. To test this hypothesis, closure was investigated after using KH2O data for calculating λE (Figure 3.13b).

Using data from the open path instrument to determine λE, the slope of the regression line in Figure 3.13b was 0.89, the same as the slope in Figure 3.13a, however the offset was improved to –37 W m^{-2} (r^2=93%). The improved offset increased the mean closure ratio to 83% (±0.4%, α=0.05) when the open path instrument was used to determine λE, however a large unresolved closure error of 17% remains. Some of the closure error may therefore be explained by deficiencies in the closed path system, but a significant closure gap remains that cannot be attributed to the closed path method of water vapour measurement *per se*.

Aubinet et al. (2000) report that closure for six EUROFLUX sites ranged from 0.7 to full closure, and note that for eddy covariance research there is generally a "common observation that the energy balance is more or less unclosed". While Twine (2000) suggests forcing closure upon energy balance components in a manner that maintains the Bowen ratio, the assumption that β is preserved for eddy covariance measurements has not been validated.

Therefore the generally accepted approach for eddy covariance research is adopted here: the lack of closure is acknowledged but unable to be completely explained.

3.4.5 Footprint analysis

Interference from mast and hut

To minimise systematic error from the EC mast interrupting air flow to the instruments, the mast was positioned southeast of instrumentation because past research indicated this was the least frequent wind direction (Thompson et al., 1999). To test for flux interference generated by the mast or hut during southeast winds, the energy balance closure ratio, $\lambda E+H/(Rn-G-J)$, is averaged through bins of 20° wind direction (Figure 3.14). Closure

ratio is consistent for all wind directions which indicates the mast configuration is not a source of error.

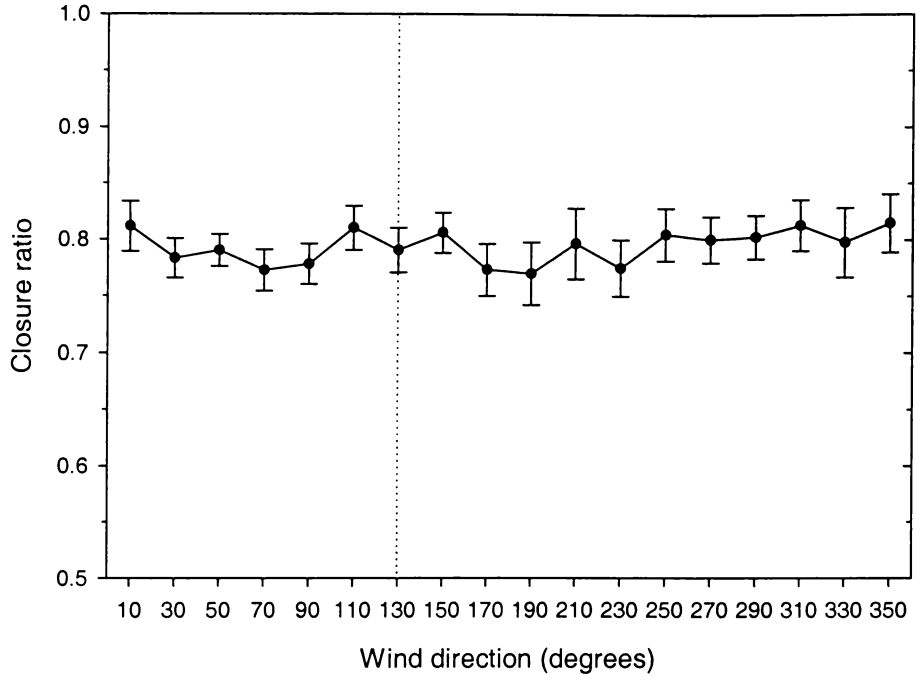

Figure 3.14 Energy balance closure ratio ($(\lambda E + H)/(R_n - G - J)$) versus wind direction for daylight data with windspeed >0.2 m s^{-1}. Data points are means for bins of 20° wind direction, with error bars showing 95% confidence intervals. Vertical dotted line indicates windward direction of mast and hut behind EC instrumentation.

Flux source area

The EC site was located so that distance to the eastern border of the bog was 290 m (Figure 3.2) but a greater distance of 360 m to the western border ensured larger fetch in the direction of prevailing westerly winds. To estimate the spatial representativeness of measured fluxes, the relative flux contribution as a function of fetch (the 'footprint') was determined following Schuepp et al. (1990). The Obukhov length (L, dimensionless) was used as a stability parameter following Schmid (1994) so that $z/L>0$ (where z is height difference between measurement and zero plane displacement heights) defines stable conditions and $z/L<0$ indicates an unstable boundary layer. Figure 3.15 shows two examples of footprints for half hourly periods with stable and unstable conditions.

With unstable conditions at 13:30 hr, 4 December 2000, the upwind distance to which flux measurements are most sensitive (x_{max}) was 17.3 m (Figure 3.15). This means that the flux source area was concentrated at approximately 17 m from the EC mast for this half hour. Under stable conditions at 21:00 hr, 6 November 2000, the source area was extended and x_{max} increased to 38.6 m.

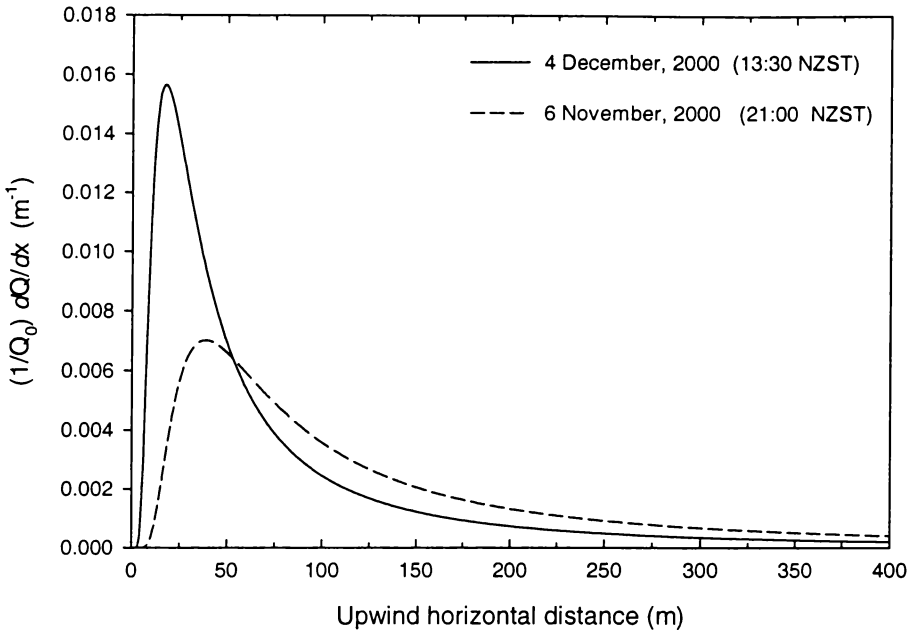

Figure 3.15 The flux footprint (relative flux contribution as a function of distance from the measurement position) for two half hourly periods: 13:30 hr, 4 December 2000 with unstable conditions and 21:00 hr, 6 November 2000 with stable atmospheric conditions.

The upwind distance to which 80% of convective fluxes are sourced (x_{80}) is commonly used as a test for adequate fetch distance (e.g. Aubinet et al., 2000; Blanken et al., 2001; Thompson et al., 1999). The plots in Figure 3.15 were chosen to demonstrate footprints approaching maximum x_{80} for the study period. With unstable conditions x_{80} was 155 m at 13:30 hr, 4 December 2000 and did not exceed 158 m throughout the study period (Figure 3.16a). Fetch is therefore validated for unstable conditions.

With stable conditions at night, x_{80} sometimes increased to over 300 m, exceeding the distance to the eastern and western boundaries. For example at 21:00 hr, 6 November 2000, x_{80} was 346 m. Wind direction was from the southwest so x_{80} did not exceed the fetch distance of over 1000 m in this direction. Fetch is adequate for all x_{80} under stable conditions except when wind is from the easterly quarter with x_{80}>290 m, or from the

westerly quarter with x_{80}>360 m. Fortunately this is a rare phenomenon (Figure 3.16b), with x_{80} exceeding the distance to the bog perimeter on 4.3% of half-hourly periods with stable conditions. This represents only 0.83% of all half-hourly periods with good quality flux data and is so rare that fetch is considered adequate for the entire study period.

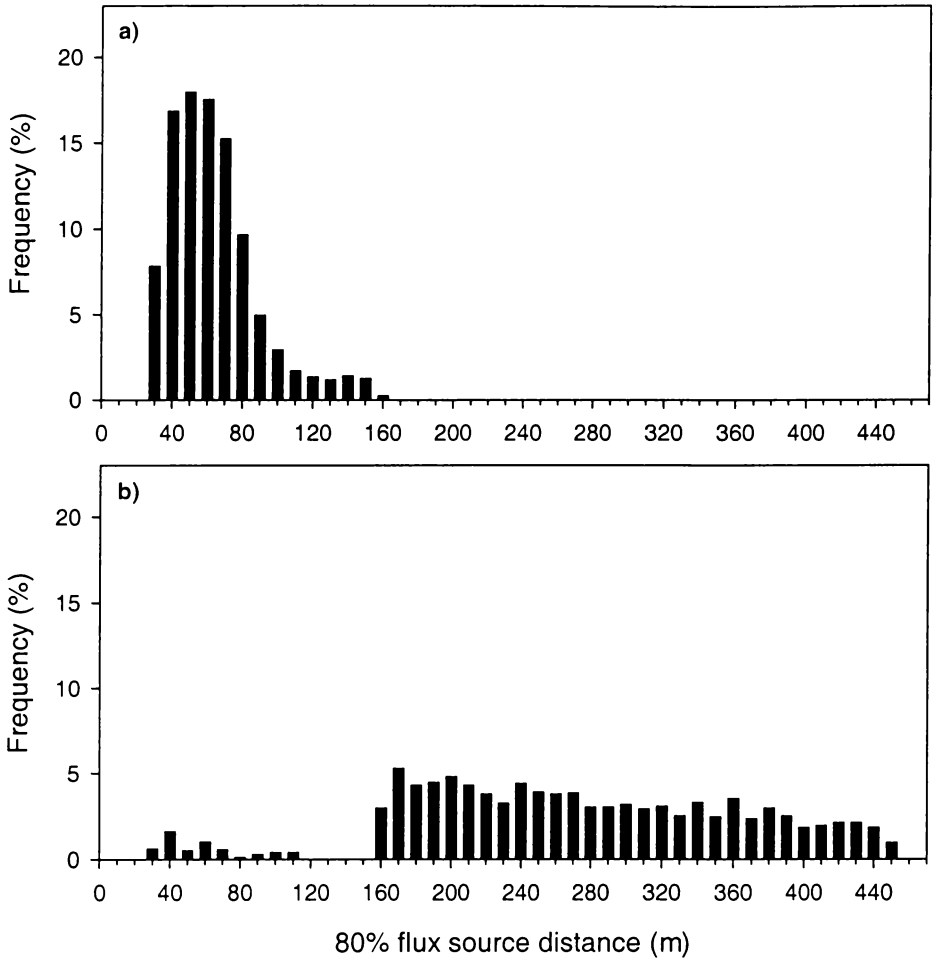

Figure 3.16 Frequency histograms of horizontal position of distance for 80% of cumulative footprint (x_{80}) under **(a)** unstable atmospheric conditions and **(b)** stable conditions.

3.5 Additional Measurements

3.5.1 Chamber measurements of respiration

Peat respiration measurements were made along two perpendicular transects near the EC site, at 3–6 weekly intervals from September 1999 and more frequently during the six

intensive field campaigns (IFC). Ten sampling sites were randomly chosen along a total distance of 110 m and a random distance up to 1 m from the edge of the transect. At each site a PVC collar was installed to a depth of 100 mm, with 10 mm above the surface as an interface for chamber measurements (Figure 3.17).

Figure 3.17 PVC collar inserted to a depth of 100 mm for chamber measurements of respiration from the peat surface.

The LI-6200 portable gas analyser with LI6000-09 chamber measurement system (LiCor, NE, USA) was used on the collars to measure fluxes of CO_2 from the peat surface. This system is described in the LI6000-09 manual and by Norman et al. (1997). CO_2 zero calibration was undertaken before every sampling cycle by scrubbing the sample air with soda lime. The instrument was also calibrated approximately every 3–4 months with a commercial span gas of known concentration. A foam gasket prevented leaks at the interface between chamber and collar.

After placing the chamber on a collar, the CO_2 concentration was drawn down to about 20 $\mu mol\ mol^{-1}$ below ambient concentration. The CO_2 concentration was measured five times over 5 $\mu mol\ mol^{-1}$ concentration increments to determine the flux of CO_2. Post-processing

of respiration data involved averaging measurements from the ten sample sites to obtain a spatial average of respiration from the peat surface (R_s, μmol m^{-2} s^{-1}).

3.5.2 Other measurements of peat properties

Ground heat flux (G, W m^{-2}) was measured with a soil heat flux plate (HFT3, Radiation and Energy Balance Systems, Seattle) at 3 cm depth. One soil heat flux plate was considered sufficient because Thompson et al. (1999) observed very small G at Moanatuatua: accounting for only 3% of midday R_n. Because G is such a small energy balance term, error caused by spatial variation of G will have a negligible influence on the energy balance.

Peat temperature was measured at 8 cm and 30 cm depths with two Campbell Scientific Inc. (CSI) 107B probes. Volumetric soil moisture content (θ_v, cm^3 cm^{-3}) was measured with a CS615 (CSI) reflectometer probe, inserted at an angle to give a vertical spatial average over the upper 100 mm of the peat profile. θ_v was corrected for temperature effects as described in the CS615 manual and a calibration polynomial (Laybourne, 2000) was used to account for the altered response of the instrument in organic peat.

3.5.3 Radiation measurements

Net radiation (R_n, W m^{-2}) was measured on a dedicated mast, 7 m east of the EC mast, at 3.5 m height with a net radiometer (Q6.7.1, Radiation and Energy Balance Systems, Seattle). R_n data were corrected for errors generated by windspeed variability (CSI, 1996). Incoming solar radiation ($K\downarrow$) was measured with a pyranometer (SR200, LiCor, NE, USA) mounted above the EC hut. Mounted adjacent to the SR200 was a LI-190SZ (LiCor, NE, USA) quantum sensor that measured photosynthetic photon flux density (PPFD, μmol m^{-2} s^{-1}): solar energy within the spectrum of photosynthetically active radiation (PAR, 0.4–0.7 μm) (Oke, 1990, pg.118).

3.5.4 Other meteorological instrumentation

Air temperature and vapour pressure were measured at 3 m height on the EC mast with a relative humidity sensor (HMP-35C, Vaisala Inc., Helsinki, Finland). Ambient air pressure was measured with a barometer (PCB220, Vaisala Inc., Helsinki, Finland) in the hut.

Windspeed and direction were measured with a cup anemometer and windvane (models A101M and W200P respectively, Vector Instruments, Denbighshire, N.Wales, UK) mounted at 3.5 m height, 6 m south of the EC mast.

Precipitation was measured with a tipping bucket raingauge (OTA, model OSK 15180–T) mounted at approximately 1.2 m height. Each tip of the raingauge buckets was equivalent to 0.2044 mm of rainfall. Water table elevation was measured and recorded with a capacitance probe (model 392, Dataflow Systems Pty Ltd. Eumundi, QLD, Australia) located near the EC hut. Calibration of the capacitance probe was conducted prior to installation. An adjacent dipwell facilitated manual measurement of depth to water table for quality control.

Leaf wetness sensors similar to the CSI model 237 were constructed and used to measure an index of canopy wetness. Sensors were constructed of a fine stainless steel wire grid attached to cotton muslin, supported on a frame of similar size and shape to a fly swat. Connected to a CR10X (CSI) datalogger, a 25 mV excitation voltage was applied to the sensors and the output voltage was recorded. The resistance of the sensor was reduced when the cotton was wet and the variation of output voltage relative to the excitation voltage was used as an index of wetness, with 100 indicating 100% wetness and 0% is fully dry.

3.6 Summary

Fluxes of water vapour and CO_2 were measured at Moanatuatua Scientific Reserve between 15 December 1998 and 15 December 2000. The field site, vegetation and climate regime at Moanatuatua were described.

The primary method of flux measurement was the eddy covariance system. A CSAT3 sonic anemometer measured virtual temperature and 3-dimensional components of windspeed at 10Hz sampling frequency. A closed path gas analyser made high frequency measurements of CO_2 and water vapour concentrations, while an open path fast response hygrometer mounted next to the CSAT3 provided a second method for determining fluxes

of water vapour. Issues and corrections required with the EC system were attended to, along with verfication that data quality meets generally accepted standards.

Energy balance closure ratios were 0.79 and 0.83 for the closed–path and open–path eddy covariance systems respectively. Lack of energy balance closure is common for eddy covariance measurements and the closure ratios of 0.79 and 0.83 for this research are above 0.70, which is the generally recognised threshold of acceptance (Aubinet et al., 2000; Kustas et al., 1991; Twine et al., 2000). Footprint analysis showed that the source area for flux measurements extended beyond the bog perimeter for only 0.83% of half-hourly periods when good quality data were obtained. Fetch is therefore considered adequate for the entire study period.

A portable gas analyser with chamber system was used to measure fluxes of CO_2 from the peat surface and a suite of meteorological supporting measurements were also described in this chapter.

4 Energy Balance and Evaporation

4.1 Introduction

This chapter provides a multi-year investigation of energy balance phenomena at a restiad bog that have previously been observed only during summer periods. Objectives of this chapter are to:

1. Investigate controls on evaporation at diurnal–annual timescales
2. Test models of evaporation that have been developed using data collected at Moanatuatua over summer
3. Describe the annual water balance at Moanatuatua.

4.2 Energy Partitioning

Previous research during summer at Moanatuatua by Thompson et al. (1999) reports evaporation rates of 2.9 mm day^{-1} with energy balance partitioning favouring the sensible heat flux. Bowen ratios (β) of 2 were common for dry canopy periods, whereas wet canopy conditions increased the importance of the latent heat flux (λE). This section extends Thompson et al.'s (1999) investigation of summer time energy balance partitioning at Moanatuatua by considering these dynamics throughout the year and reconfirming the analysis.

4.2.1 Diurnal energy balance

Summer energy balance partitioning

Figure 4.1 compares energy balance components during three days in November 1999 with contrasting states of canopy wetness and sky conditions. Mainly clear sky conditions prevailed on 19 November 1999 and leaf wetness sensors showed that the entire canopy was wet in the morning, with the upper canopy completely dry by 0800 hrs and the entire canopy had dried by mid afternoon (Figure 4.2).

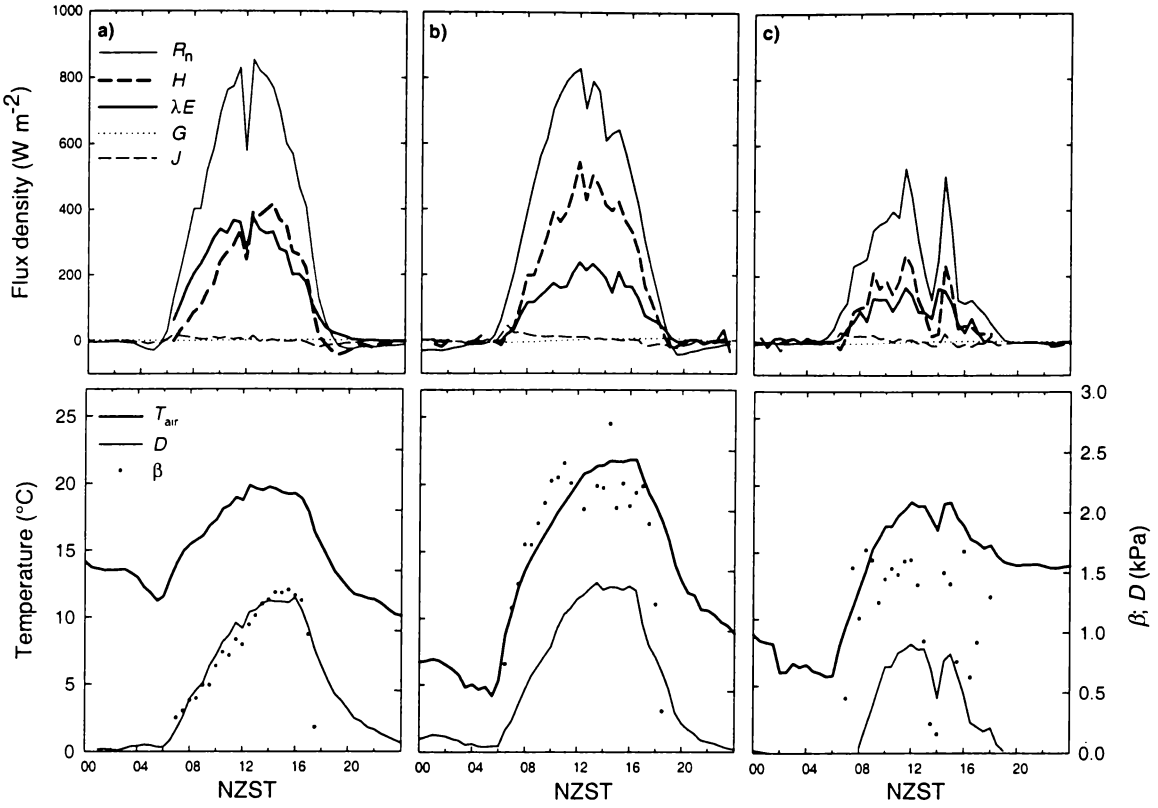

Figure 4.1 Diurnal courses of energy balance components, air temperature (T_{air}), saturation vapour pressure deficit (D) and Bowen ratio (β) for **(a)** 19 November 1999 with wet canopy in the morning and completely dry canopy by mid afternoon; **(b)** 23 November 1999 with completely dry canopy; and **(c)** 24 November 1999 with dry canopy.

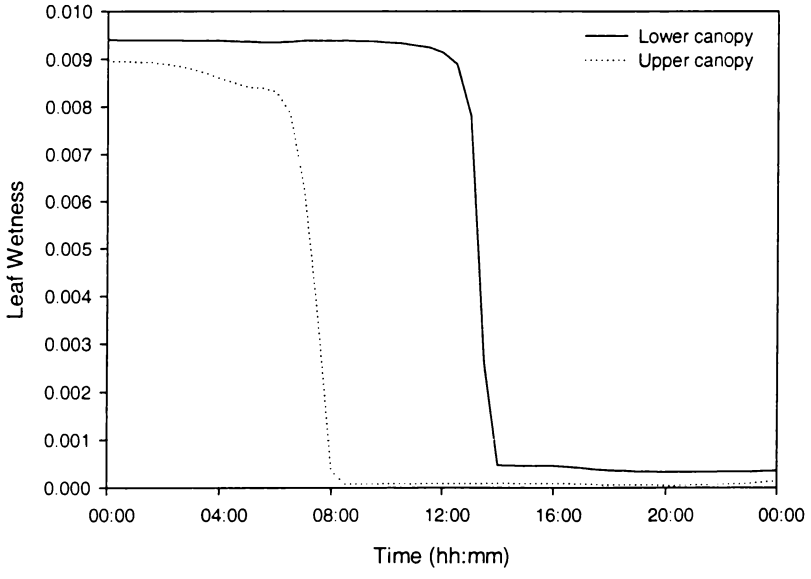

Figure 4.2 Leaf wetness index for 19 November 1999. Sensors were placed at 1.5 m and 0.5 m in the *Sporodanthus* canopy with an index less than 0.001 identifying a dry sensor (indicated by solid grey line). The mid canopy sensor was not performing on this day.

With abundant canopy moisture and R_n, λE proceeded strongly in the morning and Bowen ratios (β) were less than unity until midday (Figure 4.1a). After the canopy had dried at midday H became the dominant flux. Declining R_n later in the afternoon limited H and restricted the maximum β to 1.3 for the day. G was negligible and peaked at only 23.5 W m^{-2} throughout the entire study period. Thompson et al. (1999) also observed insignificant G at Moanatuatua, which they attributed to the dense canopy impeding solar radiation from reaching the peat surface.

Following Thompson et al. (1999), change of canopy sensible heat storage (J) may be calculated as

$$J = m\frac{\Delta T}{t}\rho_{\text{can}} \qquad \textbf{4.1}$$

where m is the thickness of the canopy, ΔT is the change in canopy air temperature (assumed from measurements of air temperature at 3.5 m height) over measurement period t and ρ_{can} is canopy dry density. At Moanatuatua, Thompson et al. (1999) note that canopy sensible heat storage is a small energy balance term. Figure 4.1 confirms this observation, with small values of J that peak in the morning compared with the late afternoon peak for G.

Figure 4.1b shows that during 23 November 1999, sky conditions and D were similar to 19 November 1999, however the canopy was dry for the entire daylight period. Under these conditions H dominated the exchange of convective energy and β exceeded 2.0 for most of the daylight period. While D was similar for the two days, the increased sensible heat flux on 23 November 1999 is reflected in higher daytime air temperatures (T_{air}). Peak λE on 23 November 1999 (Figure 4.1b) was 45% smaller than during 19 November 1999 (Figure 4.1a) while maximum H was 15% larger on the latter (dry canopy) day.

Large β on dry canopy days have been observed during previous summertime research at Waikato restiad bogs and explained by plant physiological control of transpiration and restriction of evaporation from the peat surface by the dense canopy structure (Campbell and Williamson, 1997; Thompson et al., 1999).

The effect of cloudy sky conditions on the energy balance has also been observed during summer at Moanatuatua (Thompson, 1997). Reductions of λE, T_{air} and D as a consequence of decreased R_n under cloudy skies were observed by Thompson (1997) and the cloudy day data plotted in Figure 4.1c are consistent with this. Compared with Figure 4.1b, midday β is reduced under cloudy conditions in Figure 4.1c and D is also considerably smaller during the cloudy day.

Winter energy balance partitioning

For comparison of winter and summer energy partitioning, Figure 4.3 displays diurnal courses of energy balance components for two clear sky days with dry canopy conditions. Figure 4.3a displays data collected on 7 July 2000 when R_n peaked at just 345 W m^{-2}. The summer day selected for comparison (7 February 2000, Figure 4.3b) has maximum R_n of 800 W m^{-2}, with energy partitioning and climate characteristics similar to the clear sky data plotted in Figure 4.1b and described above.

The energy partitioning dynamics for the winter day are similar to those previously described for cloudy periods, with reduced evaporative demand, lower T_{air}, β and D in Figure 4.3a than in Figure 4.3b. As with Figure 4.1, G and J are small components of the energy balance for both winter and summer days in Figure 4.3.

In winter the proportion of available radiation used for evaporation is increased, with the daily average ratio $\lambda E/R_n$ being 0.64 for 7 July 2000 and 0.34 for the summer day 7 February 2000. The summer day average $\lambda E/R_n$ ratio of 0.34 accords with Thompson's (1997) observation of average $\lambda E/R_n$ ratio of 0.35 for 17 summer days in 1996. Thompson (1997) also reported $\lambda E/R_n$ ratio of 0.40 for a cloudy day, of which the $\lambda E/R_n$ ratio 0.38 for cloudy day 25 November 1999 is consistent (Figure 4.1c). However, $\lambda E/R_n$ ratio for the winter day 7 July 2000 is considerably greater at 0.64.

This means that while R_n for the winter day in Figure 4.3a is similar to the cloudy day in Figure 4.1c, the proportion of energy used for evaporation is significantly greater during the winter day. Thompson (1997) concludes that restiad plants have an important role in restricting water loss when evaporation demand is high, however this characteristic is less

important on cloudy days when evaporation demand is lessened. Along with $\lambda E/R_n$ ratio being 50% greater, β was reduced, peaking at unity for the winter day compared to 1.5 on the summer cloudy day in Figure 4.1c. An implication of this is that stomatal control of evaporation may be less important in winter, with evaporation limited more by radiation availability.

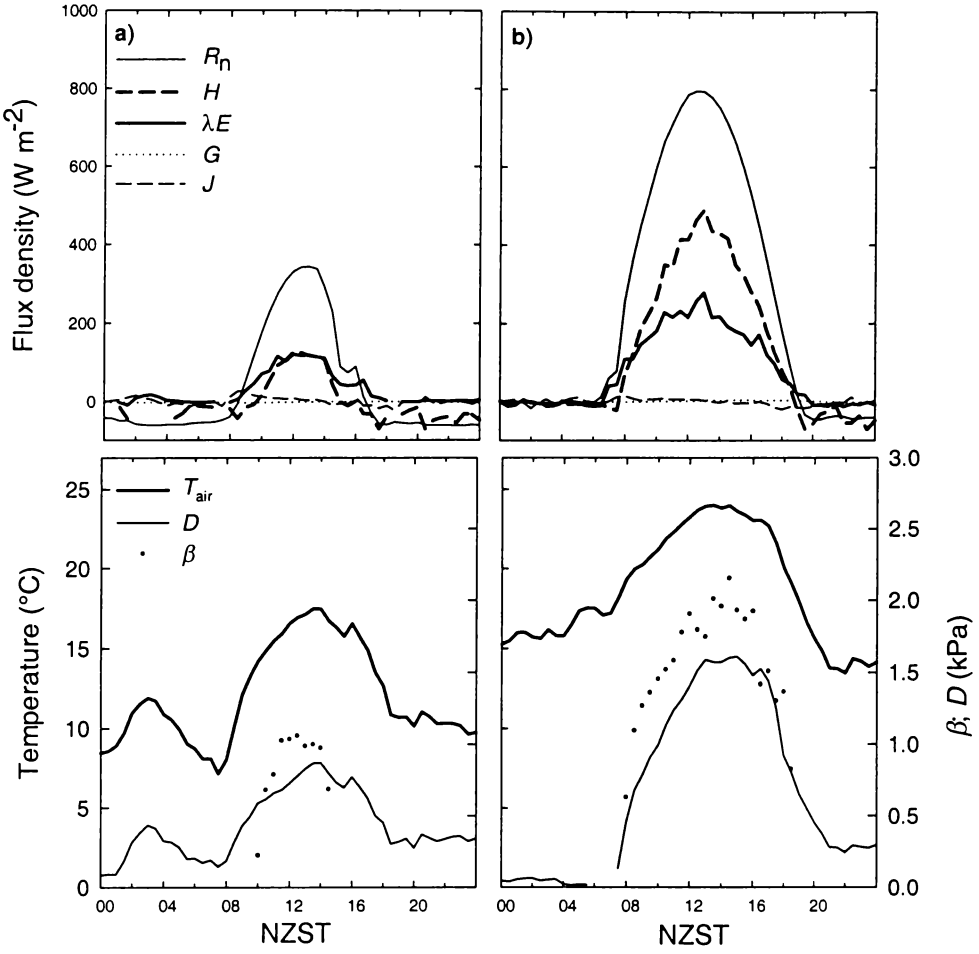

Figure 4.3 Diurnal courses of energy balance components, air temperature (T_{air}), saturation vapour pressure deficit (D) and Bowen ratio (β) for two days with completely dry canopy: **(a)** winter day 7 July 2000; and **(b)** summer day 7 February 2000.

This hypothesis is confirmed by plots of diurnal ensemble averages of energy balance components in Figure 4.4. The ensemble average energy balance plot in Figure 4.4a is for data collected during dry-canopy periods in December 1999 and 2000, replicating Thompson's (1997) average diurnal course of dry-canopy energy flux components for 17 days in December 1995.

Figure 4.4a shows maximum ensemble average R_n and λE for dry-canopy periods in December are 610 W m^{-2} and 196 W m^{-2} respectively, with H dominating the daylight flux and effecting median β of 1.36. In contrast, dry-canopy ensemble averages for July reveal maximum R_n and λE are almost halved at 327 W m^{-2} and 109 W m^{-2} respectively (Figure 4.4b). At 129 W m^{-2}, maximum H in July is more than 50% less than the December maximum of 310 W m^{-2} and accordingly, average β is reduced to 0.73 for July. Half-hourly average Bowen ratios in winter barely exceed unity and for only two hours at midday in July, while λE dominates the energy fluxes in the morning and later in the afternoon (Figure 4.4b). Conversely, mean H in December is significantly larger than mean λE for ten half-hour periods (α=0.05) and β peaks at 1.7.

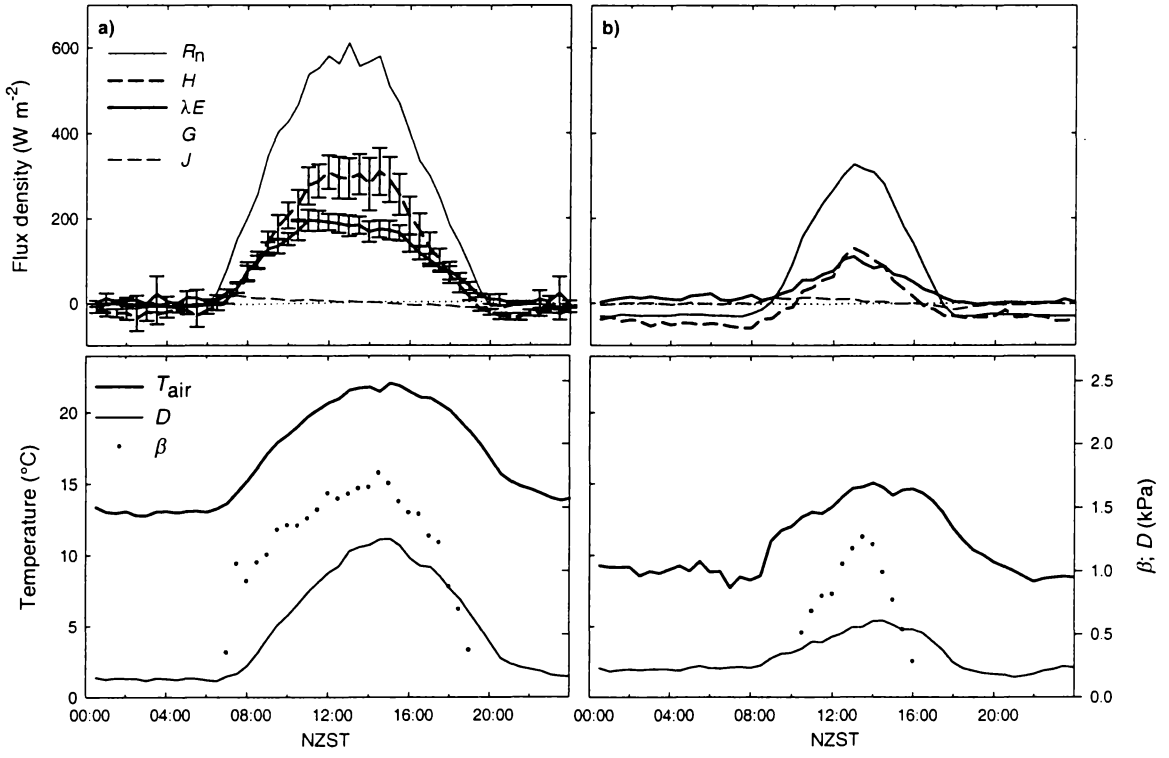

Figure 4.4 Monthly ensemble averages for **(a)** December 1999 & 2000 and **(b)** July 1999 & 2000, of half-hourly energy balance components, air temperature (T_{air}), saturation vapour pressure deficit (D) and Bowen ratio (β, dimensionless) for periods with completely dry canopy. Error bars show 95% confidence intervals in **(a)** but are omitted from **(b)** where there was no significant difference between H and λE for any half-hourly period.

An interpretation is that during winter the net radiation and evaporative demand are insufficient to force plant physiological restriction of transpiration and λE is controlled

more by availability of radiation than in summer. With different energy balance dynamics between summer and winter, there may be implications for the utility of models of evaporation developed exclusively from summer data.

Following the research of Thompson et al. (1999), Grimshaw (2000) used simple models of daily evaporation based on equilibrium evaporation (E_{eq}) to construct an annual water balance for Moanatuatua. Using data collected over summer, Thompson (1997) found the relatively more complex Penman Monteith models to be less appropriate for modelling daily evaporation than simple energy based models. While varying states of canopy wetness can confound models at the diurnal scale (Thompson, 1997), on a daily basis evaporation has been modelled as $0.80E_{eq}$ or $0.58E_{eq}$ for wet and dry days respectively (Grimshaw, 2000).

The following section tests this approach by comparing modelled evaporation with measured evaporation from the two years of eddy covariance measurements.

4.2.2 Modelling Latent Heat Flux

The utility of models of λE includes construction of annual water balances using basic meteorological records in the absence of more expensive eddy covariance data (e.g. Grimshaw, 2000). Even when eddy covariance measurements have been made, spurious and discontinuous data require replacement with modelled values for gap-filling. During the two year period 15 December 1998 – 15 December 2000 of this project, 36% of daytime λE data are missing or spurious and require modelled estimates.

Thompson (1997) determined that an equilibrium-based model provided better estimates of daily evaporation than the Penman-Monteith model due to the importance of net radiation in driving evaporation at this time scale. At diurnal time scales the Penman-Monteith equation (Equation 2.13) provided Thompson (1997) with the most realistic model of evaporation. Thompson (1997) derived r_c from relationships with D under dry and wet canopy states (r_c=187D-106 and r_c=92D-28 respectively) and r_a was determined using Equation 2.14.

Lafleur et al. (1997) used a different modelling approach to replace missing eddy covariance data by estimating β from temperature and vapour pressure and combining this

with measurements of net radiation. An alternative gap filling approach uses mean diurnal values for particular time periods based on previous and subsequent days, however it is preferred to use environmental variables such as R_n and D to estimate missing energy fluxes (Falge et al., 2001b).

Models for gap filling

To ascertain the most appropriate model for gapfilling the eddy covariance measurements, evaporation estimates determined using the Penman-Monteith (P–M) and equilibrium-based (P–T) models defined by Thompson (1997) and Thompson et al. (1999) are compared with measured evaporation during the days previously used in Figure 4.1. The following equations provide a list of the models to be tested, with further details provided in Table 4.1

$$E_{PT} = \frac{1}{\lambda}\left(0.80E_{eq}\right) \qquad \textbf{4.2}$$

$$E_{PT} = \frac{1}{\lambda}\left(0.58E_{eq}\right) \qquad \textbf{4.3}$$

$$E_{PM} = \frac{1}{\lambda}\left(\frac{s(R_n - G) + \rho c_p D / r_a}{s + \gamma(1 + r_c / r_a)}\right) \text{ where } r_c = (187D) - 106 \qquad \textbf{4.4}$$

$$E_{PM} = \frac{1}{\lambda}\left(\frac{s(R_n - G) + \rho c_p D / r_a}{s + \gamma(1 + r_c / r_a)}\right) \text{ where } r_c = (92D) - 28 \qquad \textbf{4.5}$$

$$E_{PM} = \frac{1}{\lambda}\left(\frac{s(R_n - G) + \rho c_p D / r_a}{s + \gamma(1 + r_c / r_a)}\right) \text{ where } r_c = (23D) + 9 \qquad \textbf{4.6}$$

Table 4.1 Details of models currently used to estimate evaporation at Moanatuatua. The reference equations may be consulted for descriptions of model components. Penman–Monteith models used for wet– and dry–canopy conditions are distinguished by the equation used to derive r_c from D.

Equation number	Reference Equations	Model application	Reference
4.2	2.16	Equilibrium-based model for wet canopy conditions	(Grimshaw, 2000)
4.3	2.16	Equilibrium-based model for dry canopy conditions	(Grimshaw, 2000)
4.4	2.13, 2.14	Penman-Monteith model for dry canopy conditions.	(Thompson, 1997)
4.5	2.13, 2.14	Penman-Monteith model developed for wet canopy conditions at Moanatuatua	(Thompson, 1997)
4.6	2.13, 2.14	Penman-Monteith model developed for wet canopy conditions at Kopouatai wetland	(Thompson, 1997)

These models use different parameters for dry and wet canopy states, with the latter condition distinguished by any of the leaf wetness sensors recording greater than 10% wetness. Firstly then, the P–M and P–T models were qualitatively tested against diurnal measurements of evaporation for several days (Figure 4.5). Wet and dry canopy half hourly periods were identified using leaf wetness sensor data and the selected days include dry and drying canopy conditions during clear sky and cloudy sky periods.

On 19 November 1999 the leaf wetness sensors indicate the canopy was drying until mid-afternoon when the sensors were completely dry (Figure 4.2). Dry canopy conditions prevailed during the remaining daytime periods in Figure 4.5 except for the afternoon of 22 November when 1 mm of precipitation wetted the canopy after 1500 hours.

Figure 4.5a compares measured evaporation with estimates from the Penman–Monteith ($P–M_1$) equation defined by Thompson (1997). The $P–M_1$ model underestimated evaporation on November 19th and tended to overestimate during morning periods when the canopy was dry. The overestimation may be a consequence of the dry canopy r_c being underestimated by the model. Figure 4.5b shows that underestimation of P–M evaporation on November 19th was corrected by replacing the r_c equation for wet canopy conditions with the (r_c =23D +9) model that Thompson (1997) derived for Kopouatai peat bog. Attempting to mitigate the overestimation of dry canopy evaporation by using the Kopouatai dry canopy r_c model was a failure and only accentuated the errors (not shown).

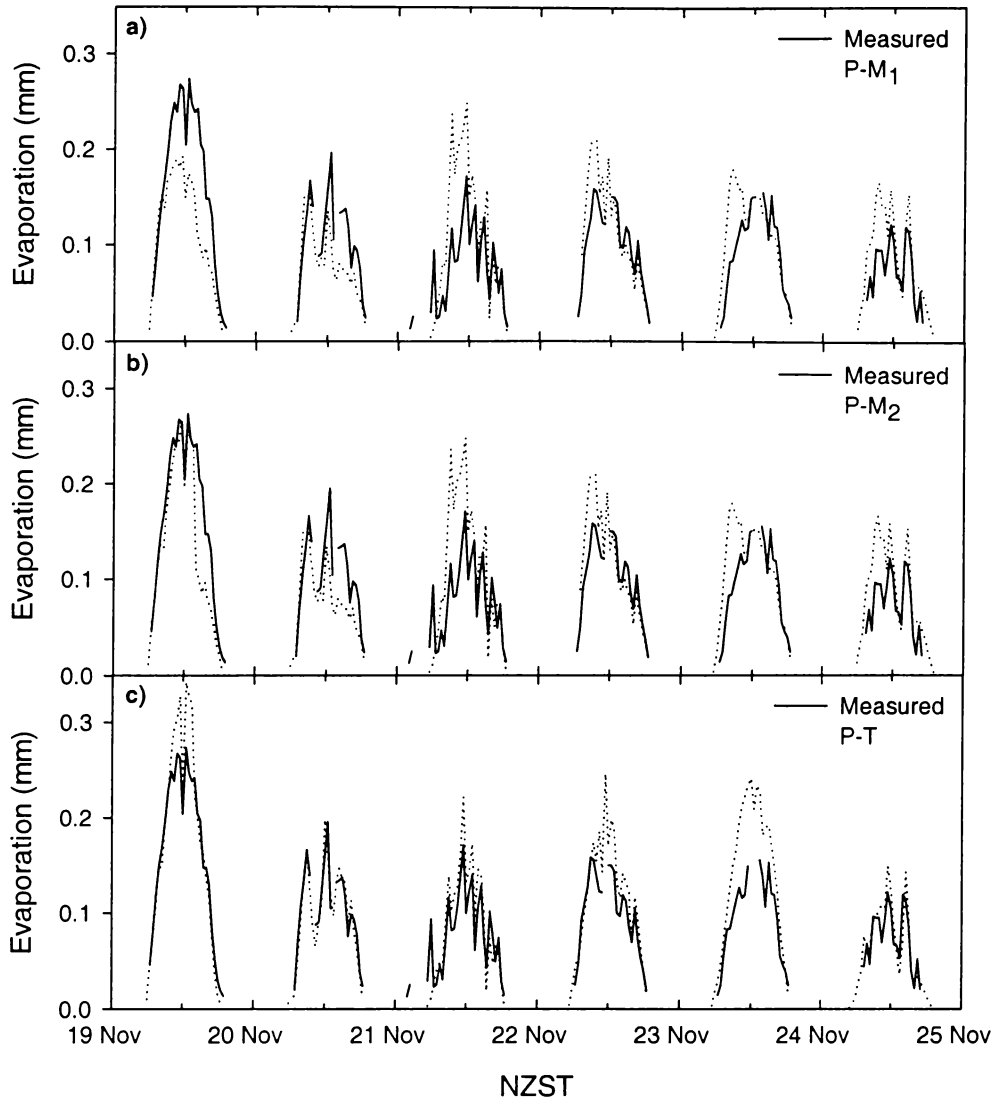

Figure 4.5 Measured and estimated evaporation for half-hourly periods on selected days 19–25 November 1999 that include the days plotted in Figure 4.3. Estimated evaporation is determined using **(a)** P–M_1: Penman-Monteith model with r_c=187D-106 and r_c=92D-28 for dry and wet canopy states respectively, **(b)** P–M_2: Penman-Monteith equation using dry-canopy model as in (a) and wet-canopy model of r_c=23D+9 developed for Kopouatai, and **(c)** P-T: equilibrium–based model.

Adopting a pragmatic approach, the Kopouatai wet canopy model of r_c will be used for P–M evaporation estimates when the canopy is not completely dry because it performs better than the wet canopy r_c model derived for Moanatuatua.

The Priestley-Taylor equation provided very reasonable estimates of evaporation apart from occasional overestimation (Figure 4.5c). The overestimation errors invariably

occurred between 1000–1500 hours when β was greater than unity and are most significant between 1030–1630 hrs on 23 November when β exceeds 2.0. This is probably due to failure of the P–T model to account for stomatal regulation of evaporation during periods that are readily identified by H overwhelmingly dominating the convective flux (refer to Figure 4.1). At all other times the P–T model provides reliable diurnal estimates of evaporation.

Models for annual water balance construction

Leaf wetness measurements were made during this project, however these data are not usually recorded at meteorological stations. For future modelling of evaporation in the absence of leaf wetness data, an index of canopy wetness is proposed here. The index is a modified version of Woods and Rowe's (1996) antecedent precipitation index (API) that was originally used to estimate the moisture condition of a catchment prior to storm events. Driving variables of the API are total rainfall and time since the occurrence of previous storms.

Because intercepted rain water evaporates faster than the soil moisture indexed by Woods and Rowe (1996), the API here only considers precipitation events up to 48 hours preceding the index (reference) time and the equation uses an exponential function for the denominator:

$$\mathrm{API} = \sum_{i=1}^{96} \frac{P_i}{1.104 \times 1.024^i} \qquad \textbf{4.7}$$

where P_i is precipitation on the ith 30min period before the reference time. A dry canopy is defined by API<1.0 with all other periods defined as wet. The exponential function used for the denominator was determined iteratively by comparing plots of API with leaf wetness sensor data.

Similar time series' as in Figure 4.6 indicated satisfactory performance of Equation 4.7 as an index of canopy wetness, albeit the return of API index from wet to dry lagged the

response of leaf wetness sensors. The wet–dry attenuation of the API was considered satisfactory because comparison of data from leaf wetness sensors with visual observations of canopy conditions at Moanatuatua suggested the response of leaf wetness sensors from wet to dry was too rapid.

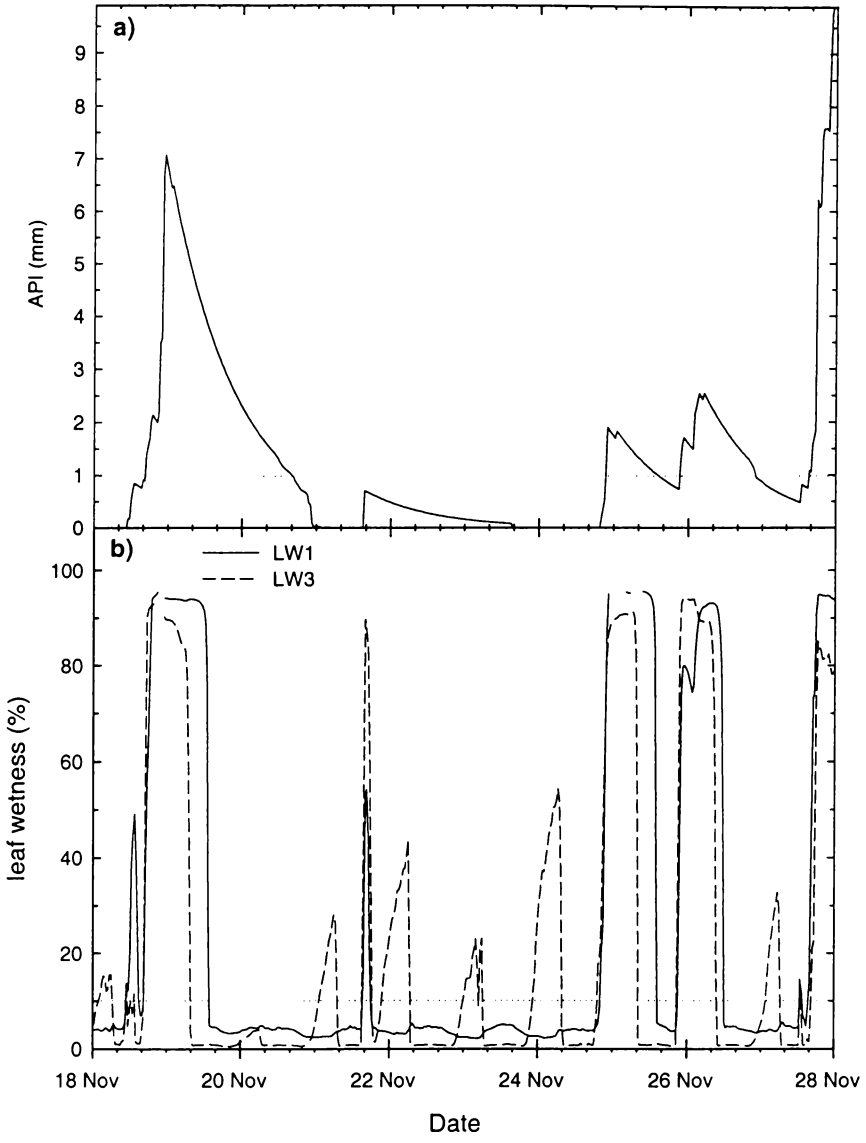

Figure 4.6 Time series' of canopy wetness indices for ten days 18–28 November 1999, determined using **(a)** antecedent precipitation index (API, Equation 4.7) and **(b)** leaf wetness sensors (LWS; mid-canopy sensor was not performing during this period). Dotted horizontal lines show arbitrary threshold where data above the line indicate wet canopy conditions. Note that for leaf wetness sensors, wet canopy conditions are identified when all data are above the threshold.

Figure 4.7 also shows that the API performs well as an index of canopy wetness for evaporation modelling purposes. The P–T results in Figure 4.7b are equivalent to those in Figure 4.5c when leaf wetness sensors were used to define the state of canopy wetness. Meanwhile the performance of the P–M estimates plotted in Figure 4.5b is improved by defining the canopy condition according to the API.

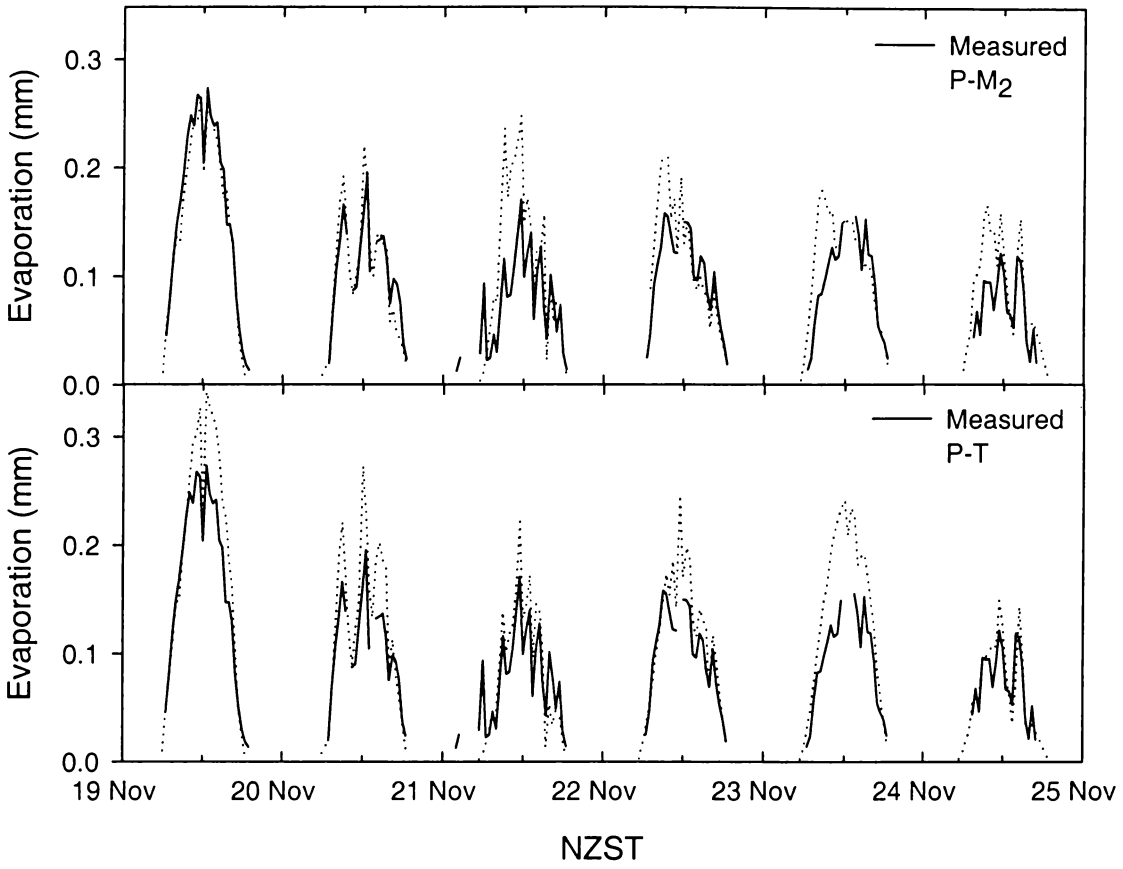

Figure 4.7 Measured and estimated evaporation for selected days 19 November 1999–25 November 1999 with antecedent precipitation index (API, Equation 4.7) used to identify the state of canopy wetness. Estimated evaporation is determined using **(a)** P–M_2: Penman-Monteith model with r_c=187D-106 and r_c=23D+9 (originally derived for Kopouatai) for dry and drying canopy states respectively, and **(b)** P–T: Priestley-Taylor model.

On the afternoons of November 19th and 20th, the P–M estimates that were underestimated in Figure 4.5b were improved so that they closely match measured evaporation in Figure 4.7a. It appears that the leaf wetness sensors may have dried earlier than the canopy on November 19–20th 1999 but after further drying during the week, the canopy was completely dry and matched the sensors later in the week. Indications are that the API not

only provides a good surrogate to the leaf wetness sensors, it may perform better than the measured leaf wetness index. The API is therefore adopted as the preferred index of canopy dryness.

Regardless of which canopy wetness indicator is employed, the P–M model still tends to overestimate evaporation during morning periods as indicated for November 21-24th on Figure 4.7a. Overestimates in the morning may be a trade-off when choosing the P–M model rather than the P–T approach that fails during periods identified by high Bowen ratios.

To test the models further, valid evaporation measurements from the two-year study period are plotted against P–M and P–T estimates (Figure 4.8). The data in Figure 4.8 are half-hourly evaporation measurements so the linear regression results can be used to evaluate the models for diurnal and long term evaporation estimates.

Using the leaf wetness sensors to distinguish wet and dry canopy conditions (hereafter referred to as the LW approach), the P–M model performed poorly with r^2=0.51 and the regression line slope was 0.81± 0.017 (α=0.05). Once again, employing the API to define canopy dryness improved the P–M approach and the slope was drawn closer (0.85 ±0.017, α=0.05) to the one-to-one line in Figure 4.8d. However, considerable scatter remains in Figure 4.8d and while r^2=0.53 is an improvement on Figure 4.7b that validates the API, it does not encourage the use of the P–M model for diurnal or long term evaporation estimates.

The P–T model also performed best with the API method (Figure 4.8c) yielding slightly better r^2=0.84 than the LW approach (r^2=0.83, Figure 4.8a). For future research at Moanatuatua when leaf wetness data are unavailable, the API is validated as a canopy wetness index by the r^2 values of models using the API being on par with those using leaf wetness sensors to differentiate wet and dry canopy periods.

The slope of the regression line for the equilibrium based evaporation model (E_{PT}) is 15% steeper than the one to one line, while the Penman Monteith model regression line slope was underestimated by a similar amount. P–T evaporation is distinguished as superior to the P–M model by a greater r^2 for the regression line and the y-intercept approximating

zero whereas the P–M regression line has a zero offset of 0.03 mm. The scatter causing the unacceptable r^2 for P–M regression line is obvious in Figure 4.8d.

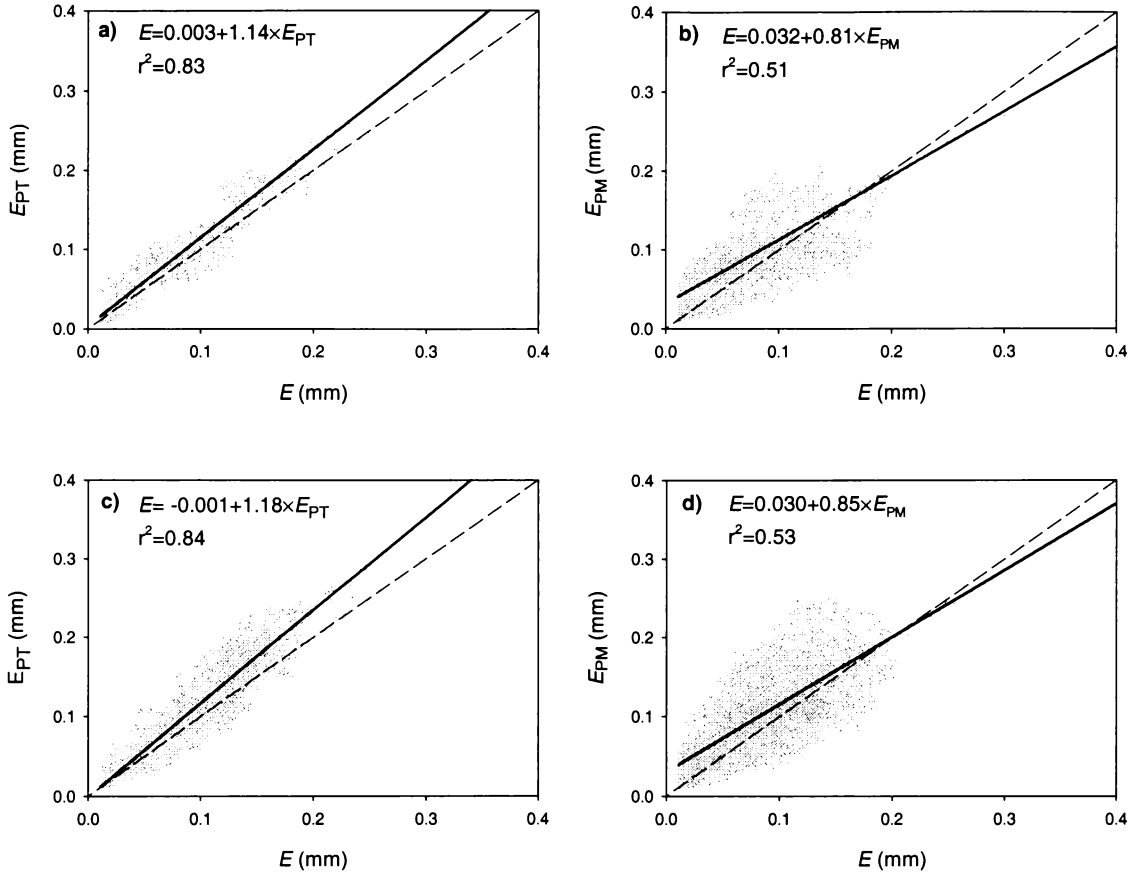

Figure 4.8 Measured versus modelled half-hourly evaporation using valid daylight 30 min eddy covariance measurements between 15 December 1998 and 15 December 2000. Modelled values are determined using **(a)** equilibrium-based Equations 4.2 and 4.3 with leaf wetness sensors to define canopy state **(b)** Penman–Monteith Equations 4.4 and 4.6 using leaf wetness sensors. Plots **(c)** and **(d)** are the same as (a) and (b) respectively, except API (Equation 4.7) is used to determine canopy wetness.

Compared with the one–one line in Figure 4.8c, the steeper slope of the regression line demonstrates that P–T evaporation is overestimated when atmospheric demand for evaporation is high, as described for 24 November 1999 in Figure 4.7b. However r^2=0.85 shows the variation of measured evaporation is more adequately explained by the P–T model than P–M which yielded r^2=0.53. This contradicts Thompson's (1997) conclusion that the P–M model is most suitable for diurnal modelling of evaporation.

An explanation is that the P–M approach is superior when evaporation demand is high in the middle of the day because of the model's ability to incorporate plant responses to extreme evaporation demand. The incorporation of r_c in the P–M model is superior to the radiation driven P–T model on clear sky, dry canopy days when D is high and stomata respond by restricting transpiration.

This phenomenon was particularly apparent to Thompson (1997), whose study was confined to midsummer days, however evaporation dynamics vary throughout the year. While P–T overestimates when evaporation demand is high, P–M overestimates when measured evaporation is low. This is a trade off between the models and is also demonstrated by the P–M model regression line overestimating at low values of measured evaporation in Figure 4.8d.

Figure 4.9 is a diurnal plot of modelled and measured evaporation for a day in winter and suggests that the P–T overestimate is negligible when low atmospheric demand for evaporation exists in winter. Whereas the P–T overestimate may be confined to summer, the overestimation of P–M evaporation occurs in Figure 4.9 and indicates this may be a year-round phenomenon.

Figure 4.10 demonstrates that evaporation drivers vary between seasons. Winter ensemble average r_c is significantly lower and average r_a greater for almost all of the daylight periods than summer. This results in the canopy being more decoupled from atmospheric demand in winter and radiation becomes more important as a driver of evaporation. This has been alluded to previously in the text referring to Figure 4.3 and Figure 4.4. The data in Figure 4.10 supports the hypothesis made earlier that only during summer is the net radiation budget and evaporative demand sufficient to force plant physiological restriction of transpiration.

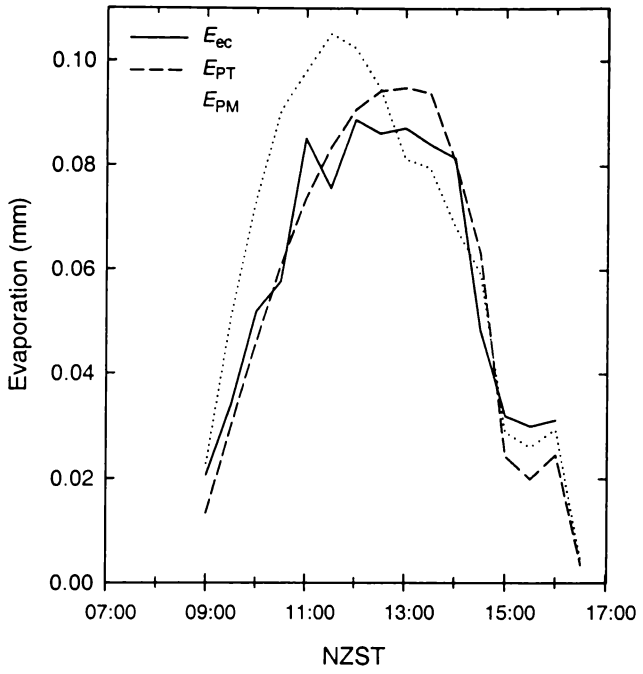

Figure 4.9 Diurnal course of measured (E_{ec}) and modelled evaporation (E_{PT} and E_{PM} are equilibrium–based and Penman–Monteith models respectively) for 7 July 2000: a clear sky day with dry canopy.

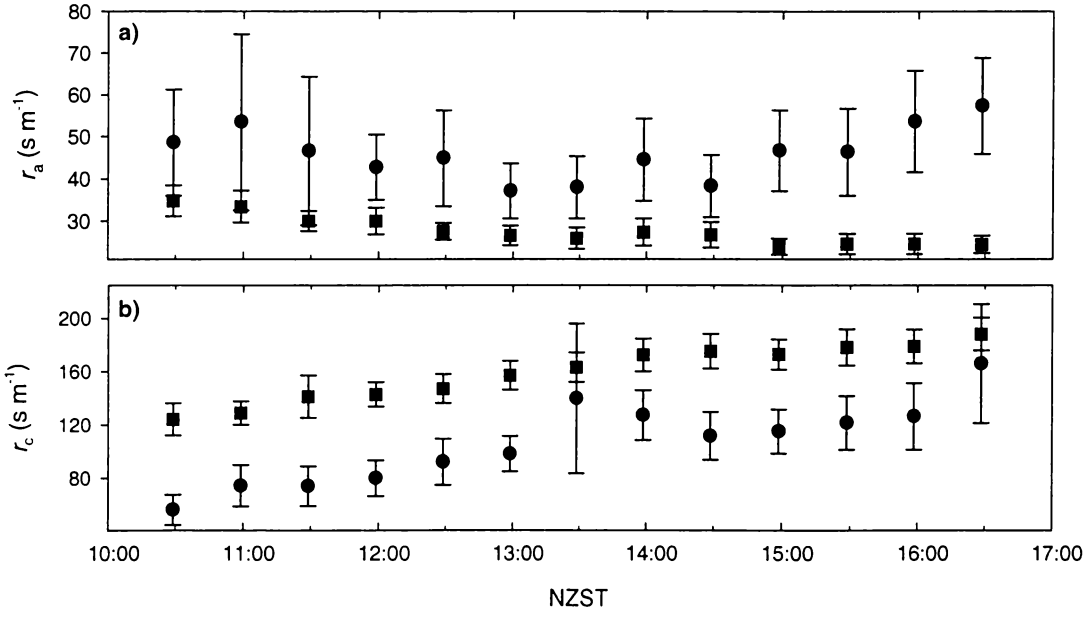

Figure 4.10 Ensemble mean daylight (1030–1630 hr) course of **(a)** aerodynamic resistance (r_a, derived using Equation 2.14) and **(b)** canopy resistance (r_c, derived using Equation 2.15). Data are for dry canopy conditions during winter (Jun–Aug 1999 & 2000; circles) and summer (Dec–Feb 1999 & 2000; squares). Error bars are 95% confidence intervals.

Further evidence of this hypothesis is provided by Figure 4.11. Thompson et al. (1999) concluded that the sensible heat flux dominates the energy balance at Moanatuatua and β in excess of 2 were common. These observations are true for summer periods, however Figure 4.11 shows that for the two years of this research only a small percentage of dry canopy periods are characterised by β>2. The 95% confidence interval of mean β is 1.02 ±0.013 and only 5% of dry canopy daylight periods had β>2. The annual mean β of approximately unity indicates that latent heat flux equals sensible heat flux on an annual basis.

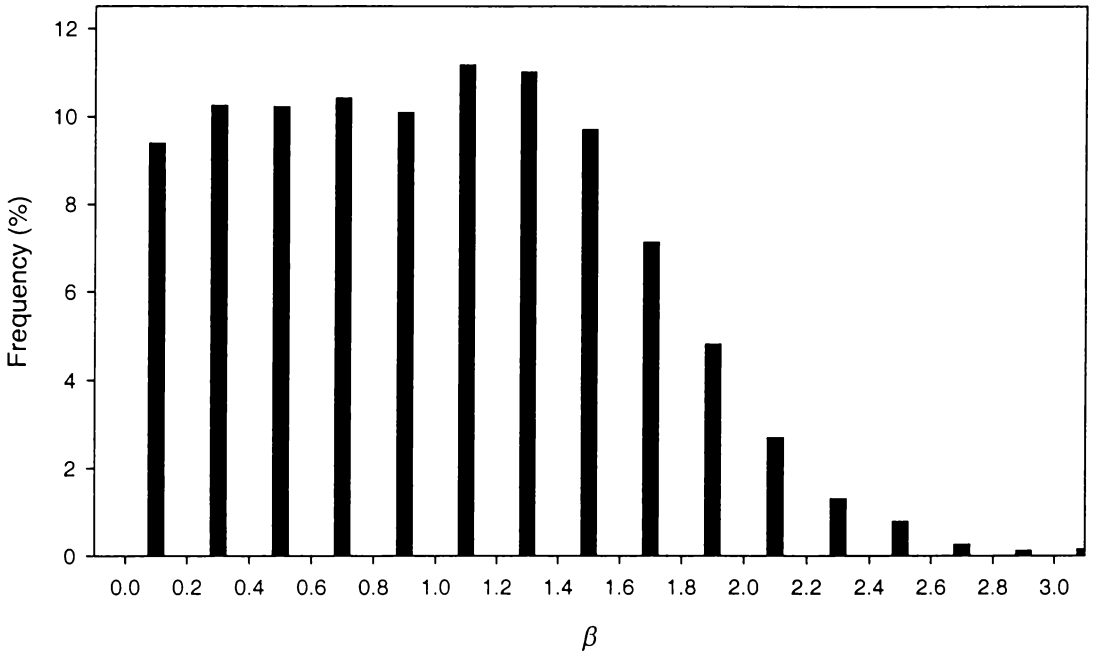

Figure 4.11 Frequency distribution of half-hourly Bowen ratio (β, dimensionless) determined using daylight (1000–1630 hr) eddy covariance data for dry canopy conditions throughout the entire study period. Mean β is 1.015 ± 0.013 (α=0.05).

Excessive summertime β are a consequence of large saturation vapour pressure deficits and high air temperatures associated with peak annual R_n and minimum precipitation (Figure 3.6). Plant physiological restriction of transpiration is important for maintaining high water table at Waikato peat bogs under these conditions (Campbell and Williamson, 1997; Thompson et al., 1999). However the high frequency of rainfall events, reduced R_n and lower air temperatures at other times of the year ensures the plant canopy is more frequently wet. This minimises the need for regulation of transpiration by *Sporodanthus* and *Empodisma* except during relatively rare periods indicated by large β. In general, λE

is controlled more by availability of radiation than by the plant controls observed during summer.

For the purposes of this research the P–M approach is not required for gap filling. The principle of parsimony demands the choice of the simplest model from a set of otherwise equivalent ones and the equilibrium–based model (Equation 2.18) minimises inconsistencies and ambiguities in this case. For future estimates of annual water balance components at Moanatuatua, the conclusion of Thompson (1997) is confirmed that the equilibrium–based model also provides better estimates at long-term time scales than the Penman–Monteith equation.

To demonstrate the sensitivity of evaporation estimates to the choice of model, Figure 4.12 displays cumulative plots of measured and modelled evaporation for the year 10 July 1999 – 10 July 2000. This 12 month period was chosen because it has the least gaps in the data (22% of data are missing or spurious). Gaps are filled using Equation 2.16 (E_{PT}) with α=0.8 and α=0.58 for wet and dry canopy periods respectively, where dry canopy conditions are identified by API<1.0 (Equation 4.7). Ideally the measured evaporation (E_{ec}) should be gap free because E_{PT} is being compared to E_{ec}. However the main objective of this analysis is to compare the two models P–T and P–M, and the bias introduced by gap filled values will be the same for testing both models.

Using the P–T approach for gap filling reduced missing data from 22% to 0.14% of all daytime half hourly values and the few remaining missing data points were interpolated. Total E_{ec} for the 12 month period was 633 mm and to test the sensitivity of gap filling models, E_{PM} was substituted for missing data previously replaced with E_{PT}. The plot was indistinguishable from the E_{ec} in Figure 4.12 and total evaporation was 639 mm. For the 12 month period 10 July 1999 – 10 July 2000, the influence of gap filling method was therefore negligible.

As a further test of sensitivity, all daylight periods were modelled using equilibrium–based (E_{PT}) and Penman–Monteith (E_{PM}) models. At 705 mm, E_{PT} overestimated E_{ec} by 11% while E_{PM} was an exaggeration of 16% at 732 mm (Figure 4.12). Error from the P–T

model is less than the P–M approach and is considered the superior method for annual water balance estimates.

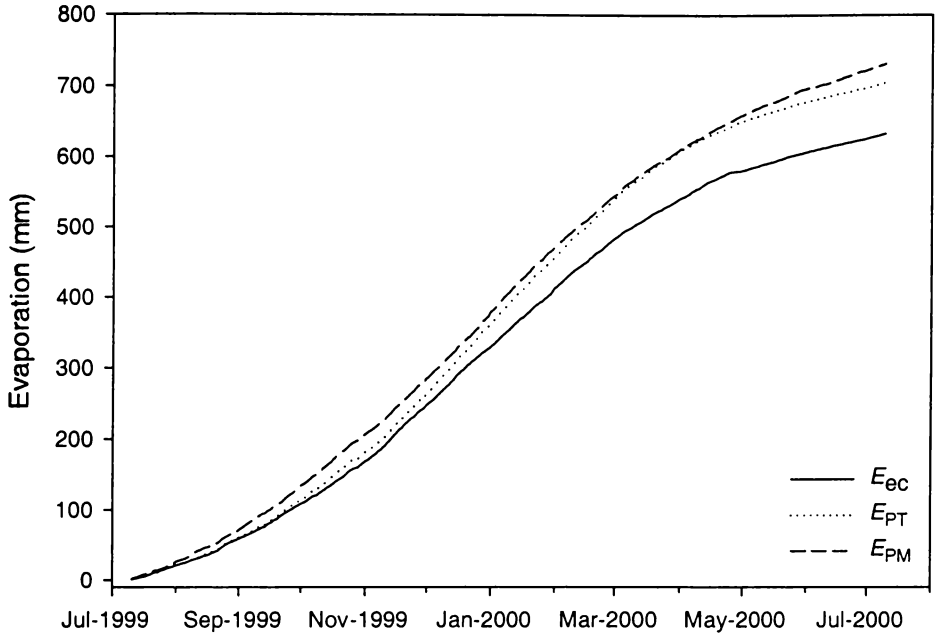

Figure 4.12 Cumulative evaporation between 10 July 1999 – 10 July 2000. E_{ec} is daytime (R_n>10 W m^{-2}) evaporation measured with the eddy covariance system and gap filled with equilibrium–based modelled values; E_{PT} is equilibrium–based evaporation modelled for wet and dry canopy; E_{PM} is estimated using Penman–Monteith equations for wet and dry canopy.

4.3 Annual water balance

The annual water balance was calculated using the assumptions described by Grimshaw (2000): vertical groundwater flow (G) and surface runoff (R) are assumed to be zero and precipitation (P) is assumed to be the sole input. With these assumptions, the annual water balance equation for Moanatuatua becomes

$$Q_w = P - E - \Delta S_w \qquad \textbf{4.8}$$

where Q_w is lateral groundwater discharge and ΔS_w is change in storage estimated by multiplying the change in water table elevation (ΔW) by specific yield of the peat (S_y). An

increase in water table elevation indicates water added to storage and is represented by a negative number.

For the upper 50 cm of peat at Moanatuatua, average S_y has been determined as 0.32 (Grimshaw, 2000) and was used here for calculating ΔS_w.

4.3.1 Annual evaporation

Figure 4.13 is a plot of daily evaporation for the two-year study period between 15 December 1998 and 15 December 2000. Using the P–T approach for gap filling, 35% of the data in Figure 4.13 were modelled and the remaining 0.19% missing half-hourly data were interpolated.

A 45 day running mean demonstrates the seasonal variation of evaporation at Moanatuatua. The running mean peaked at 3.1 mm d^{-1} and 2.8 mm d^{-1} for December 1998 and 1999 respectively. Winter minima were 0.7 mm d^{-1} for both 1999 and 2000. The minimum and maximum running mean of daily evaporation were in phase with net radiation and not the seasonal variation of D. Once again this is a reflection of the importance of R_n in driving evaporation at this time scale.

4.3.2 Water balance partitioning

Cumulative plots of water balance components in Figure 4.14 show precipitation (P) inputs exceed evaporation (E) from May–October, 1999 and April–November, 2000 with evaporation losses dominating the water balance at other times. Negative slope of the residual (P-E) plot in Figure 4.14 indicates periods when evaporation dominated the water balance and a positive slope shows when P was greater than E. Total evaporation for the two years was 1284 mm, compared with E_{PT} and E_{PM} of 1378 mm and 1393 mm respectively (not shown).

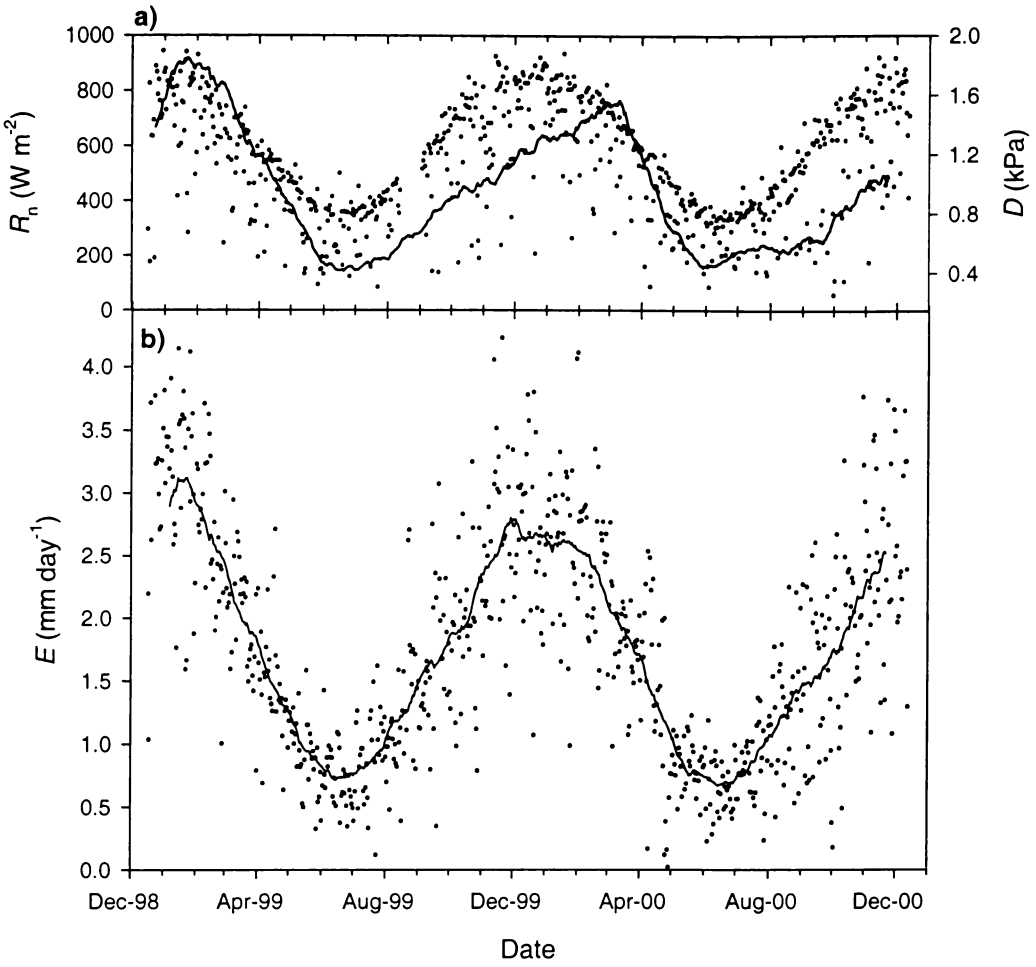

Figure 4.13 Interannual course of **(a)** daily maximum net radiation (R_n, points) and 45 day running mean of daily maximum vapour pressure deficit (D, solid line); and **(b)** Daily evaporation (E, points) with 45 day running mean of daily evaporation (solid line) between 15 December 1998 – 15 December 2000. E is daytime (R_n>10 W m^{-2}) evaporation measured with the eddy covariance system and gap filled with P–T modelled values.

Annual totals of water balance components are listed in Table 4.2. The water balance results here are similar to those estimated by Grimshaw (2000), with 64% of annual precipitation being lost as evaporation in both years (Grimshaw estimated 60% for 1999). Despite the second year being drier, with 10% less precipitation, evaporation losses were also lower and remained 64% of annual precipitation in 2000.

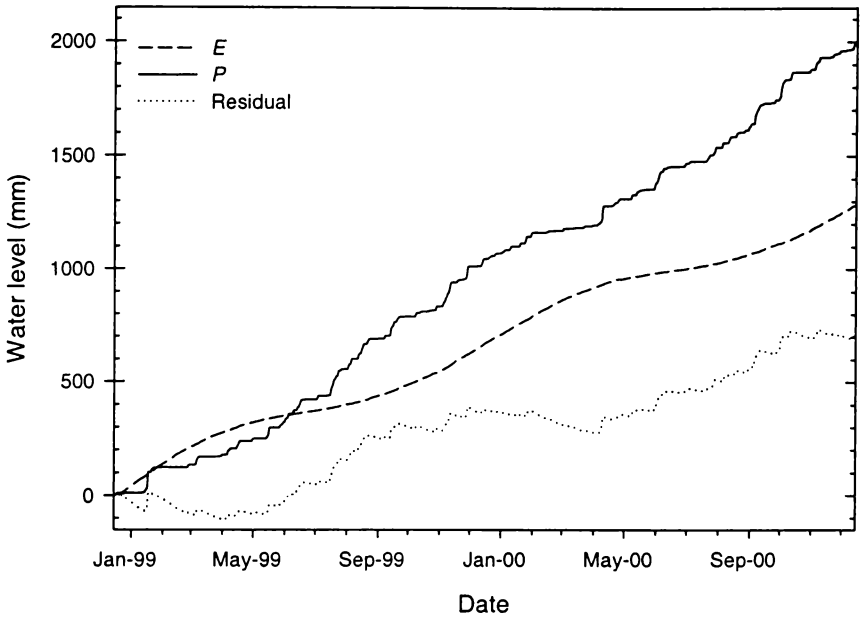

Figure 4.14 Interannual water balance for Moanatuatua peat bog. *P* is cumulative precipitation (mean of precipitation measurements from the eddy covariance site and meteorological station), *E* is evaporation and *P–E* is the residual component of the water balance.

Table 4.2 Annual water balance components 15 December 1998 – 15 December 2000 for Moanatuatua, using gap filled E_{ec} measurements. Data are in mm units. Precipitation values are the mean of measurements from the eddy covariance site and meteorological station.

	15/12/1998–15/12/1999	15/12/1999–15/12/2000
P	1046.00	953.00
E	670.00	614.00
P–E	376.00	339.00
ΔW	68.00	–141.00
ΔS_w	21.76	–45.12
Q_w (residual)	354.24	384.12

In 1999 water was added to storage while in 2000 water was released from storage, so that discharge from the bog (Q_w) was 34% and 40% of annual precipitation for both years. These results are equivalent to those calculated by Grimshaw (2000) using evaporation estimates entirely modelled using the equilibrium–based models described in this chapter.

4.4 Summary

This chapter augments previous research at Moanatuatua bog that investigated energy balance phenomena during a summer period. Eddy covariance measurements between 15 December 1998 and 15 December 2000 were used to investigate controls on evaporation at diurnal–annual timescales. Models of evaporation that were previously developed from data collected over a summer period were tested and the annual water balance at Moanatuatua was described.

The main findings of this chapter are:

- The dominant convective fluxes at Moanatuatua were H and λE, with β in excess of 2 sometimes observed during summer when the plant canopy was dry. In winter, the proportion of available radiation used for evaporation was increased and the role of stomatal regulation of transpiration was less important than during summer. On an annual basis, periods with $\beta > 2$ were rare and mean β was approximately unity, indicating that λE equals H.

- Net radiation and evaporative demand are generally insufficient to force plant physiological restriction of transpiration and λE is controlled more by availability of radiation than by stomatal controls observed during summer.

- Equilibrium-based models were superior to the Penman-Monteith equation for gap filling measurements of evaporation. For evaluating the annual water balance at Moanatuatua the evaporation component may be reliably estimated using equilibrium–based models exclusively, with α=0.80 and α=0.58 for wet– and dry–canopy periods respectively. A simple method for identifying wet and dry canopy conditions based on antecedent precipitation was described.

- For both years of this research, 64% of annual precipitation was removed as evaporation. Groundwater discharge (Q_w) was 34% and 40% for the first and second year of the study respectively, with water added to and released from storage during the first and second years respectively.

5 The Carbon Budget at Moanatuatua

5.1 Introduction

This chapter describes the variability in CO_2 and carbon exchange from diurnal to interannual time scales. Missing or spurious eddy covariance data are supplemented with modelled values and the models were also applied to data over a four year period to estimate interannual variation of the carbon budget. In order to model missing data, processes that govern nocturnal respiration losses and daytime CO_2 uptake are investigated.

While the models are based upon the premise that variability of CO_2 flux is driven by incident PPFD and peat temperature, this chapter is fundamentally a descriptive one and the intention is to provide carbon budget estimates. Explanations of CO_2 sequestration processes and the relationships with peat bog hydrology are reserved for Chapter 6, along with prediction of CO_2 exchange modification for climate change scenarios.

5.2 Diurnal variation

The diurnal trend of CO_2 flux (NEE) between 01 December 1999 and 06 December 1999 is shown in Figure 5.1a. The meteorological convention is adopted such that negative values of NEE indicate uptake of CO_2 and positive NEE indicates CO_2 loss from the ecosystem.

Nocturnal respiration between 01 December 1999 and 06 December 1999 averaged 1.77 ± 0.27 (α=0.05) μmol m^{-2} s^{-1}, which is not significantly different from 1.82 ± 0.27 (α=0.05) μmol m^{-2} s^{-1} observed by Lafleur et al. (2001) during summer nights at Mer Bleue peat bog in Ottawa, Canada. Peak daytime NEE ranged between –9.5 and –7.8 μmol m^{-2} s^{-1} and is similar to the range of –8.4 to –7.1 μmol m^{-2} s^{-1} observed by Lafleur et al. (2001).

Also congruent with the results of Lafleur et al. (2001) is the observation that peak uptake occurs in the late morning, at around 1100–1200 NZST.

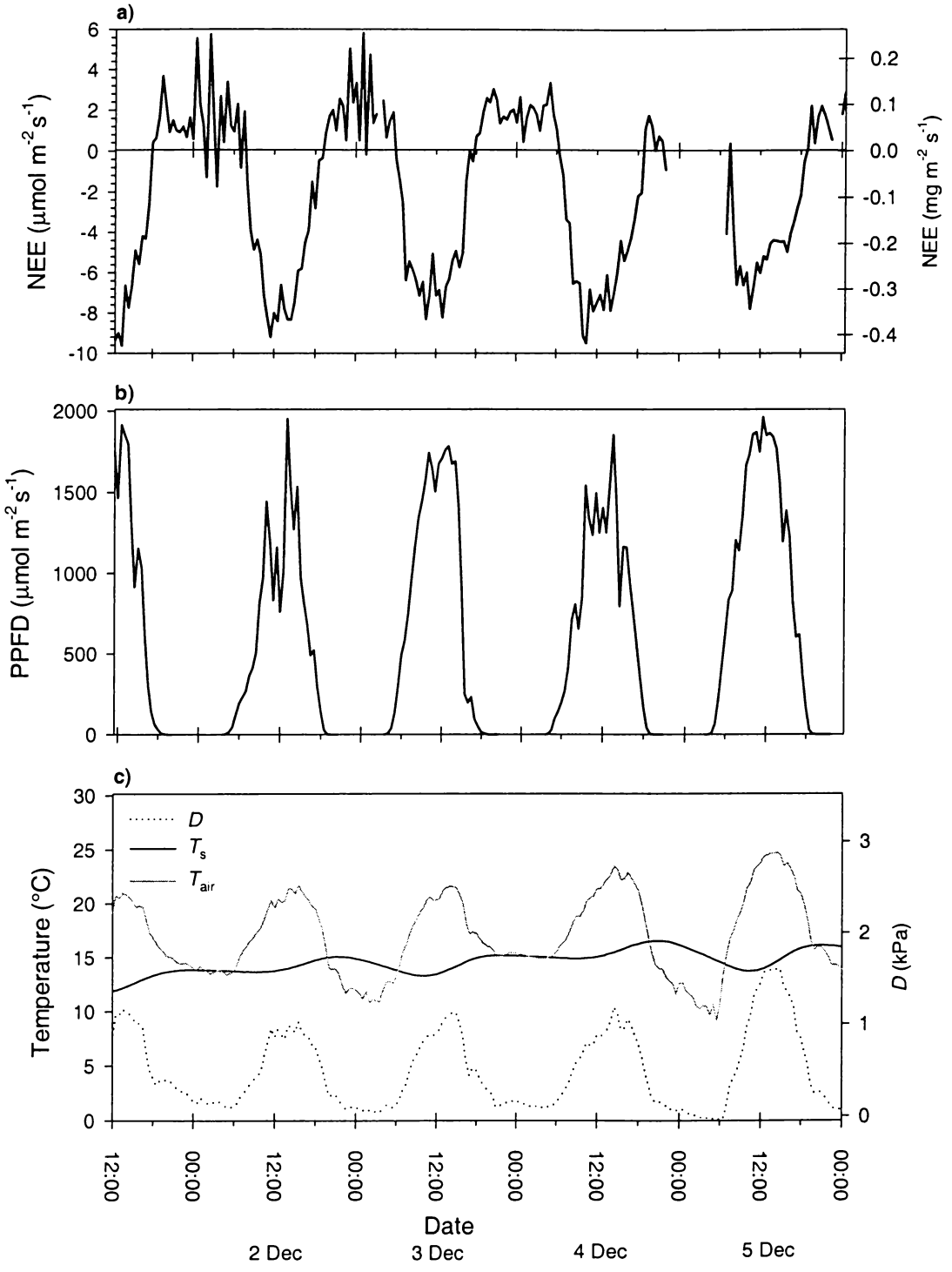

Figure 5.1 Diurnal variation of: **(a)** net ecosystem exchange (NEE); **(b)** photosynthetic photon flux density (PPFD); and **(c)** air temperature (T_{air}) , 8cm peat temperature (T_s) and vapour pressure deficit (D) for the period 01 December 1999 – 06 December 1999.

The observed diurnal trend of NEE is consistent with hypotheses from previous work at Waikato bogs that propose midday stomatal closure by restiad vegetation limits evaporation in the afternoon (Campbell and Williamson, 1997). Measurements of stomatal conductance for *E. minus* have indicated greatly reduced values in the afternoon (Sharp, 1995). This is believed to be a strategy to minimise plant uptake of acidic water by maximising carbon uptake in the morning when D is low and evaporation demand is the least (Campbell and Williamson, 1997).

Maximum diurnal sequestration of carbon in the morning has also been reported for other ecosystems such as Sahelian savannah (Moncrieff et al., 1997c), Brazilian rain forest (Grace et al., 1996), boreal jack pine (Baldocchi and Vogel, 1996) and wheat crops (Baldocchi, 1994). In contrast, maximum NEE has been observed in the afternoon at temperate deciduous forests (Baldocchi and Vogel, 1996) and over C_4 corn crops (Baldocchi, 1994).

For the period shown in Figure 5.1, the greatest daytime sequestration of CO_2 occurred on 2 and 4 December with average daytime NEE of 5.4 μmol m^{-2} s^{-1} and 5.5 μmol m^{-2} s^{-1} respectively. The least daytime accumulation of CO_2 occurred on 5 December, when the average flux was 4.5 μmol m^{-2} s^{-1}. The PPFD record (Figure 5.1b) indicates that 2 and 4 December were cloudy days and received less PPFD than 5 December which was a mainly clear sky day. The reduced CO_2 uptake on the latter day is therefore not attributable to less solar radiation available for photosynthesis. Campbell and Williamson (1997) hypothesised that plant physiological response to increased vapour pressure deficit is likely to include stomatal closure to minimise water use. This hypothesis may explain the reduction of NEE on 5 December (Figure 5.1).

Also, the smallest peak daytime fluxes occurred on clear sky days (3 and 5 December), while the largest peak fluxes were on partly cloudy days (2 and 4 December). The increased daytime CO_2 flux on the cloudy days might indicate the augmentation of photosynthesis due to various effects associated with the presence of clouds. Gu et al. (1999) suggest that increased diffuse radiation and decreased water stress, soil temperature and air temperature associated with cloudy conditions were responsible for enhancing

carbon uptake under cloudy conditions at a boreal aspen forest. These phenomena are investigated in Chapter 6.

Mean diurnal trends of CO_2 exchange over summer 2000 and winter 1999 are plotted in Figure 5.2. The uptake of CO_2 in winter is reduced by shorter day length and reduction of PPFD as shown by the narrower period of uptake and reduced peak of daytime CO_2 sequestration. Total daytime CO_2 sequestration was 9.14 (±0.88) $mgCO_2$ m^{-2} for the summer ensemble average and is significantly greater (α=0.05) than 3.22 (±0.59) $mgCO_2$ m^{-2} total daytime uptake for the winter ensemble.

Because less nocturnal data are available, the size of confidence intervals is increased for the nightly half hourly periods. Consequently, not all of the nocturnal summer respiration ensemble averages are significantly different from winter data. However sufficient quantity of data for summer and winter are available for half hourly periods at 0100, 2000, 2130 and 2230 hours to suggest that nocturnal ensemble average respiration is reduced in winter.

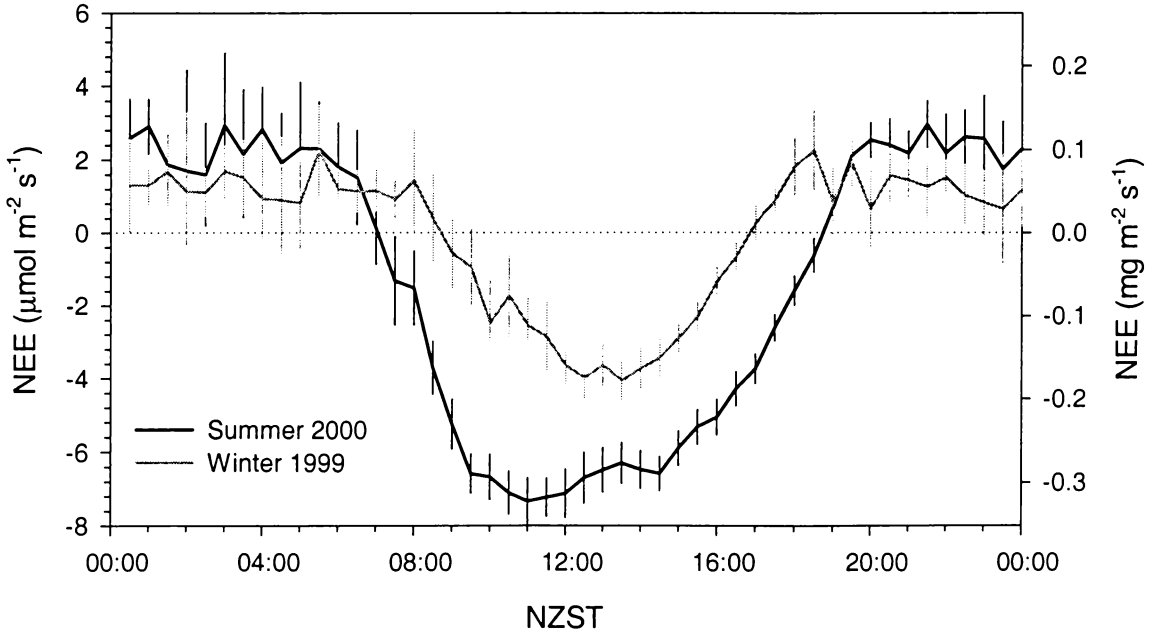

Figure 5.2 Diurnal course of ensemble average NEE for summer (1 December 1999 – 1 March 2000) and winter (1 June – 1 September 1999). Points are the half-hourly average of measured data with 95% confidence intervals as error bars.

This may be intuitively expected because peat temperatures are cooler in winter: there is strong evidence (α=0.01) that mean T_s for the summer of 2000 (15.7±0.054 °C) is larger than for winter of 1999 (9.6±0.084 °C). Lloyd and Taylor (1994) note that rates of soil respiration across a wide range of ecosystem types may be determined by a simple relationship with soil temperature.

While some ensemble averaged nocturnal CO_2 losses are reduced for winter in Figure 5.2, this is accompanied by reduction of daytime carbon sequestration. The sum of the daily ensemble mean NEE for winter indicates a small average sink strength of 0.12 $gCO_2\ m^{-2}\ d^{-1}$ for winter days in 1999. The sum of the 1999/2000 summertime ensemble averaged data suggests a strong mean sink strength of 4.94 $gCO_2\ m^{-2}\ d^{-1}$.

Whereas peak ensemble average NEE occurs in morning during the summer months, in winter it occurs in the early afternoon (Figure 5.2). This is consistent with discussion in the previous chapter, suggesting that during winter the net radiation budget and evaporative demand are insufficient to force plant physiological restriction of transpiration. A hypothesis to explain this is that midday stomatal closure occurs as a response to large *D* in summer months, but not during winter when *D* is small (Figure 3.6).

The previous chapter suggested that evaporation is driven by radiation except during uncommon periods throughout the year with dry canopy, clear sky and large *D*. During these rare periods, stomatal closure limits evaporation. Because photosynthesis is also regulated by stomatal activity, an interpretation of Figure 5.2 is that photosynthesis is generally driven by PPFD, but is limited by large *D* on summer afternoons.

5.3 Gap filling methods to replace missing data

A major issue when using eddy covariance to produce long-term datasets of CO_2 fluxes is how to deal with gaps in the data. For the two-year research period, valid data were collected for 45% of half hourly periods and the remaining data were either absent or spurious (Figure 5.3). This study uses non-linear regression methods that are considered superior to techniques such as mean diurnal variation for modelling missing data (Falge et al., 2001a). Valid data were obtained for 52% of half hourly periods between 11 July

1999 and 11 July 2000 and this 12-month period was chosen for model development because it has the least missing data.

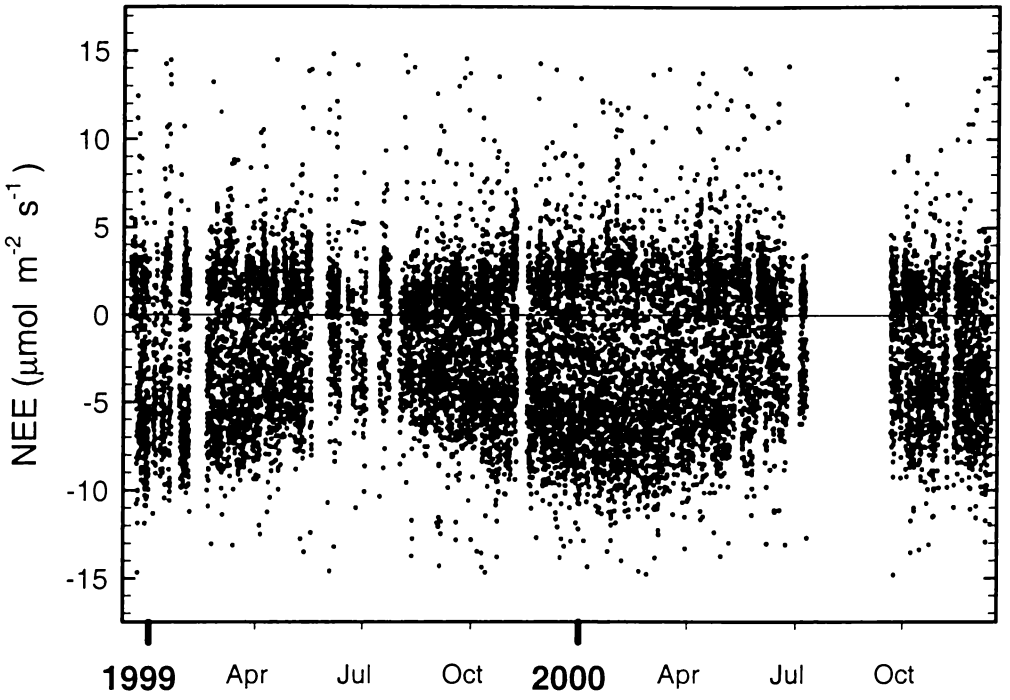

Figure 5.3 Valid half-hourly measurements of NEE for the two-year study period 15 December 1998 – 15 December 2000. Gaps are a consequence of missing data due to instrument failure or spurious data that were filtered from the dataset.

5.3.1 Respiration model

Missing and spurious nighttime data were modelled using Equation 5.1. Ecosystem respiration (R_e) is measured as the nocturnal ($R_n \leq 0$) eddy flux and is plotted against peat temperature measured at 8 cm depth (Figure 5.4). Following Lloyd and Taylor (1994, hereafter referred to as the Lloyd & Taylor model) an Arrhenius type equation is used as a respiration model and is expressed in terms of the respiration rate at 10°C (R_{10}). Because of strong scatter in results (Figure 5.4), nocturnal eddy fluxes were averaged over 0.5 °C bins and the binned averages were used to construct the respiration model. Binned averages were also used by Schmid et al. (2000) to model respiration and are appropriate for gap filling annual datasets because this time scale is the same as that used to determine binned averages.

The optimum R_{10} value was determined by iteratively increasing an estimate of R_{10} (in steps of 0.001 μmol m^{-2} s^{-1}) to find the greatest r^2 for the function

$$R_e = R_{10} e^{308.56\left(\frac{1}{56.02} - \frac{1}{T_s - 227.13}\right)} \qquad \textbf{5.1}$$

where T_s (K) is peat temperature at 8 cm depth. Using this procedure, R_{10} of 1.604 μmol m^{-2} s^{-1} was identified by maximum r^2=0.91 for the binned averages.

Respiration from the peat substrate was measured using the Li-6200 chamber system at irregular intervals between 9 September 1999 and 6 December 2000. Data are plotted in Figure 5.5 with a Lloyd & Taylor type model (Equation 5.1) indicating R_{10} = 1.535 μmol m^{-2} s^{-1} (r^2= 0.51). The plot of modelled R_e with an R_{10} of 1.604 μmol m^{-2} s^{-1} is analogous to modelled R_s (Figure 5.5). For modelling purposes, this suggests that nocturnal above-ground respiration is negligible at Moanatuatua. This is consistent with observations at a boreal aspen forest, where above-ground respiration was insignificant compared with nocturnal respiration from the soil (Black et al., 1996).

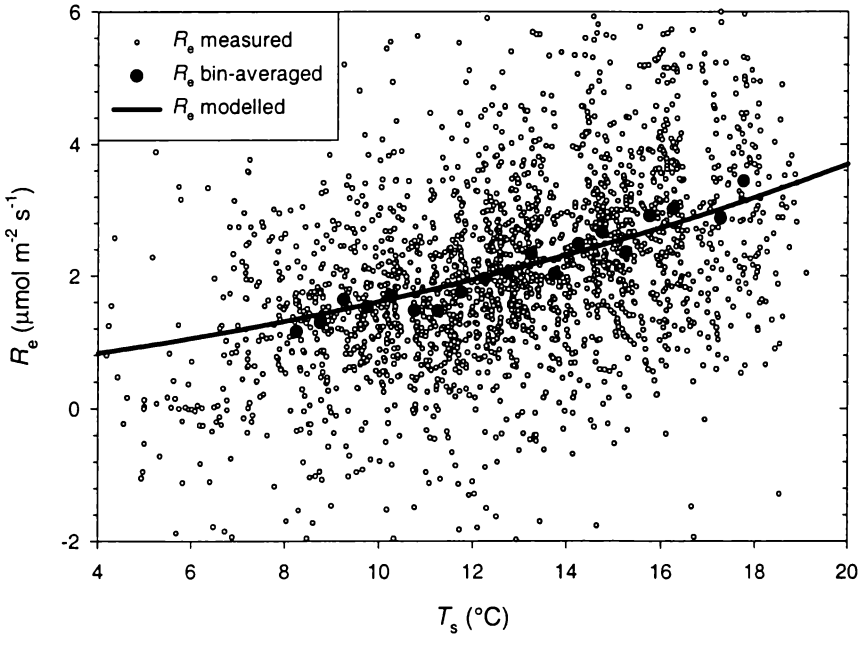

Figure 5.4 Ecosystem respiration (R_e) vs peat temperature measured at 8 cm depth (T_s) between 11 July 1999 and 11 July 2000. R_e data averaged in bins of 0.5 °C width are used to construct the Lloyd & Taylor model with R_{10} = 1.604 μmol m^{-2} s^{-1} (r^2 = 0.91).

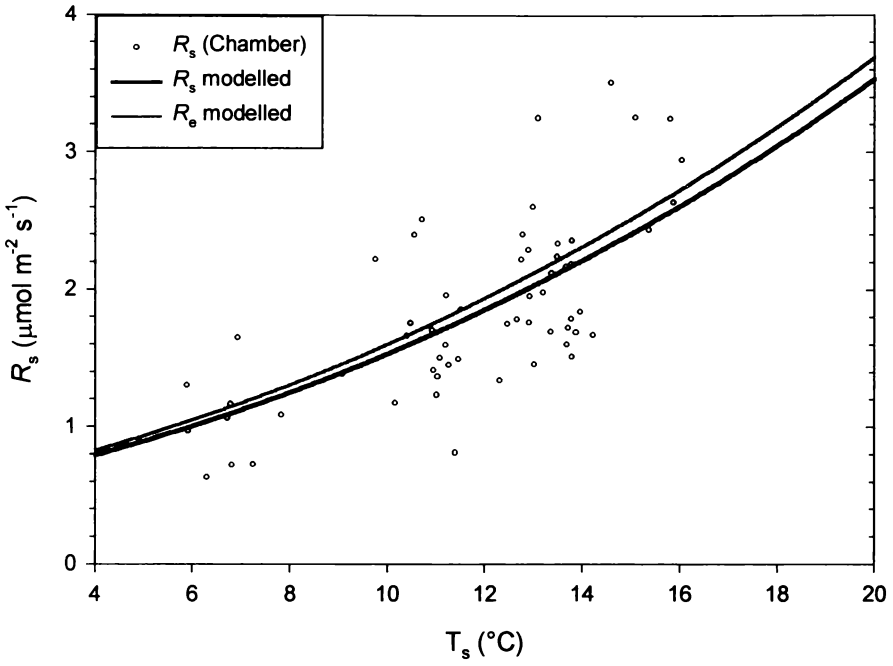

Figure 5.5 Respiration from peat (R_s) vs peat temperature measured at 8 cm depth (T_s) between 9 September 1999 and 6 December 2000. Each datum is an average of measurements from 10 sites sampled at approximately the same time. The R_s model is a Lloyd & Taylor equation with R_{10} = 1.535 µmol m^{-2} s^{-1} (r^2 = 0.51). The model of R_e from Figure 5.4 is shown for comparison.

Water table elevation has been shown to be a significant influence on R_e at wetland and tundra ecosystems, with respiration generally increasing as water tables are lowered (Aerts and Ludwig, 1997; Armentano and Menges, 1986; Clymo et al., 1998; Freeman et al., 2001; Oechel et al., 1998; Shearer, 1997). In a controlled laboratory experiment, Hodge (2002) measured respiration rates from cores of Moanatuatua peat with temperature maintained at 10°C and water table varied between 10 and 60 cm depth. Hodge (2002) concluded that water table elevation had a significant influence on respiration rates from Moanatuatua peat cores and the Lloyd & Taylor model failed to exclusively predict observed respiration.

Figure 5.6 is a plot of R_e versus depth to water table between 11 July 1999 – 11 July 2000. Nocturnal eddy fluxes were averaged over 40 mm water table depth bins and the binned averages were used to overcome scatter for modelling purposes, as in Figure 5.4. While there appears to be a slight decrease of R_e at shallower water table depths, the use of binned averages as input data failed to yield a suitable model of R_e and a linear regression

model explained only 30% of the variance (Figure 5.6). An implication of this is that, compared with peat temperature, depth to water table is not a significant control of nocturnal eddy fluxes at Moanatuatua. Using the Lloyd & Taylor model with $r^2 = 0.91$, peat temperature is a more appropriate predictor of R_e at annual time scales.

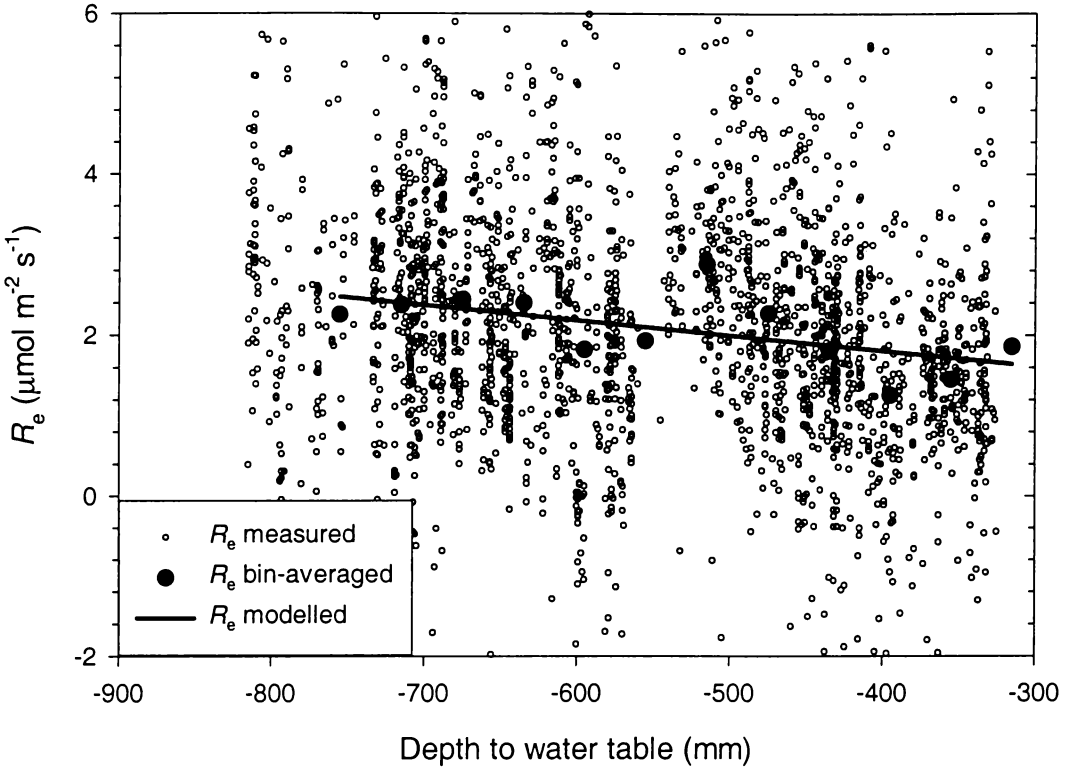

Figure 5.6 Ecosystem respiration (R_e) vs depth to water table (WT) between 11 July 1999 and 11 July 2000. R_e data were averaged over bins of 40mm depth and a linear regression model (R_e=0.0019WT +1.047) was fitted to binned averages with $r^2 = 0.30$.

With temperatures controlled at 10 °C, Hodge (2002) observed respiration rates of 1.075 µmol m^{-2} s^{-1} for cores with water maintained at 60 cm below the surface. Between 11 July 1999 and 11 July 2000, the average water table depth below ground was 56 cm (i.e. ≈60 cm) at Moanatuatua and R_{10} was 1.60 µmol m^{-2} s^{-1}. The difference of approximately 0.5 µmol m^{-2} s^{-1} between the Moanatuatua R_{10} value from field data and Hodge's (2002) laboratory observations may be explained in several ways:

Firstly, the cores in Hodge's (2002) experiment were maintained at 10°C through their entire depth. Vertical temperature stratification exists in the field and this has elsewhere

been suggested as an explanation why water table position may have limited influence on respiration rates in field conditions (Moore and Dalva, 1993).

Secondly, living material was excluded from Hodge's (2002) cores however living roots exist in the peat profile at Moanatuatua. Respiration from roots below the soil collars is measured by the chamber system at Moanatuatua and is certainly accounted for with nocturnal eddy fluxes. It is likely that some, if not most, of the disparity between Hodge's (2002) R_{10} and field observations is due to autotrophic (i.e. root) respiration being included in field measurements.

It is also believed that deeper peats are decay resistant and lowering the water table may have relatively little impact of respiration rates at these sites (Hogg et al., 1992). This phenomenon is especially pertinent for peatlands with a water table that is already > 20 cm below the surface (Hogg et al., 1992), which may have been the case for Moanatuatua (Shearer, 1997). For wetlands with deep peat profiles where the water table is not close to the surface, temperature has a much greater effect on CO_2 release than water table elevation (Hogg et al., 1992). Petrone et al. (2001) also noted that the respiration component of the CO_2 flux was primarily temperature controlled at a restored peatland in Québec, Canada.

Lastly, Hodge's (2002) cores were 70 cm long. Some of the methane that is produced below 70 cm depth in the field, but rises through the profile, may oxidise to form CO_2. This would augment CO_2 release but would not be accounted for in Hodge's (2002) experiment.

An exploration of these hypotheses warrants further attention in future research.

5.3.2 Modelling missing daytime data

Gross ecosystem production (GEP) is determined as NEP + R_e which is the difference between daytime (PPFD > 0) eddy fluxes and modelled respiration where R_e is estimated using Equation 5.1 (R_{10}=1.604 μmol m^{-2} s^{-1}). Half-hourly GEP are plotted against PPFD in Figure 5.7.

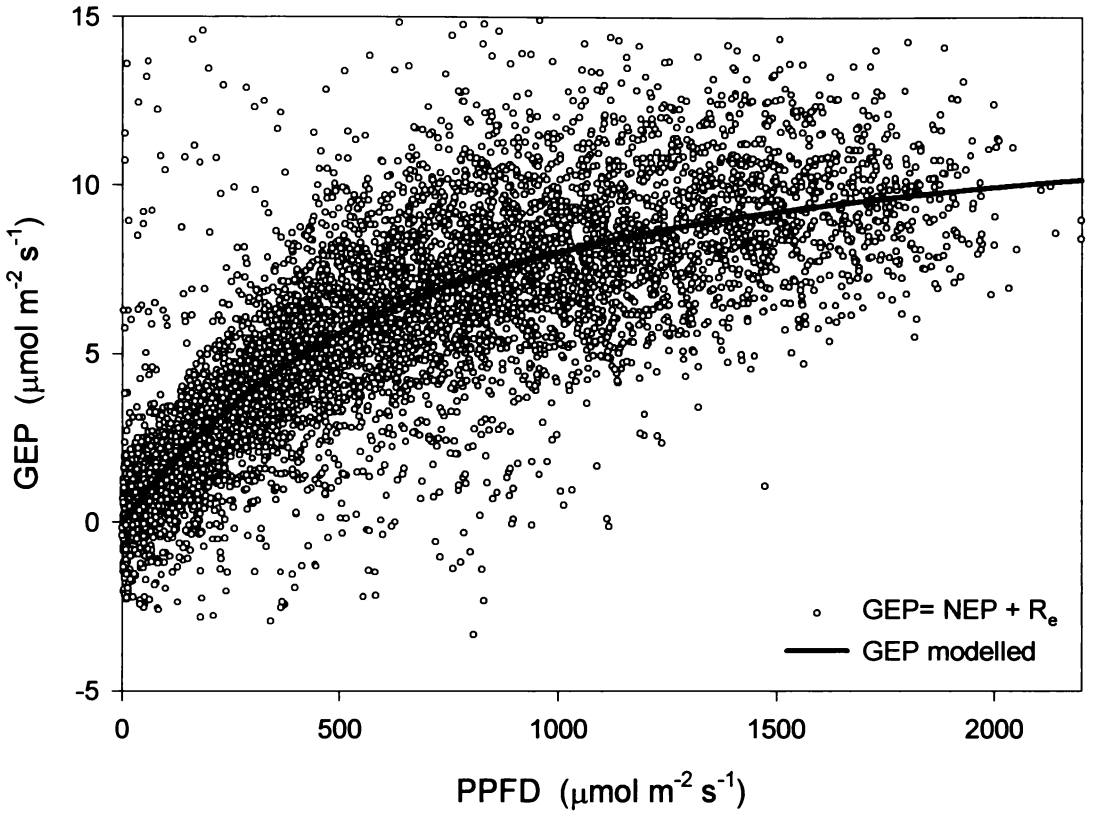

Figure 5.7 GEP vs. PPFD for daytime data collected between 11 July 1999 and 11 July 2000. NEP is –NEE, measured using eddy covariance. The non-rectangular hyperbolic model is determined with Equation 5.2 ($r^2 = 0.63$).

Following Farquhar and Wong (1984), a non-rectangular hyperbolic equation with physiologically meaningful parameters was used to model GEP as a function of PPFD. The curve was fitted to the data using a non-linear regression technique with the quadratic formula

$$\mathrm{GEP}_{\mathrm{mod}} = A - \frac{\sqrt{B-C}}{2.0 \times \theta} - R_{\mathrm{d}} \qquad \textbf{5.2}$$

where $\mathrm{GEP}_{\mathrm{mod}}$ = modelled GEP; $A = (\alpha_q \times \mathrm{PPFD}) + A_{\max}$; $B = (\alpha_q \times \mathrm{PPFD} + A_{\max})^2$; and $C = 4.0 \times \alpha_q \times \mathrm{PPFD} \times \theta \times A_{\max}$ for α_q = initial slope of the curve (a.k.a. the quantum yield); $A_{\max}$ = maximum rate of CO_2 uptake at saturating irradiance; θ = the convexity of

the hyperbola; and the y-intercept is dark respiration (R_d) of CO_2 from plants (Whitehead, pers. comm.[2]).

Using Sigmaplot software (SPSS Inc.), iterative curve optimisation identified the parameters in Table 5.1.

Table 5.1 Input parameters used in Equation 5.2 for modelling GEP

Parameter	Value	Units
α_q	0.01695	μmol CO_2 / μmol photons
A_{max}	12.5855	μmol m^{-2} s^{-1}
θ	0.3618	(dimensionless)
R_d	0.0	μmol m^{-2} s^{-1}

The negligible value of R_d is consistent with the hypothesis drawn from Figure 5.5 that above-ground respiration at Moanatuatua is insignificant, however Falge et al. (2001a) caution against the estimation of respiration rates via extrapolation of light response curves.

5.3.3 Model validation

Data collected between 15 December 1998 and 15 December 2000, but excluding the period 11 July 1999 to 11 July 2000 (i.e. data used for model calibration), were used to test the models of R_e and NEE (where NEE = –GEP + R_e).

Figure 5.8 shows that modelled R_e is a reasonable approximation of mean ecosystem respiration. The poor r^2=0.04 indicates the model would be inadequate for evaluating half-hourly R_e and is a consequence of using binned averages for construction of the model intended exclusively for long term gap filling. However the linear regression line is a reasonable approximation of the 1:1 line on Figure 5.8, with slope and intercept of 0.95±0.12 and 0.17±0.29 μmol m^{-2} s^{-1} respectively, demonstrating that the model is appropriate for long term gap filling.

[2] Personal communication with Dr. David Whitehead, Manaaki Whenua Landcare Research, Lincoln, NZ.

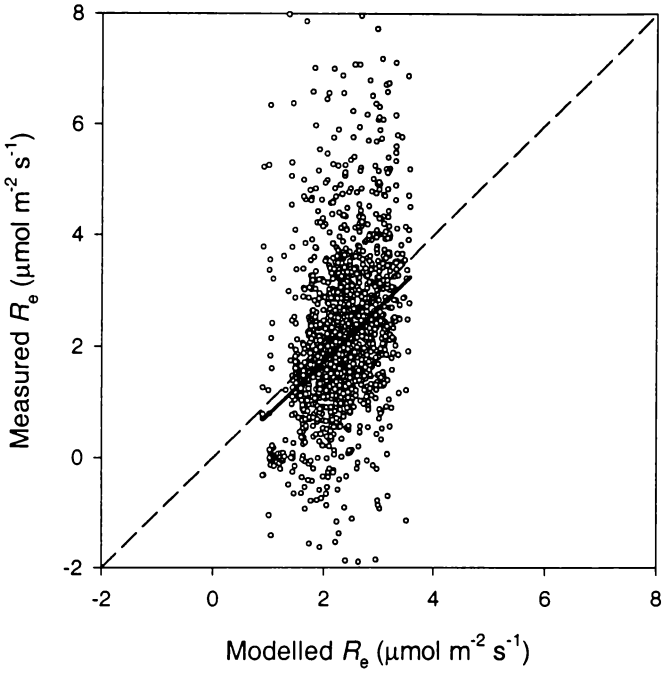

Figure 5.8 Modelled vs measured ecosystem respiration (R_e) for all data 15 December 1998 – 15 December 2000, except those used for model calibration. Dashed line is one-to-one line. Solid line is linear regression model NEE_{mod}=0.95NEE–0.17 (r^2=0.04).

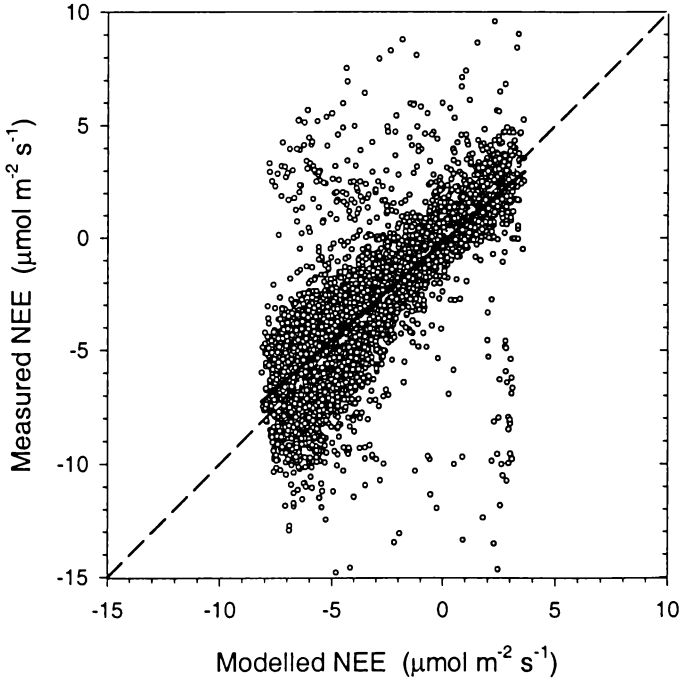

Figure 5.9 Modelled vs measured NEE for all data 15 December 1998 - 15 December 2000, except those used for model calibration. Dashed line is one-to-one line. Solid line is linear regression model NEE_{mod}=0.87NEE–0.19 (r^2=0.56).

Likewise, Figure 5.9 illustrates the appropriateness of the NEE model for gap filling of long-term datasets. Table 5.2 sums fluxes across periods with good quality eddy covariance measurements between 15 December 1998 and 15 December 2000 and shows that totals of modelled and measured carbon fluxes were in reasonable agreement.

Table 5.2 Sum of measured and corresponding modelled carbon fluxes for period 15 Dec 1998 to 15 Dec 2000, excluding half-hourly periods with spurious eddy covariance measurements and data used for model calibration.

	Modelled ($tC\ ha^{-1}$)	Measured ($tC\ ha^{-1}$)	% Error (meas-mod) /meas
Nocturnal R_e	0.817	0.765	-6.8%
Daytime NEE	-3.476	-3.171	-9.6%
Total	-2.658	-2.406	-10.4%

Despite the large scatter of modelled versus measured respiration and poor r^2 of the linear regression model, at annual time scales the R_e model overestimates measurements by 6.8%. Using a combination of the R_e and NEE models overestimates sequestration at annual time scales by 10.4%. This level of uncertainty is consistent with other research: Schmid et al. (2000) report 10% uncertainty of their annual sequestration estimate. Both the R_e and NEE models are therefore validated for gap filling at annual time scales.

5.4 Seasonal variation

For the model calibration period 11 July 1999 to 11 July 2000, 52% of data were valid and 48% were missing or spurious and thus have been modelled. For the two-year period 15 December 1998 to 15 December 2000, 45% of data were credible and the remaining 55% have been modelled.

Gap filled CO_2 data were averaged over 24 hour periods and have been plotted in Figure 5.10 with a 15-day running mean to illustrate seasonal trends. The running mean reveals that the Moanatuatua ecosystem was a CO_2 sink for most of the year, switching to a source for a brief period in each winter.

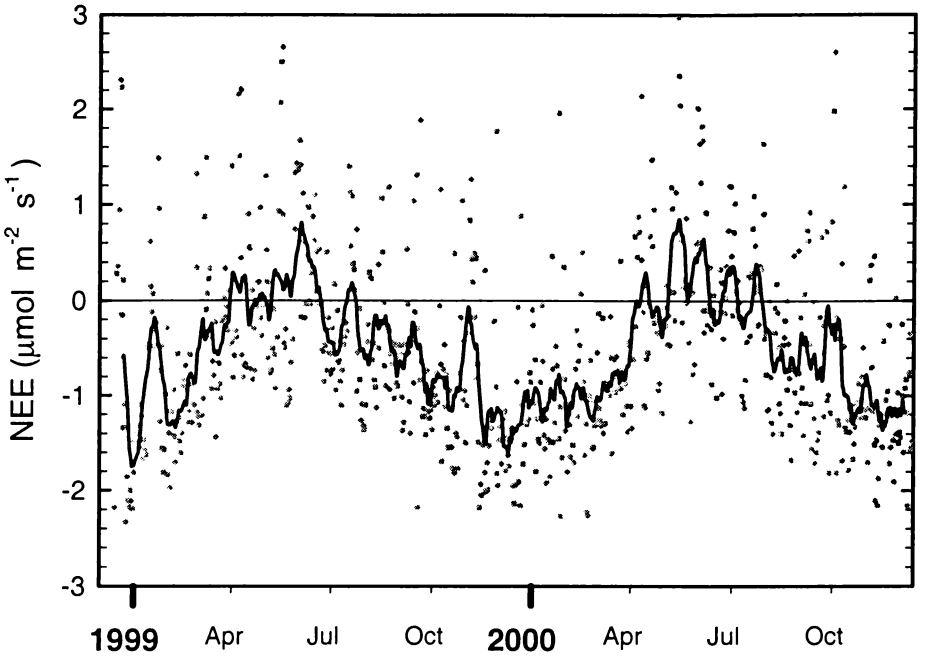

Figure 5.10 Seasonal variation of daily mean NEE at Moanatuatua bog between 15 December 1998 and 15 December 2000 (points). Negative values indicate periods when the ecosystem was a sink of atmospheric CO_2. Bold line is the 15-day running mean.

Figure 5.11 shows average monthly NEE expressed as mean half-hourly flux density. This plot also illustrates seasonal variation and shows that Moanatuatua peat bog is a sink of CO_2 for most of the year. Negative values indicate net carbon sequestration that occurs when monthly respiration losses are exceeded by daytime photosynthetic uptake of CO_2. The bog switched from being a sink to a source of CO_2 earlier in 1999 than in 2000, as did the switch back to being a carbon sink at the end of winter 1999.

The magnitude of monthly mean NEE ranged from a sink strength of –1.36 µmol m^{-2} s^{-1} in December 1999 to a source of 0.38 µmol m^{-2} s^{-1} in May 2000. This is equivalent to a total gain of 43.7 gC m^{-2} in December 1999 and a total loss of 12.2 gC m^{-2} in May 2000. At a former true raised peat bog in the Netherlands, Nieveen et al. (1998) measured CO_2 exchange ten years after the water table had been restored from previously drained levels. Nieveen et al. (1998) observed monthly average CO_2 flux densities ranging between –1.5 µmol m^{-2} s^{-1} and 0.54 µmol m^{-2} s^{-1}, however the sequestration period was only three months long and the bog was a source of CO_2 for nine months of the year.

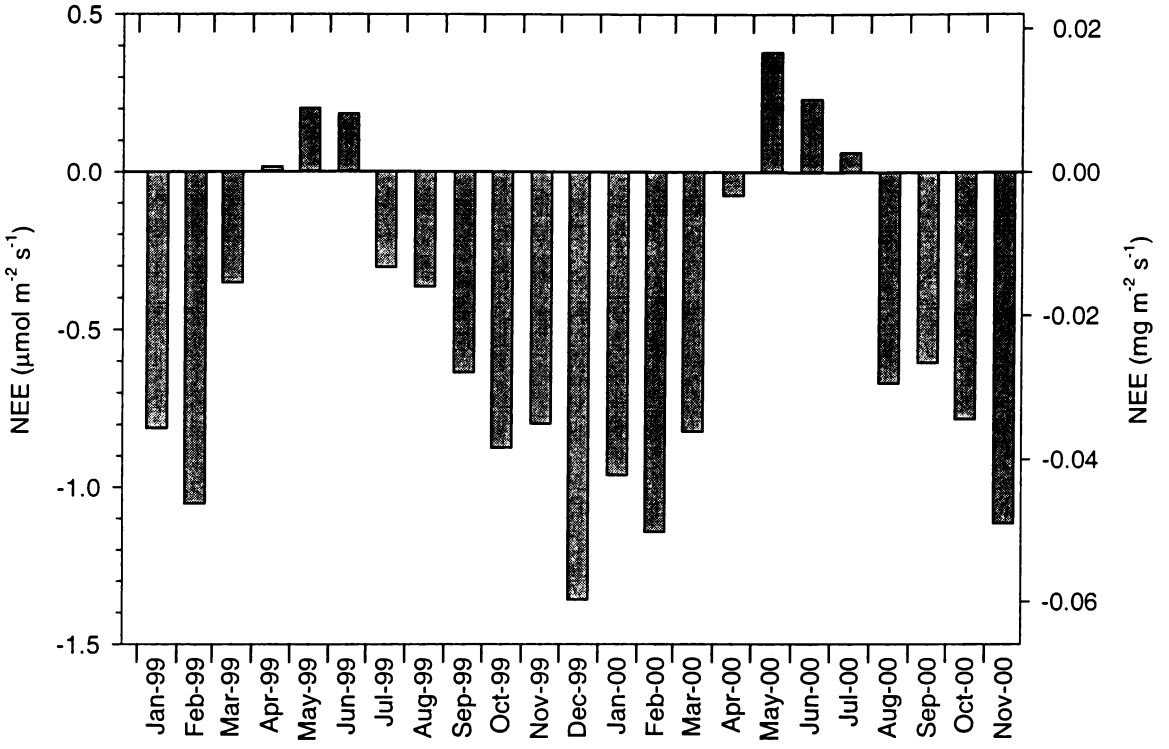

Figure 5.11 Monthly variation of CO_2 flux beginning January 1999 and ending November 2000. Negative values denote periods of CO_2 sequestration while positive fluxes indicate months of net CO_2 release to the atmosphere.

Seasonal variability of carbon exchange at other Northern Hemisphere wetlands also differs from the Moanatuatua results. Decreased temperatures and daylengths along with periods of snow cover restrict the growing season duration at high latitude wetlands. For example at a Canadian temperate peat bog (lat. 45°N), Lafleur et al. (2001) observed a growing season limited to seven months of the year. Further north, boreal and Arctic peatlands are sources of CO_2 for most of the year, except during a short growing season approximately three months in duration (Joiner et al., 1999; Lafleur et al., 1997; Vourlitis and Oechel, 1999).

Other ecosystems also exhibit seasonal variation of CO_2 exchange that are different to Moanatuatua. Variation of carbon uptake at temperate deciduous forests is regulated by phenological timing of the growing season that ranges from five to seven months (Baldocchi et al., 2001). While not constrained by senescence, seasonal variation of carbon exchange for coniferous forests varies according to latitude and continental

position that affect growing season length and climatic regime respectively. A Finnish coniferous forest exhibited seasonal variation of carbon uptake similar to deciduous forests because respiration losses exceeded photosynthetic production during winter (Baldocchi et al., 2001). In contrast, a similar biome in Oregon sequestered carbon for most of the year except during a hot dry summer when the ecosystem switched to a source of CO_2 (Baldocchi et al., 2001).

The Moanatuatua seasonal variation resembles that observed at a temperate humid coniferous forest in the southeastern United States (Ameriflux Duke site), where carbon is assimilated for most of the year except for a month or two in winter (Baldocchi et al., 2001).

While the length of growing season for many deciduous forests is shorter than for Moanatuatua, the range of seasonal variation in fluxes is similar. At Moanatuatua the 15-day running mean ranged between -1.75 μmol m^{-2} s^{-1} and 0.8 μmol m^{-2} s^{-1}, compared with a seasonal range of -1.5 μmol m^{-2} s^{-1} to 0.38 μmol m^{-2} s^{-1} when averaged on a weekly basis for deciduous forests (Baldocchi et al., 2001). The magnitude for coniferous forests is less, so that while the Duke site had a similar length of growing season compared to Moanatuatua, the seasonal range was attenuated between -1.13 μmol m^{-2} s^{-1} and 0.19 μmol m^{-2} s^{-1} (Baldocchi et al., 2001).

5.5 Annual and interannual carbon exchange

Gap-filled CO_2 fluxes (gCO_2 m^{-2} d^{-1}) are converted to carbon fluxes (gC m^{-2} d^{-1}) using ratios of atomic mass, where gC = 0.273 gCO_2 (Greco and Baldocchi, 1996). Converted data are used to illustrate annual carbon sequestration (Figure 5.12). The cumulative plot in Figure 5.12 shows the seasonal variation of carbon exchange where a negative gradient indicates carbon assimilation and a positive gradient reveals periods of carbon release to the atmosphere.

While the annual total carbon sequestration was similar for both years, the seasonal variation was different. Of particular interest is the timing of the switches from carbon sink to carbon neutral in March 1999 and in April 2000, the latter year lagging the former by a month. The switch from carbon neutral to a source of atmospheric carbon occurred in

May during both years (Figure 5.12) and the bog was a stronger carbon source in winter 2000 than during the winter of 1999 (Figure 5.11 and 5.12). The return to a negative gradient in June 1999 and six weeks later at the end of July 2000 indicates the switch when the bog promptly reverted to being a carbon sink.

To explain this seasonal behaviour, Figure 5.13 allows comparison between running means of PPFD and T_s for 1999 and 2000. In March 1999, the 45-day running mean of PPFD was less than during the same period in 2000, whereas T_s was greater during the former period. Reduced photosynthesis due to decreased radiation inputs during March 1999 would therefore have been accompanied by increased respiration as a consequence of higher peat temperatures. This offers an explanation for the switch to carbon neutral in March 1999 whereas in March 2000 the bog remained a sink of atmospheric carbon.

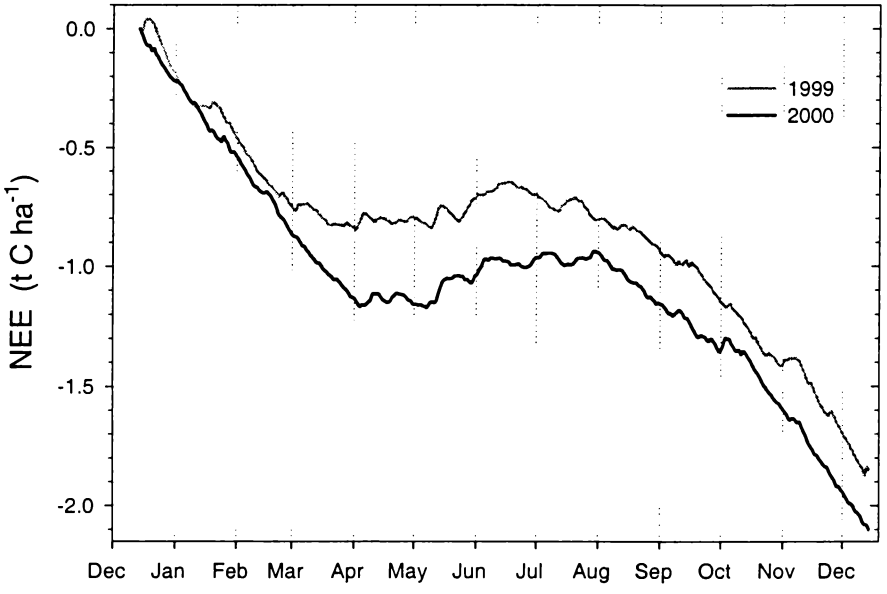

Figure 5.12 Cumulative net ecosystem exchange (NEE) for 1999 (15 December 1998 –15 December 1999) and 2000 (15 December 1999 – 15 December 2000). Measured data are gap filled using modelled values. Annual sequestration is 1.85 tC ha^{-1} for 1999 and 2.10 tC ha^{-1} for 2000.

During winter 2000, the bog was a stronger source of CO_2 than the preceding winter (Figure 5.12) and, because PPFD was similar during both winters, this may be explained exclusively by warmer peat temperatures causing greater respiration losses in winter 2000. Minimum PPFD occurs in June, however the minimum peat temperature is lagged by 4 weeks in 1999 and 8 weeks in 2000.

The switch when the bog reverted to being a carbon sink in June 1999 (Figure 5.12) is probably a consequence of respiration losses being minimised by cooler peat temperatures while photosynthesis was augmented as PPFD increased (Figure 5.13). The switch back to carbon sink after winter 2000 lagged the 1999 response by six weeks because peat temperatures were warmer and respiration losses would have been greater than during the same period in 1999.

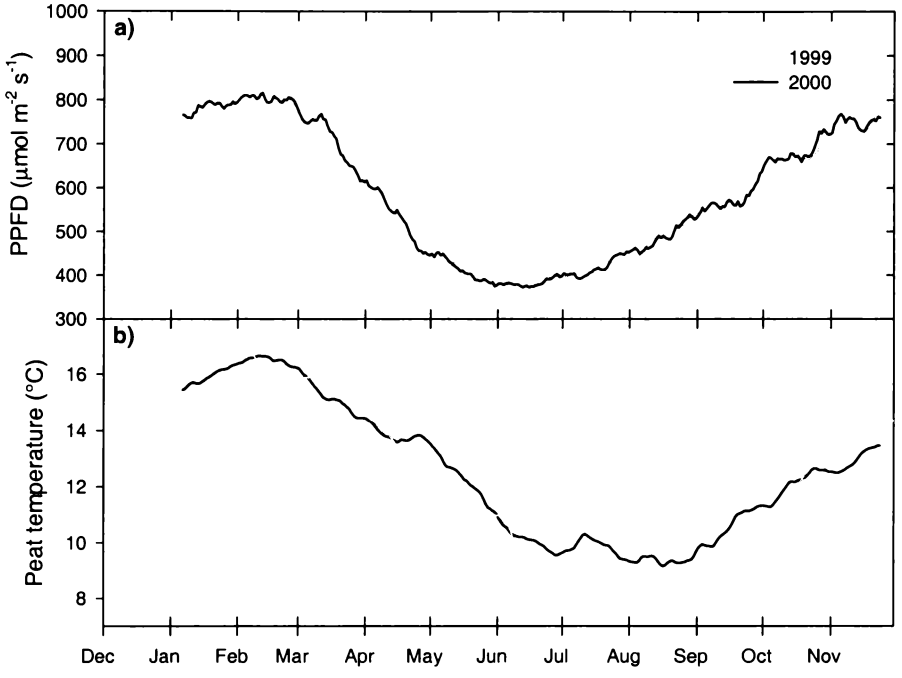

Figure 5.13 45-day running means of **(a)** mean daytime PPFD; and **(b)** daily mean peat temperature at 8 cm depth (T_s).

5.5.1 Model extrapolation beyond the two-year measurement period

Data from a meteorological station at Moanatuatua, 200 m east of the eddy covariance site, were collected between 1996-2000. These data are used for additional assessment of the interannual variability of carbon sequestration. Incident solar radiation is used to calculate PPFD described by the regression equation shown in Figure 5.14, with units µmol m^{-2} s^{-1}. Peat temperature data from Moanatuatua meteorological station were spurious due to damaged cables and records of T_s from Kopouatai restiad peat bog (90 km north of Moanatuatua) were used instead.

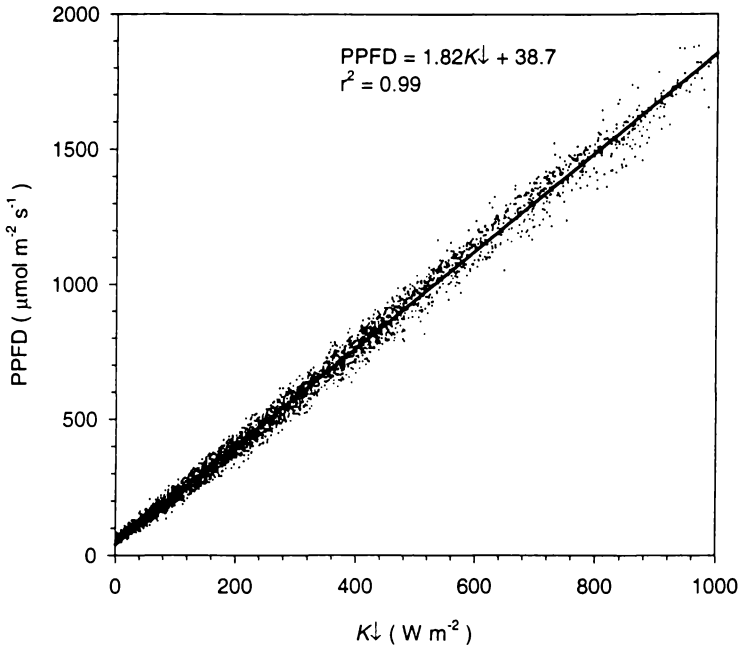

Figure 5.14 $K\downarrow$ versus PPFD measured at Moanatuatua between 15 December 1998 and 15 December 2000. Linear regression model of PPFD is shown.

A cumulative 2-year plot of modelled and measured PPFD reveals qualitative and quantitative agreement between measured PPFD and modelled values using $K\downarrow$ as input data (Figure 5.15). To ascertain the validity of using peat temperature data from Kopouatai peat bog, Figure 5.16 is a plot of eddy site T_s vs. soil temperature measured at Kopouatai meteorological site. Peat temperature measured at Kopouatai (T_{sKop}) provides a reasonable surrogate of T_s measured at Moanatuatua eddy site.

Two year's of cumulative NEE data are plotted in Figure 5.17. Gap filled eddy covariance data indicate a total sequestration of 3.97 tC ha^{-1} for this two year period and models are included in Figure 5.17 for comparison. The equations used for gap filling were used in stand-alone mode using PPFD and T_s data collected at the eddy site and meteorological stations.

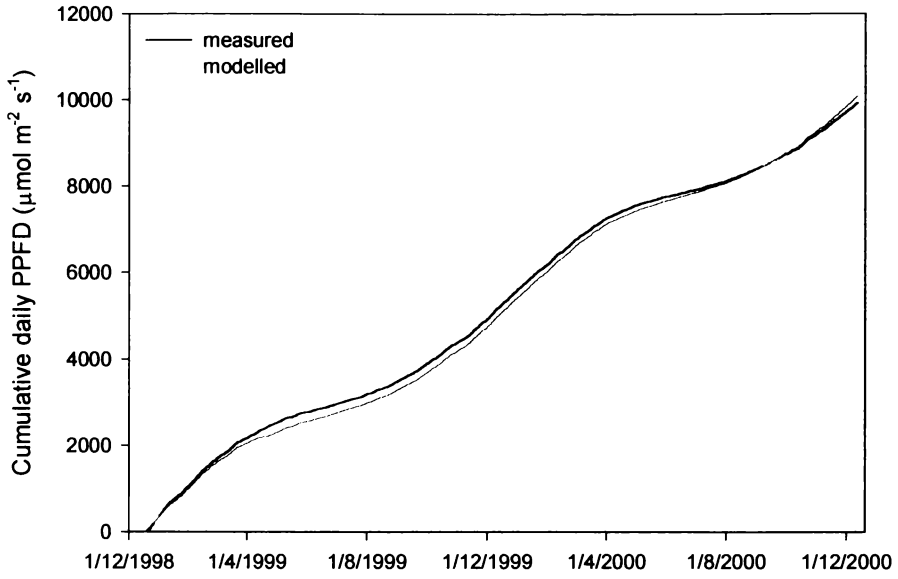

Figure 5.15 Cumulative plot of half-hourly PPFD for two years at Moanatuatua. Measured data were recorded with LI-190SZ quantum sensor. Modelled values were estimated with linear regression equation (see Figure 5.14), where $K\downarrow$ was measured at Moanatuatua meteorological station.

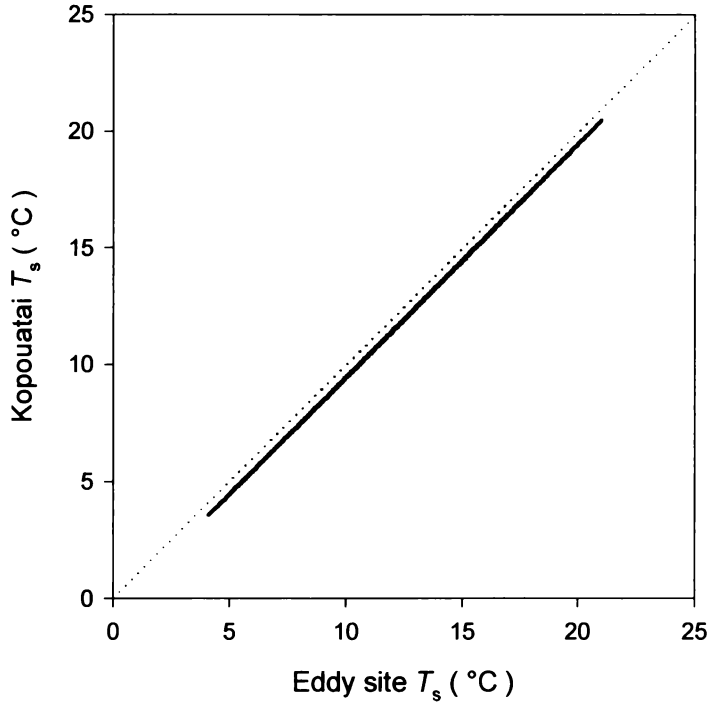

Figure 5.16 Peat temperature (T_s) measured at Moanatuatua eddy site vs. contemporaneous T_s data from Kopouatai meteorological station. Data represent the period 15 December 1998 – 15 December 2000. Solid line is linear regression (T_s=1.0006T_{sKop}-0.56, r^2 =93%). Dotted line is 1:1 line.

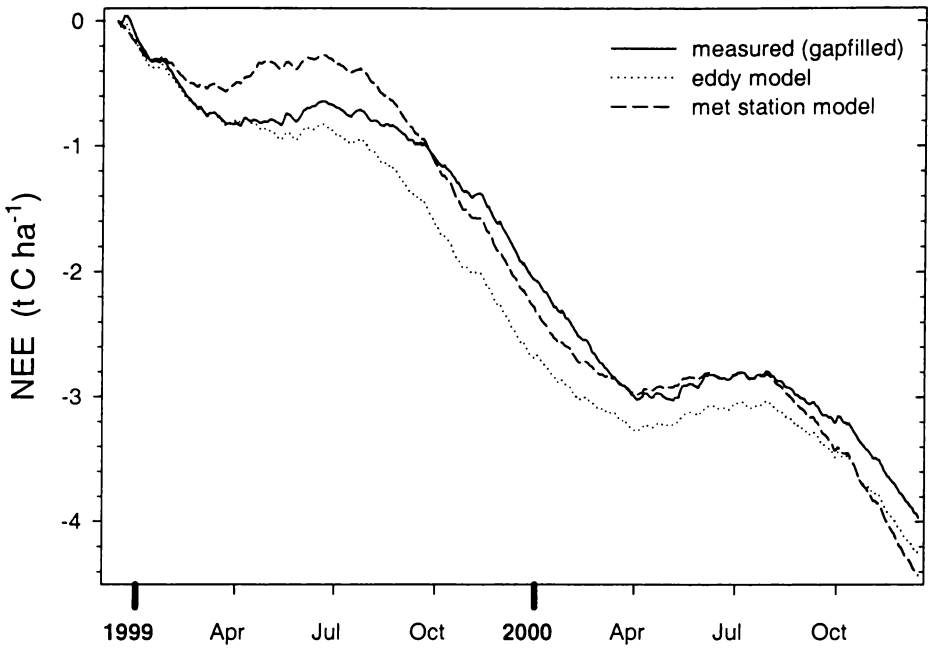

Figure 5.17 Cumulative NEE over two years from 15 December 1998 to 15 December 2000. The measured curve is obtained using gap filled eddy covariance data and is the most realistic estimate with a total sequestration of 3.97 tC ha^{-1} for the two years. The eddy model uses data measured at the eddy site, while the meteorological (met) station model uses data from Moanatuatua and Kopouatai meteorological stations.

With estimated sequestration of 4.25 tC ha^{-1}, the eddy model is in reasonable qualitative and quantitative agreement with the observed NEE, albeit not as remarkably so as the agreement demonstrated by Schmid et al. (2000) in a similar exercise.

To test the utility of data from the meteorological stations in providing a longer-term model of interannual NEE, a cumulative plot of modelled NEE is shown for comparison with the eddy model (Figure 5.17). The meteorological station model generally mimics the eddy model except for a period of over-estimation in winter 1999 and underestimate in spring 2000.

Caution must be exercised with interpreting these results. As noted by Schmid et al. (2000), validation of carbon exchange models by comparison with gap filled eddy covariance data (e.g. Figure 5.17) is not strictly judicious. A percentage of the eddy covariance data are modelled and therefore not completely independent of the model. Figure 5.17 is most appropriate for verifying that NEE at Moanatuatua was driven

primarily by incident solar radiation and peat temperature under the climatic regime of 1999–2000.

For the purposes of modelling seasonal–interannual NEE in this research, a limitation is that gap-filled eddy covariance data are used to verify the NEE models. Future research could overcome this limitation by contemporaneously measuring NEE by eddy covariance and alternative means, such as incremental biomass measurements (e.g. Schmid et al., 2000). The models developed here should not be used, under any circumstances, for estimating short–term carbon budgets. However they are useful for indicating trends of carbon exchange over seasonal–interannual periods.

A major objective of this analysis was to test the validity of measurements from meteorological stations at Moanatuatua and Kopouatai as input data for NEE models. The meteorological station model overestimates the measured observation by a small percentage, as does the eddy model (Table 5.3). $K\downarrow$ and T_s data from the Moanatuatua and Kopouatai meteorological stations respectively appear to provide reasonable estimates of annual and interannual carbon sequestration at Moanatuatua peat bog.

Table 5.3 Estimates of carbon accumulation over two years 15 December 1998 to 15 December 2000. The measured value is the most realistic, while eddy and meteorological station models are determined using input data from the eddy site, Moanatuatua and Kopouatai meteorological stations respectively. Over-estimation is the percentage that modelled values exceed measured.

	NEE (tC ha^{-1})	Over-estimation (%)
measured/gap filled	3.95	
eddy model	4.25	6.8
Met. station model	4.43	11.6

$K\downarrow$ measured at Moanatuatua met station is used with T_{sKop} to construct a four-year plot of cumulative NEE (Figure 5.18). The cumulative plots of modelled NEE for 1999 and 2000 in Figure 5.18 have been compared with measured data (Figure 5.17, Table 5.4). Cumulative NEE was similar for the years 1998–2000 and the 1998 annual budget was similar to 1999 and 2000 measured NEE (Table 5.4). 1997 differed from the other years,

being carbon neutral for only a few weeks. Consequently, an estimated 3.24 tC ha^{-1} was sequestered during 1997: at least 46% more than other years (Table 5.4).

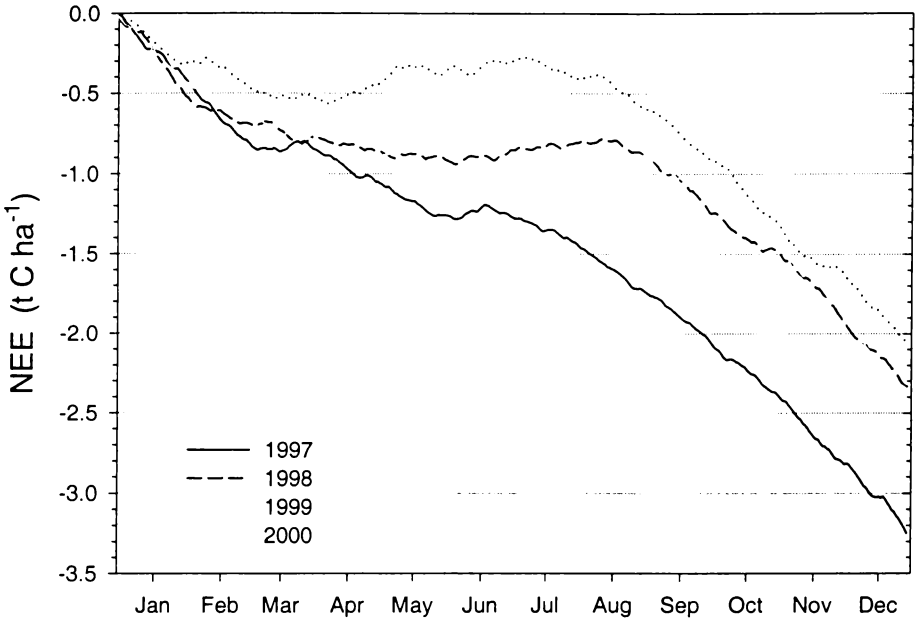

Figure 5.18 Modelled carbon sequestration (NEE) at Moanatuatua wetland 15 December 1996 – 15 December 2000.

Table 5.4 Estimates of annual carbon accumulation 15 December 1996 – 15 December 2000. Data from meteorological stations were used to model NEE.

	Modelled NEE (tC ha^{-1})	Measured NEE (tC ha^{-1})
2000	2.37	2.10
1999	2.06	1.85
1998	2.33	
1997	3.25	

Because the NEE models have only two inputs, PPFD and T_s, an explanation for the disparate timing of source-sink switching in 1997 and 1998 should not be too elusive. PPFD was similar between 1997 and 1998, but peat temperatures were generally cooler in 1997 (Figure 5.19). This was especially apparent during winter 1997. Therefore respiration losses would have been reduced in 1997, leading to the increased annual sequestration. The brief periods of carbon neutrality in March and June 1997 were caused by temporary increase of T_s at those times (Figure 5.19a).

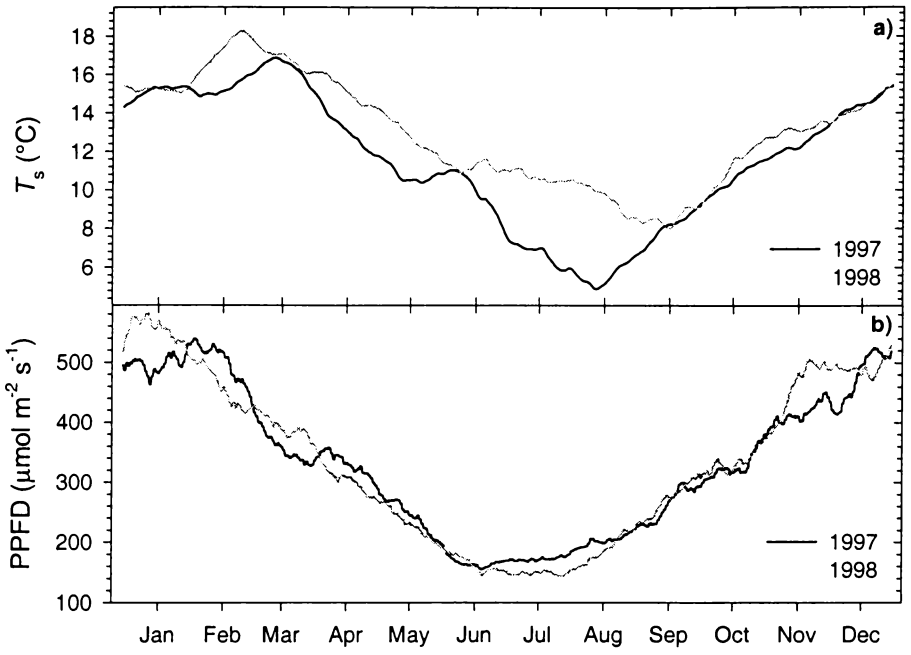

Figure 5.19 30-day moving averages of **(a)** peat temperature (T_s) at Kopouatai and **(b)** incident PPFD at Moanatuatua meteorological station.

A Tukey's pairwise comparison of mean annual T_s reveals strong evidence that the peat temperature was cooler in 1997 than the other three years, however there is no evidence that any of the years 1998–2000 had significantly different mean annual T_s (Table 5.5). Figure 5.19b shows seasonal variation in daily PPFD, estimated using $K\downarrow$ for 1997 and 1998. The 30-day running mean of PPFD for 1997 is similar to the plot for 1998 and Table 5.6 indicates there is no significant difference in the annual mean of daily PPFD measured during any of the years 1997–2000.

This evidence suggests that the difference in modelled NEE between 1997 and 1998 is a consequence of reduced respiration losses in 1997, rather than increased photosynthetic production (GEP). Figure 5.20 verifies that greater annual accumulation of carbon in 1997 compared with 1998 was a consequence of decreased respiration losses in 1997, while modelled GEP was similar for the two years.

Table 5.5 Multiple comparisons of mean annual peat temperature (°C) measured at Kopouatai meteorological station: Tukey's method (** indicates α=0.01)

Comparison	$(\bar{x}_i - \bar{x}_j)$	$(\bar{x}_i - \bar{x}_j) \pm 0.91$
1997 -1998	-1.33	(-0.42, -2.24)**
1997 -1999	-1.21	(-0.30, -2.12)**
1997 -2000	-1.24	(-0.33, -2.15)**
1998 -1999	0.12	(1.03, -0.79)
1998 -2000	0.09	(1.00, -0.82)
1999 -2000	-0.03	(0.88, -0.94)

Table 5.6 Analysis of variance table for mean annual PPFD (μmol m^{-2} d^{-1}) measured at Moanatuatua meteorological station, 1997–2000.

Source of variation	SS	df	MS	F	P-value
Between groups	67025	3	22342	0.223	0.881
Within groups	1.46E+08	1456	100298		
Total	1.46E+08	1456			

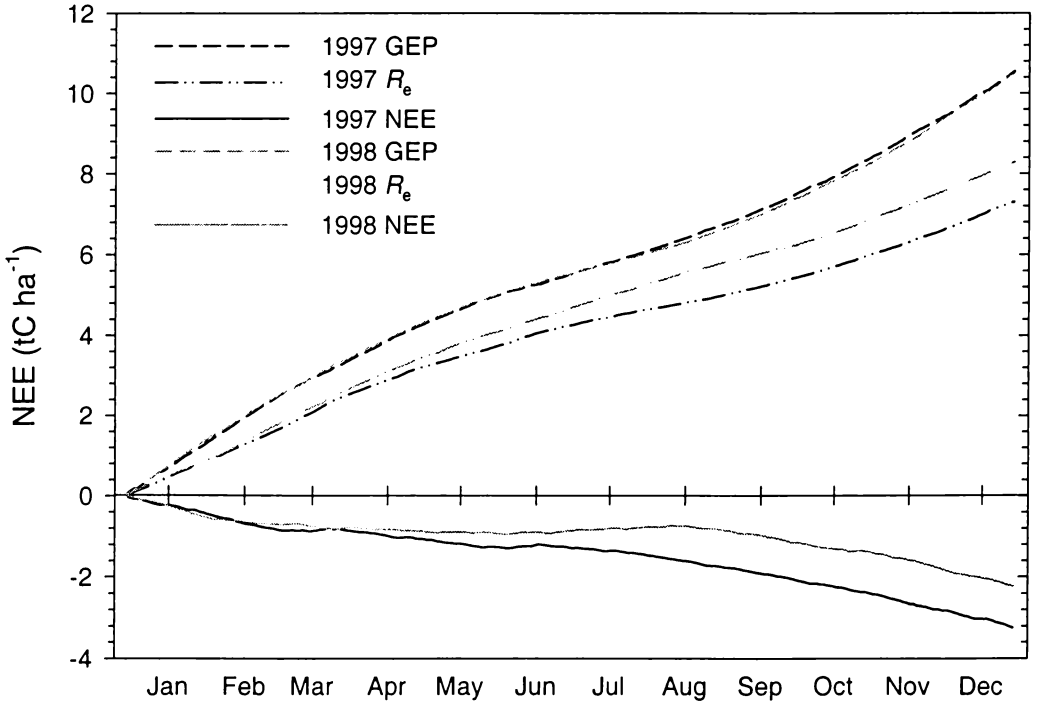

Figure 5.20 Modelled annual cumulative carbon balance components at Moanatuatua for 1997 and 1998 (15 December 1996 to 15 December 1998).

The annual sequestration of carbon at Moanatuatua (1.85 and 2.10 tC ha^{-1} for 1999 and 2000 respectively) is compared to that of other ecosystems in Table 5.7. Annual sequestration at Moanatuatua was greater than that reported for other wetlands around the world, and greater than sequestration at mature Boreal aspen and Amazonian rain forests (Table 5.7). Disturbed forests such as the slash pine described by Clark et al. (1999) sequester more carbon than those that have reached a long-term steady state (Baldocchi et al., 2001).

Annual measured NEP at Moanatuatua is similar to that observed at a temperate mixed hardwood forest (Schmid et al., 2000), however the seasonal dynamics of this ecosystem differs to Moanatuatua. While the rate of carbon sequestration during the growing season is greater at the mixed hardwood forest than at Moanatuatua, senescence reduces photosynthetic activity to almost nil during the winter at the former site. The seasonal variation of NEP is attenuated at Moanatuatua, so that annual sequestration almost matches that observed at the mixed hardwood forest.

Table 5.7 Annual carbon sequestration of Moanatuatua compared with results from other ecosystems. NEP data are annual except where indicated otherwise.

Reference	Ecosystem	Annual NEP (tC ha^{-1})
Nieveen et al. (1998)	Former raised bog (Netherlands)	- 0.97
Shurpali et al. (1995)	Boreal peatland (growing season)	-0.71 – 0.32
Clark et al. (1999)	Cypress wetland	0.37 – 0.84
Lafleur et al. (2001)	Ombrotrophic bog (Ottawa, Canada)	0.68
Grace et al. (1996)	Amazonian rain forest	1.02
Chen et al. (1992)	Boreal aspen	1.4 – 1.8
This research	**Moanatuatua peat bog**	**1.85 – 2.10**
Schmid et al. (2000)	Indiana deciduous forest	2.4
Wofsy et al. (1993) and Goulden et al (1996)	Northern hardwood (oak-maple)	2.0 – 5.0
Greco & Baldocchi (1996)	Southern hardwood	5.25
Clark et al. (1999)	Slash pine plantation	6.1 – 7.4

5.6 Summary

At the diurnal scale, carbon uptake is maximised during summer mornings. Diurnal courses of ensemble average NEE were constructed for both summer and winter. Summertime ensemble NEE peaked at 7.33 (±0.6) μmol m^{-2} s^{-1}, while nocturnal respiration losses were in the order of 2–3 μmol m^{-2} s^{-1}. During winter respiration losses were reduced because of cooler peat temperatures, however uptake of CO_2 was also decreased by shorter daylength and peak ensemble average NEE was reduced to 4.1 (±0.5) μmol m^{-2} s^{-1}. The sum of the daily ensemble mean NEE for winter indicates a small average gain of 0.12 gCO_2 m^{-2} d^{-1}, whereas a strong daily sink of 4.94 gCO_2 m^{-2} d^{-1} was observed for the summer ensemble average.

Models were developed for gap filling, with respiration driven by temperature and GEP modelled based on inputs of PPFD. Moanatuatua bog was a carbon sink for almost all of 1999 and 2000, apart from 2–3 months during autumn–winter when the wetland was a source of CO_2. The seasonal trend of carbon exchange was different between 1999 and 2000, mainly because the variation of peat temperature differed between the two years. A modelling exercise showed that carbon exchange is most sensitive at interannual timescales to variation of respiration, driven by temperature variability.

Annual carbon sequestration was 1.85 tC ha^{-1} for 1999 and 2.10 tC ha^{-1} for 2000. This is greater than rates of sequestration observed at other wetlands and similar to mature forest ecosystems.

6 Controls of carbon exchange

6.1 Introduction

Moanatuatua bog is an accumulation of carbon that has been sequestered from atmospheric CO_2 and stored as peat for more than 13 000 years (Clarkson et al., 1999; Newnham et al., 1995; Shearer, 1997). This research provides only a snapshot of contemporary carbon sequestration rates at Moanatuatua. To facilitate assumptions regarding long term peat condition and ecosystem health following modifications to climate or hydrology, it is necessary to understand the processes that control rates of carbon accumulation.

Since the Taupo eruption 1800 years BP, it is believed that peat has accumulated at a rate of 1mm yr^{-1} at Moanatuatua bog and this height growth is equivalent to mass increments of 0.34 tC ha^{-1} yr^{-1} (Schipper and McLeod, 2002). This rate is an order of magnitude less than 1.98 tC ha^{-1} yr^{-1} average accumulation measured for the two years of this research, suggesting that the rate of peat accumulation has been augmented by relatively recent environmental perturbation. With bulk density 0.06 t m^{-3} and carbon content 52% in peat above the Taupo tephra (Schipper and McLeod, 2002), 1.98 tC ha^{-1} yr^{-1} equates to possible peat accumulation of 6.35 mm yr^{-1}. This anomaly is especially surprising considering recent suggestions that the lowered water table at Moanatuatua may have increased rates of peat degradation (Shearer, 1997).

To investigate this irregularity, the processes that control carbon accumulation rates and the role of hydrology at Moanatuatua bog are considered. Long term implications for climate change scenarios are also examined so that the consequences of global warming may be estimated.

6.2 Radiation use efficiency

Radiation use efficiency, RUE, has been used to describe the effectiveness of ecosystems in using PAR to produce biomass and is the quantity of CO_2 assimilated per unit of solar radiation absorbed (Moncrieff et al., 1997c). Commonly expressed as the ratio of daily CO_2 uptake (NEP) to PPFD, RUE may be useful for explaining variation of ecosystem production during periods of climatic variation such as cloudy versus clear-sky days (Hollinger et al., 1994).

Canopy quantum efficiency (Moncrieff et al., 1997c) or marginal quantum yield (Hollinger et al., 1994) is another gauge of RUE, defined by the initial slope of the relationship between canopy CO_2 flux and PPFD (0–500 μmol m^{-2} s^{-1}). The marginal quantum yield is radiation use efficiency maximised as PPFD approaches zero: when shallow solar angle and low light intensity maximises the quantum efficiency (Wofsy et al., 1993).

6.2.1 Marginal quantum yield

The initial slope of the GEP model in Figure 5.7 is α_q = 0.017, indicating annually-averaged marginal quantum yield at Moanatuatua bog is 0.017 μmol CO_2 μmol $PPFD^{-1}$. Table 6.1 lists marginal quantum yields determined with eddy covariance observations for various ecosystems and study periods. The Moanatuatua marginal quantum yield is the same as α_q = 0.017 μmol CO_2 μmol $PPFD^{-1}$ for aggregated data sets from northern bogs (Frolking et al., 1998) while at a restored bog in the Netherlands, Nieveen (1998) observed α_q= 0.026 μmol CO_2 μmol $PPFD^{-1}$. Moncrieff et al. (1997c) found marginal quantum yield ranged between 0.012 and 0.020 μmol CO_2 μmol $PPFD^{-1}$ at Sahelian savannah and millet sites. Much smaller values were observed on bush covered sites, where α_q= 0.0059 and 0.0029 μmol CO_2 μmol $PPFD^{-1}$ were observed during well-watered and water stressed periods respectively (Moncrieff et al. 1997c). Quantum yields up to α_q= 0.055 μmol CO_2 μmol $PPFD^{-1}$ have been observed for forests, while greenhouse experiments have revealed quantum yields as high as 0.070 μmol CO_2 μmol $PPFD^{-1}$ for C_3 plants.

Compared with other ecosystems in Table 6.1, the Moanatuatua observation of α_q= 0.017 μmol CO_2 μmol $PPFD^{-1}$ suggests the vegetation has a relatively low efficiency at using radiation to sequester atmospheric carbon. However the smaller than average marginal

quantum yield at Moanatuatua is possibly a consequence of the oligotrophic environment rather than poor performance from the vegetation *per se*.

To survive in the oligotrophic environment, the restiad vegetation uses xerophytic characteristics including reduced individual leaf area and sunken stomata (Sharp 1995). Even if they could compete ecologically with the restiads at Moanatuatua, other plant species in Table 6.1 would probably have their marginal quantum yield restricted by the physiological inability to cope with oligotrophic conditions. With α_q=0.017 μmol CO_2 μmol $PPFD^{-1}$ and α_q=0.023 μmol CO_2 μmol $PPFD^{-1}$ for northern bogs and nutrient-rich fens respectively (Table 6.1), the results of Frolking et al. (1998) suggest that marginal quantum yield of bog ecosystems is restricted by paucity of nutrients.

Table 6.1 Marginal quantum yield (α_q) = initial slope of light response curves (GEP vs PPFD) for a range of ecosystem types worldwide.

Description	α_q (μmol CO_2 μmol $PPFD^{-1}$)	Reference
Sahelian bush (water stressed)	0.0029	Moncrieff et al. (1997c)
Sahelian bush (well watered)	0.0059	Moncrieff et al. (1997c)
Sahelian savannah	0.012	Moncrieff et al. (1997c)
Moanatuatua bog	**0.017**	**This study**
Northern peat bogs	0.017	Frolking et al. (1998)
Sahelian millet	0.020	Moncrieff et al. (1997c)
NZ *Nothofagus* forest (excluding winter)	0.022	Hollinger et al. (1994)
Northern fens	0.023	Frolking et al. (1998)
Crops (mean of several studies)	0.023	Ruimy et al. (1995)
Restored raised peat bog (Netherlands)	0.026	Nieveen et al. (1998)
Forests (mean of several studies)	0.035	Ruimy et al. (1995)
Black Spruce forest	0.040	Goulden et al. (1997)
Boreal forest (mean seasonal α_q)	0.042	Hollinger et al. (1999)
Deciduous forest (midsummer)	0.040–0.055	Wofsy et al. (1993)
C3 plants (greenhouse experimental maximum)	0.060–0.070	Farquhar et al. (1980)

It would be misleading to suggest that restiad vegetation at Moanatuatua is inefficient at assimilating carbon. One explanation for restiads dominating the Moanatuatua ecosystem

is that, relative to other plant families, they are efficient at maximising photosynthesis *in that environment*. Moreover, α_q is an indicator of photosynthetic (or GEP) efficiency, yet bog ecosystems may be efficient at sequestering carbon (NEP) via minimisation of respiration losses rather than astonishing rates of photosynthesis (Clymo, 1983). Therefore while some ecosystems exhibit larger rates of photosynthetic carbon assimilation (i.e. GEP) in more ideal environments, their respiration losses are greater than wetland ecosystems.

A more important application of radiation use efficiency may be to predict the perturbation of carbon sequestration through change in solar radiation receipt as a consequence of climate change via global warming. Clymo (1983) notes that peat accumulation is the result of photosynthetic production rate exceeding the rate of decay and both of these rates are generally low in bogs. A small decrease in photosynthetic productivity or radiation use efficiency can have a profound effect on the delicate relationship between production and decay, switching the bog from a sink to a source of atmospheric carbon. The relatively low marginal yield at Moanatuatua indicates a low rate of photosynthetic production compared to other ecosystems. Therefore a small decrease in radiation use efficiency may have a significant negative impact on the peat accumulation process and ecosystem welfare.

An investigation of climate change scenarios is therefore warranted; especially the effect on radiation use efficiency of modified cloud cover according to IPCC (2001a) predictions.

6.2.2 Effect of clouds on CO_2 exchange

An observed worldwide increase of cloud cover throughout the last century has been attributed to climate change associated with global warming (IPCC, 2001b). Climate change predictions include an intensified westerly air flow over New Zealand (IPCC, 2001b) and this is likely to generate increased cloud cover in the Waikato.

Cloud cover has several effects on carbon sequestration. Uptake of carbon may be reduced because of a decrease in solar radiation available for photosynthesis and ecosystems might switch from sink to source of CO_2 if climatic variations increase cloud cover (Fan et al., 1990). Alternatively, for the same magnitude of clear-sky PPFD, the presence of clouds can increase CO_2 assimilation via improved radiation receipt within the canopy due to a higher diffuse fraction or through reduction in vapour pressure deficit (Gu et al., 1999).

Compared with clear sky solar radiation, diffuse radiation promotes photosynthesis by reducing shadows within the canopy (Roderick et al., 2001). Respiration losses may also be reduced through lower air and soil temperatures associated with increases in cloudiness (Gu et al., 1999).

To investigate the effect of increased cloud cover on peat accumulation at Moanatuatua, the radiation use efficiency was assessed for cloudy and clear sky periods. A cloudiness index was defined according to the ratio $C_{ind}=K\downarrow/K_m$ of measured to modelled solar radiation receipt. Clear sky radiation (K_m) was modelled by determining the extraterrestrial solar radiation, K_{ex}, (following Gu et al., 1999) and multiplying by a transmissivity coefficient, τ, found to equal 0.76 by plotting for many clear sky summer and winter days as in Figure 6.1.

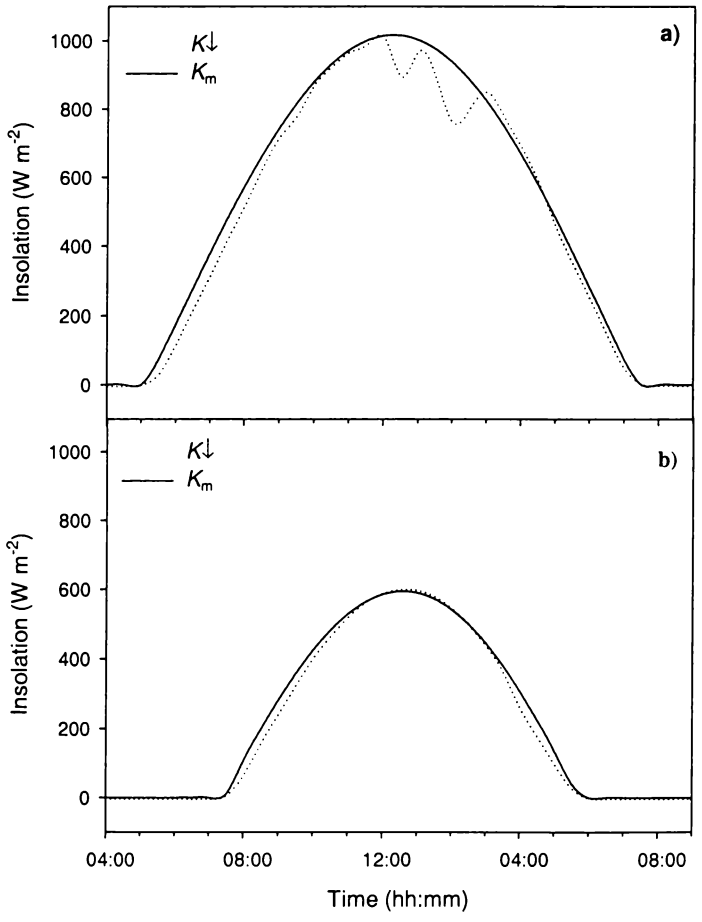

Figure 6.1 Determination of transmissivity coefficient (τ). Modelled (K_m) and measured ($K\downarrow$) insolation for clear sky day in **(a)** summer (23 November 1999) and **(b)** winter (8 August 1999) at Moanatuatua. K_m is calculated as extraterrestrial solar irradiation multiplied by $\tau = 0.76$.

The cloudiness index was determined for all half-hourly periods when K_m>100 W m^{-2}. Half-hourly periods of flux measurements are defined as cloudy when C_{ind}<0.25, and clear skies identified by C_{ind}>0.90. Partly cloudy periods with 0.90>C_{ind}>0.25 are not considered because to make a general statement of the effect of cloudiness on NEE, this analysis will compare RUE under clear sky and obviously cloudy conditions.

Figure 6.2 shows diurnal courses of modelled and measured $K\downarrow$ for: a) 24 February 2000 with mostly clear sky conditions and b) 21 December 1999, a cloudy day. By 0830 hours on 24 February 2000 the cloudiness index is above 0.90 which is the threshold indicating clear skies. Two periods during the afternoon when $K\downarrow$ dips below K_m are defined as partly cloudy by C_{ind} that decreased to approximately 0.7 in Figure 6.2a. Cloudy skies prevailed for almost all of 21 December 1999, with $K\downarrow$ much lower than K_m throughout the day (Figure 6.2b). The cloudiness index remained below the threshold 0.25 for almost the entire day (Figure 6.2d) which indicates cloudy conditions except for 1100 hours when C_{ind} exceeded 0.25 and is partly cloudy by definition.

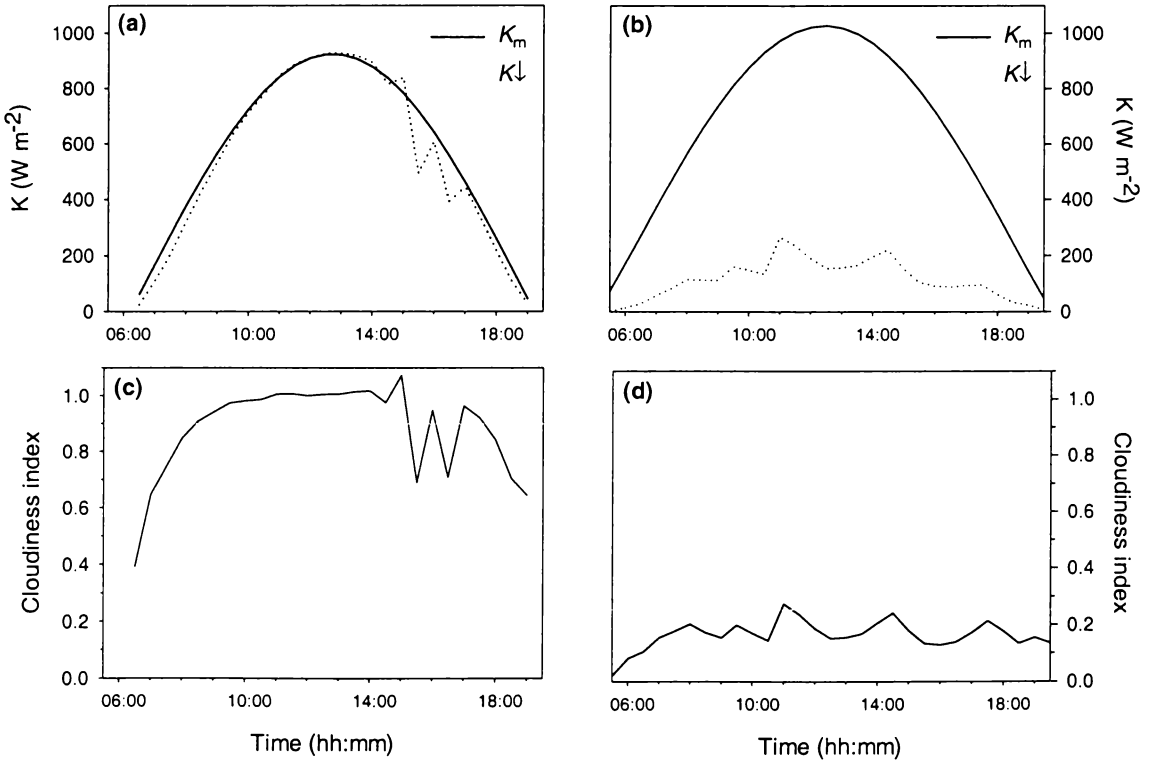

Figure 6.2 Determination of cloudiness index for a mostly clear sky day (plots **a** and **c**, 24 February 2000) and a cloudy day (plots **b** and **d**, 21 December 1999). As in **Figure 6.1**, K_m is calculated as extraterrestrial solar irradiation multiplied by $\tau = 0.76$.

Figure 6.3 shows RUE as the net ecosystem exchange of carbon plotted against PPFD under cloudy and clear skies. Except under extremely low magnitudes of PPFD, carbon sequestration is higher during cloudy periods than for clear-sky periods with the same PPFD (Figure 6.3).

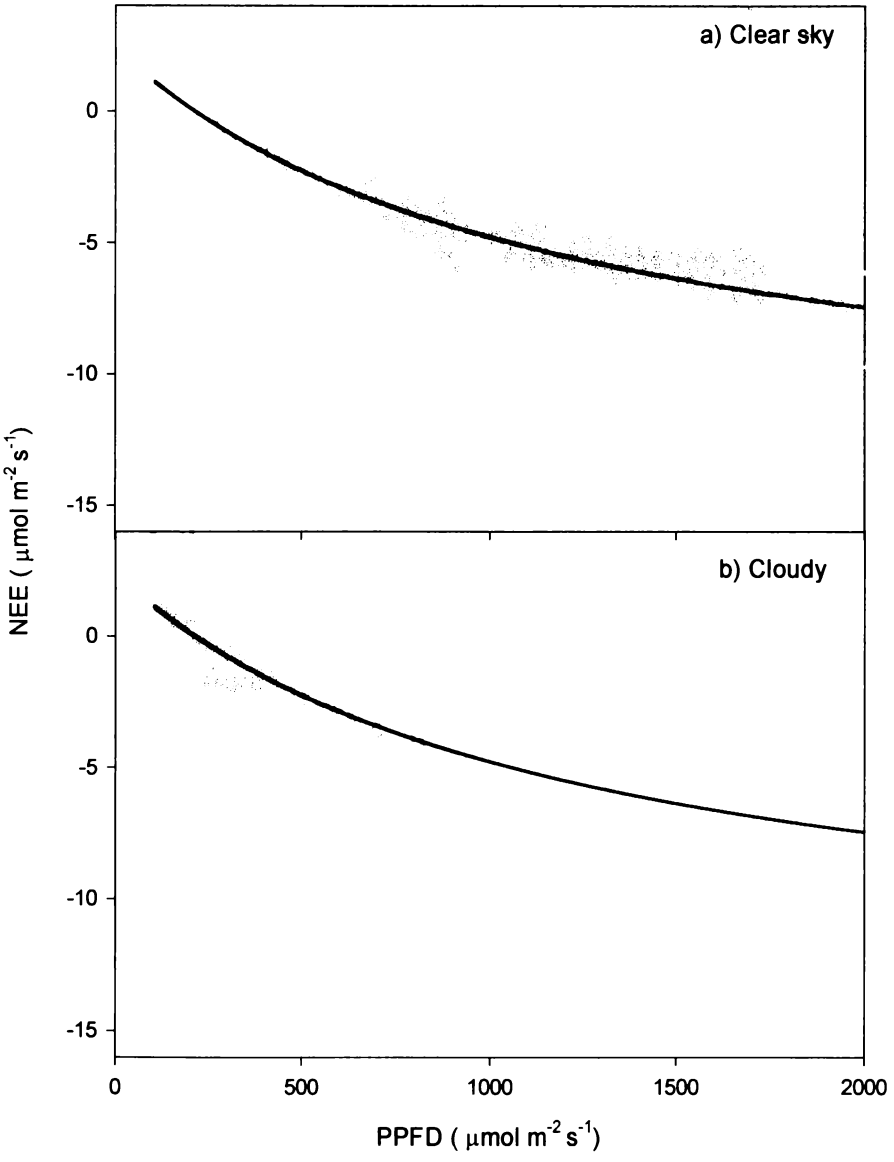

Figure 6.3 The net ecosystem exchange (NEE) as a function of PPFD at Moanatuatua under **(a)** clear sky and **(b)** cloudy conditions for half-hourly periods between December 1998 and December 2000. Solid line on both plots is the hyperbolic best fit line (NEE (μmol m^{-2} s^{-1}) = -16.05 [18.96 × 887.07]/[887.07 + PPFD]; r^2=0.55, n=3041) for clear sky data during the entire study period.

This result is consistent with other studies where higher RUE observed under cloudy conditions was such that carbon uptake was not reduced for increased frequency and magnitude of cloudiness (Fan et al., 1995; Goulden et al., 1997; Gu et al., 1999; Hollinger et al., 1994). Baldocchi et al. (2001) noted that marginal quantum yield under cloudy skies was nearly double that with direct, clear-sky radiation at a Scots pine forest in Finland. This phenomenon has been attributed mainly to the increase in diffuse radiation (Goulden et al., 1997; Hollinger et al., 1994) or a combination of diffuse radiation plus reductions in water stress, air temperature and soil temperature associated with cloudy skies (Gu et al., 1999).

The radiation receipt *per se* is reduced in winter however the reference line in Figure 6.4 shows data points for clear sky and cloudy days follow the same pattern of RUE in winter as in summer. Figure 6.5 also suggests there is no difference in mean daily RUE between seasons. An unpaired t-test revealed no significant difference ($p=0.16$) between the mean daily RUE averaged over summer and winter (4.0 and 3.7 mmol C mol^{-1} PPFD respectively).

Because the vapour pressure and soil moisture deficits, along with air and peat temperatures are reduced in winter (Figure 6.6) yet RUE is similar, these variables apparently have an insignificant effect on RUE and are not likely to be driving the cloudiness effect. By eliminating these variables, diffuse radiation remains as the sole candidate responsible for the impact of cloudiness on RUE.

In summary, increased cloudiness at Moanatuatua would reduce the magnitude of direct solar radiation available for photosynthesis, however this would be offset by improved radiation use efficiency as a consequence of more abundant diffuse radiation. Hence there would be insignificant impact on carbon accumulation rates via reduced PPFD as a consequence of increased cloudiness at Moanatuatua.

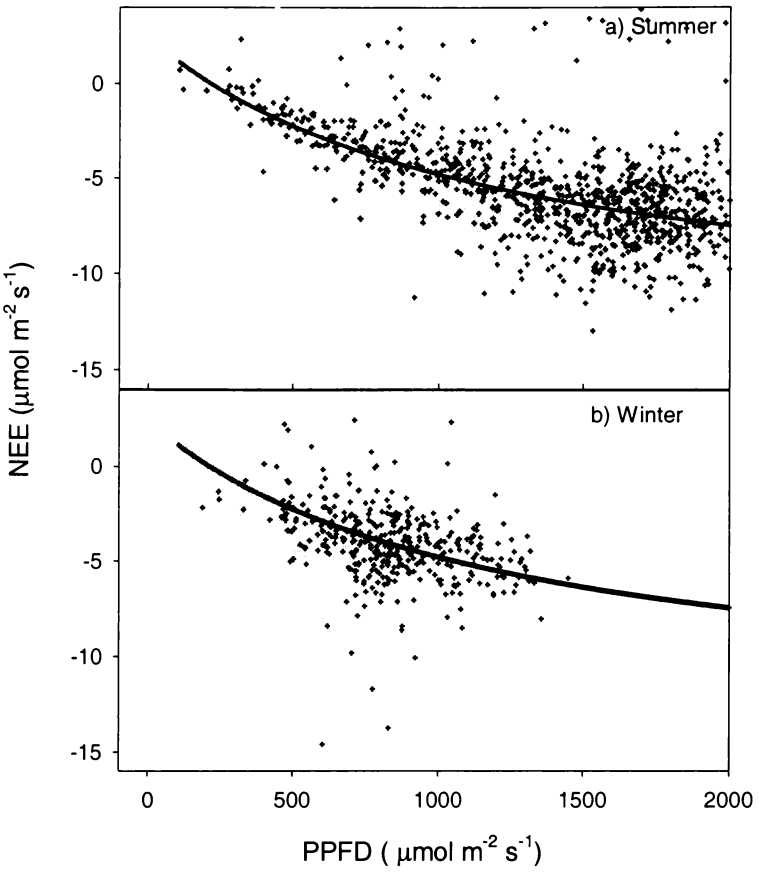

Figure 6.4 Radiation use efficiency under cloudy (grey dots) and clear sky (crosses) conditions during summer (Dec., Jan., Feb.) and winter (Jun., Jul., Aug.) at Moanatuatua. Solid line for comparison is the hyperbolic best fit line from **Figure 6.3** for clear sky data during the entire study period.

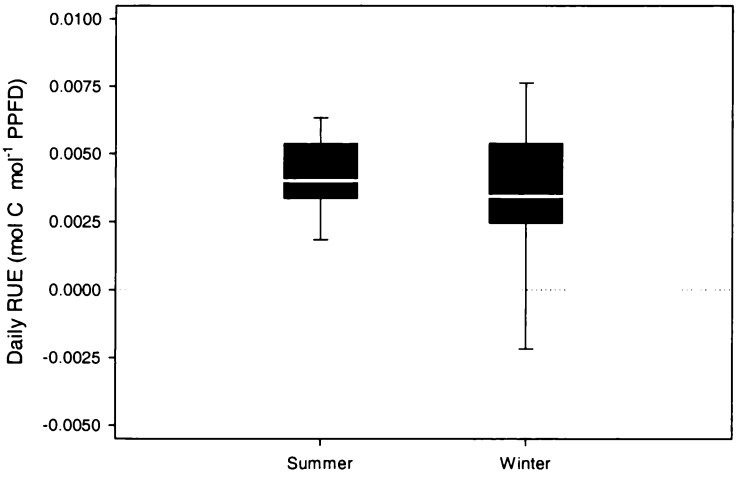

Figure 6.5 Box and whiskers plots of daily radiation use efficiency (RUE) observed during daylight (PPFD>50 μmol m^2 s^{-1}) periods over summer (Dec.–Feb.) and winter (Jun.–Aug.) at Moanatuatua. Boxes show 25th and 75th percentiles with a white line at the median, whiskers indicate 10th and 90th percentiles and outliers are included as grey dots.

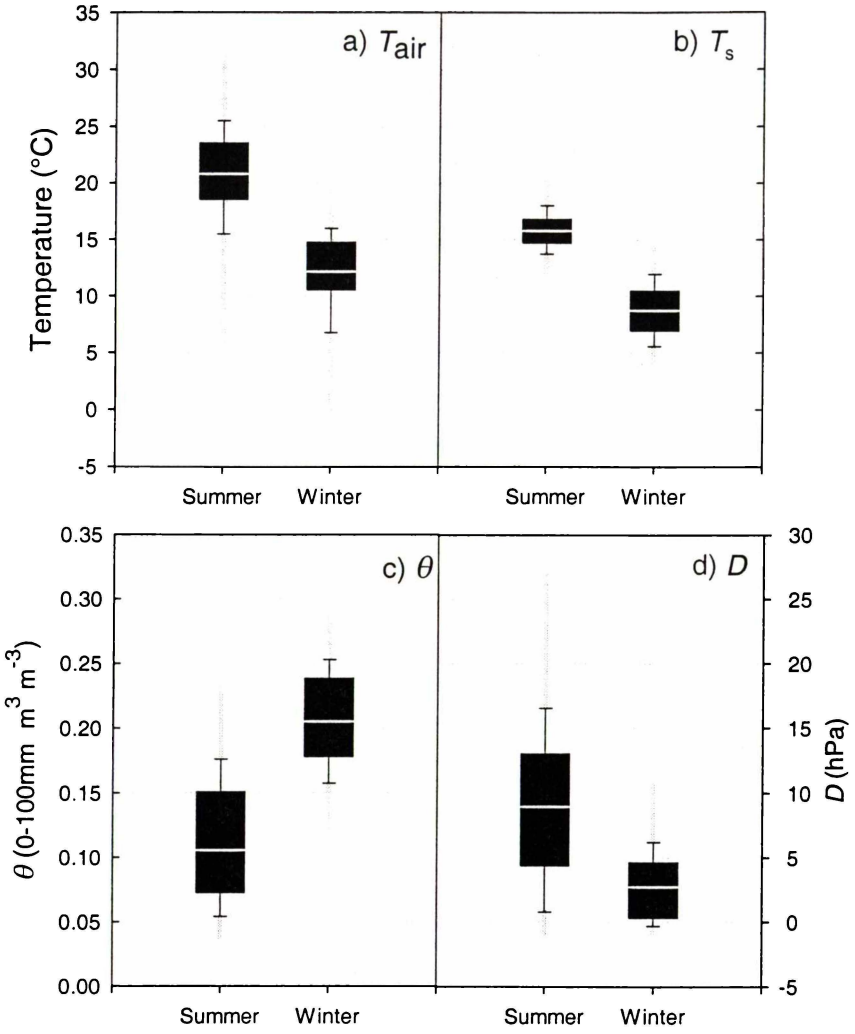

Figure 6.6 Box and whiskers plots of environmental variables observed during daylight (PPFD>50 μmol m^2 s^{-1}) periods over summer (Dec.–Feb.) and winter (Jun.–Aug.) at Moanatuatua. Plots show: **(a)** air temperature; **(b)** peat temperature at 80 mm depth; **(c)** volumetric peat moisture content (θ) averaged over 0-100 mm depth; **(d)** air saturation vapour pressure deficit (D). Boxes show 25th and 75th percentiles with a white line at the median, whiskers indicate 10th and 90th percentiles and outliers are included as grey dots.

Annual mean of daily RUE at Moanatuatua was 3.8 mmol C mol^{-1} PPFD and this is at the lower–mid end of a range (2–10 mmol C mol^{-1} PPFD) identified by Ruimy et al. (1994) over all vegetation types (cited in Valentini et al., 1995). Daily RUE at Moanatuatua is comparable to estimates of Ruimy et al. (1994) for temperate deciduous forests and grasslands, less than coniferous and equatorial evergreen forests and greater than estimates for tropical forests.

Figure 6.5 shows daily RUE at Moanatuatua does not vary seasonally and this is also worthy of comparison with other studies. In contrast, at a deciduous forest, Wofsy et al. (1993) observed decline of RUE to zero during winter senescence. Hunt et al. (2002) and Valentini et al. (1995) found the same occurred during drought at a New Zealand tussock grassland and a Californian grassland respectively. Reduced leaf area was a cause of the decline in RUE for these studies, with change in species composition also considered important by Hunt et al. (2002).

In a previous study at Moanatuatua, summertime leaf area index (LAI) was measured as 2.35 using the Chen and Black (1992) method for non-flat, living leaves (Thompson et al., 1999). Similar daily RUE during summer and winter in Figure 6.5 suggests that LAI does not vary seasonally at Moanatuatua. The upper 75th percentile of daily RUE at Moanatuatua is 5.5 mmol C mol^{-1} PPFD: larger than 4.5 mmol C mol^{-1} PPFD peak daily RUE reported by Hunt et al. (2002) for tussock grassland, but four times smaller than that of Wofsy et al. (1993) for deciduous forest. A major reason for these differences would be the corresponding LAI which was 0.5 (Hunt et al., 2002) and 3.5 (cited in Ruimy et al., 1995) respectively for the other studies.

It is perhaps surprising that variation of *D* does not provide a significant explanation for the difference between cloudy and clear sky RUE. After all, the diurnal pattern of NEE shown in Figure 5.1 supports Campbell and Williamson's (1997) hypothesis that stomatal closure late in the morning at restiad bogs is a plant physiological response to increased vapour pressure deficit that minimises water use. To further examine the role of *D* on RUE, the confounding effect of diffuse radiation was eliminated by summarising RUE for various classes of *D* during clear sky periods only (Figure 6.7).

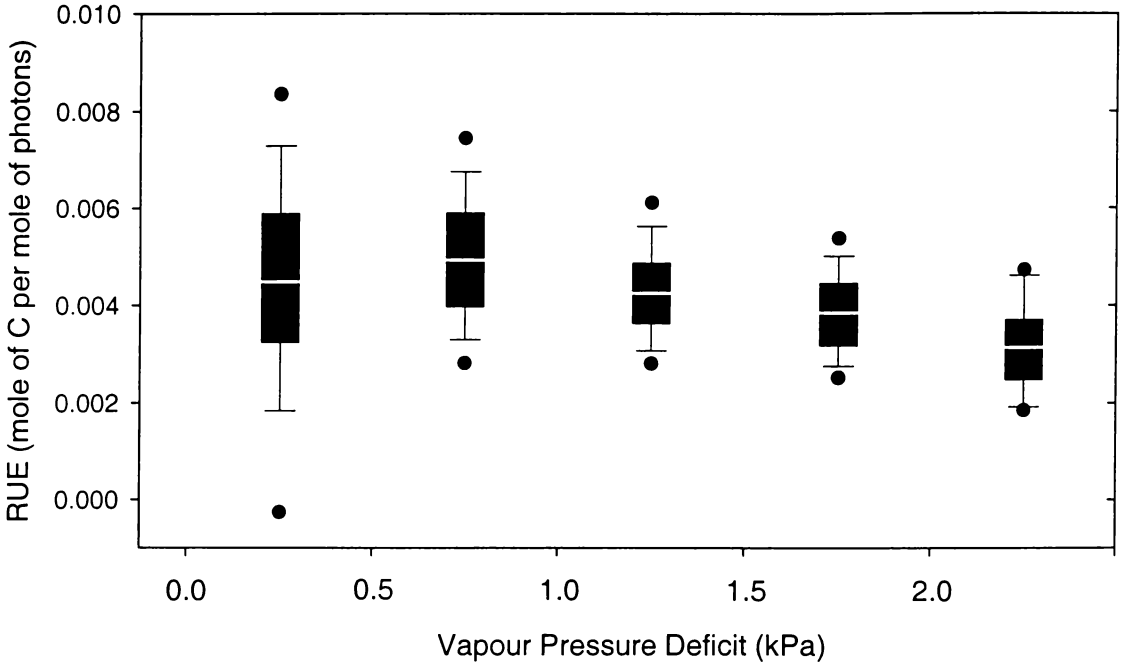

Figure 6.7 Radiation use efficiency as a function of *D* under clear sky conditions at Moanatuatua (half-hourly data). Boxes show 25th and 75th percentiles with a white line at the median, whiskers indicate 10th and 90th percentiles and 5th and 95th percentiles are included as black dots.

A Tukey's test (α=0.05) revealed significant differences between pairs of mean RUE for all classes of *D* except between (Figure 6.7, from left) boxes 1 and 3 and between boxes 4 and 5. Caution is required when interpreting these results. While the mean values of RUE are different, the magnitude of the difference is not great and the only significant decline in RUE is for *D*>1.5 kPa which represents less than 6% of daylight periods.

Thus while *D* may be important for explaining variation of diurnal NEE, the general effect of *D* on RUE does not appear to be significant for anticipating the long-term impact of climate change at Moanatuatua. This is consistent with conclusions in Chapter 4 that stomatal regulation of transpiration by *Sporodanthus* and *Empodisma* is not significant except during relatively rare periods indicated by large β. Photosynthesis is also regulated by stomatal closure and Figure 6.7 supports the hypothesis that stomatal closure driven by high evaporative demand is an infrequent phenomenon.

6.3 Hydrological interactions with peat production

It is believed that peat degradation has occurred at Moanatuatua as a consequence of a lowered water table (Shearer, 1997) and the development of peat bogs is dependant on their hydrological regime (Clymo, 1983). A 5% increase in annual rainfall predicted for the Waikato over the hundred years to 2080 (IPCC, 2001b) is likely to have consequences for the hydrological regime at Moanatuatua bog. This section investigates the impact that modification of precipitation may have on carbon sequestration and hence peat accumulation and ecosystem health. The validity of the assumption that Moanatuatua peat has degraded via water table lowering is also examined.

The effect of hydrology is introduced by investigating the water use efficiency (WUE).

6.3.1 Water Use Efficiency

The ratio of NEP to E (mg CO_2 g H_2O^{-1}) is a common and useful index of water use efficiency (WUE) at the canopy scale (Baldocchi, 1994). To illustrate this, the diurnal course of ecosystem WUE for a clear sky day and dry canopy is plotted in Figure 6.8 along with plots of its constituents: NEP and λE. Data from periods when PPFD<500 μmol m^{-2} s^{-1} were excluded because WUE is overly sensitive to low levels of solar irradiance (Baldocchi et al., 1985; Nieveen, 1998). In the early morning, photosynthesis proceeded strongly while D was low and atmospheric demand for evaporation was low (Figure 6.8); a strategy believed to optimise the growth performance of restiad vegetation (Sharp, 1995). WUE is maximised in the early morning as a consequence (Figure 6.8b).

WUE decreased during the day as D increased, recovering slightly late in the afternoon as D declined. This phenomenon is consistent with the field observations of Baldocchi (1994) for wheat and corn crops and Moncrieff at al. (1997c) for Sahelian millet. Sharp (1995) also observed maximum WUE during the early morning, using cuvette measurements of an *E. minus* specimen during a shadehouse experiment conducted over a 24 hour period.

In the absence of water stress the WUE of canopies with rough surfaces such as forests may be exclusively dependent on D (Baldocchi et al., 1987). This seems to be the case for Figure 6.8, with large WUE in the early morning when D was low, followed by a decrease of WUE as D increased later in the morning.

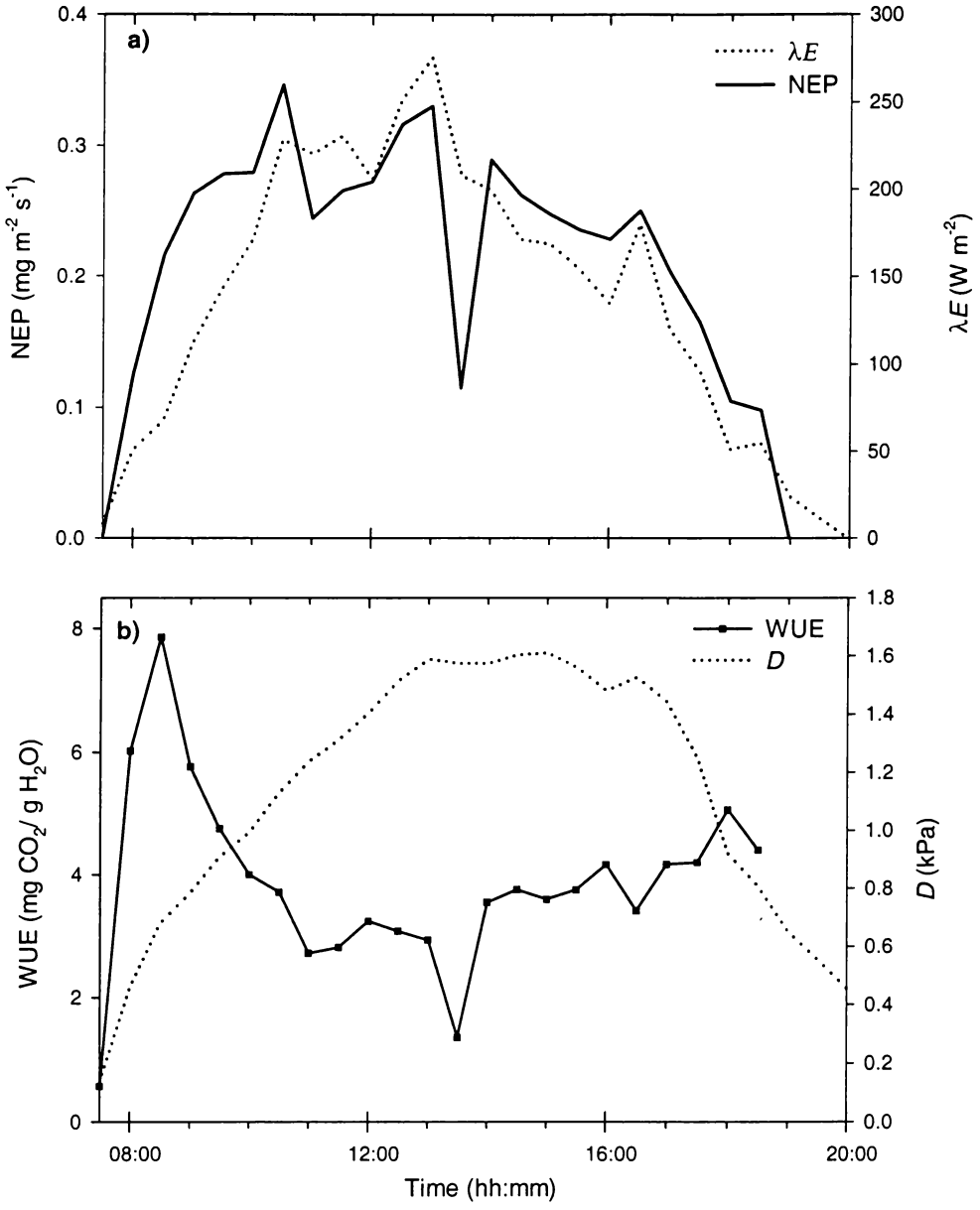

Figure 6.8 Diurnal variation of **(a)** net ecosystem production (NEP) and latent heat flux (λE); **(b)** water use efficiency (WUE) and vapour pressure deficit (D). Data are for 7 February 2000: a clear sky day with dry canopy and windspeed ranging between 2.5–4.5 m s^{-1}.

To test for a general relationship between WUE and D, half-hourly measurements are plotted in Figure 6.9. Due to considerable scatter at low D, there is no obvious relationship between the two variables. Conventional wisdom holds that WUE is usually greatest at low D, however a clear relationship is not apparent at low D in Figure 6.9.

Thompson et al. (1999) found evaporation rates were sensitive to variations of canopy wetness at Moanatuatua. Under wet canopy conditions β were as low as 0.5 whereas with dry canopy conditions H was the dominant flux, with β around 2 (Thompson et al., 1999). Because evaporation underpins WUE, the canopy wetness phenomenon is likely to be a source of variation in WUE.

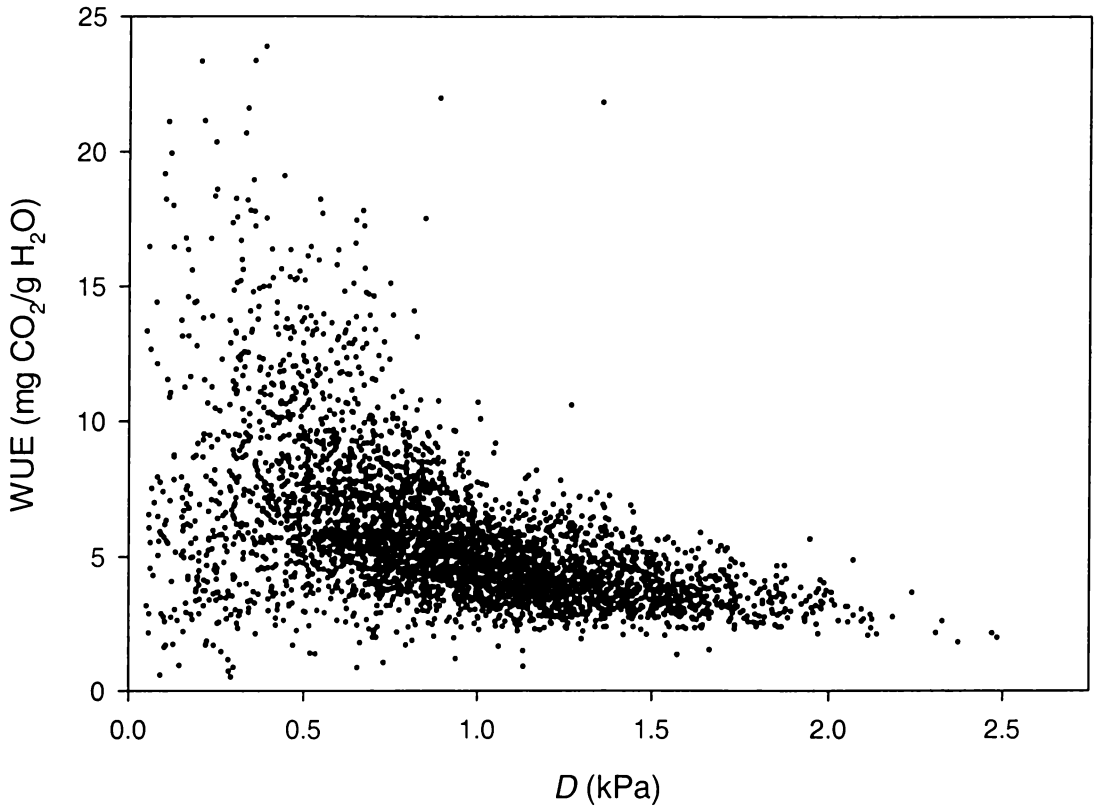

Figure 6.9 Relationship between water use efficiency (WUE) and vapour pressure deficit (*D*) for half-hourly periods between December 1998 and December 2000.

In this research, canopy wetness is defined using data from the leaf wetness sensors, with a wet or dry canopy identified by observations for all sensors being greater or less than 10% respectively. The transition from wet to dry canopy during 23 March, 2000 is illustrated in Figure 6.10, with the canopy totally wet at daybreak but drying at all levels by 1500 hours. Later in the evening the mid-canopy became wet again: a likely consequence of dew since there was no precipitation on 23 March, 2000. Figure 6.11 shows that WUE is also sensitive to variations of canopy wetness and this helps explain the scatter at low *D* in Figure 6.9.

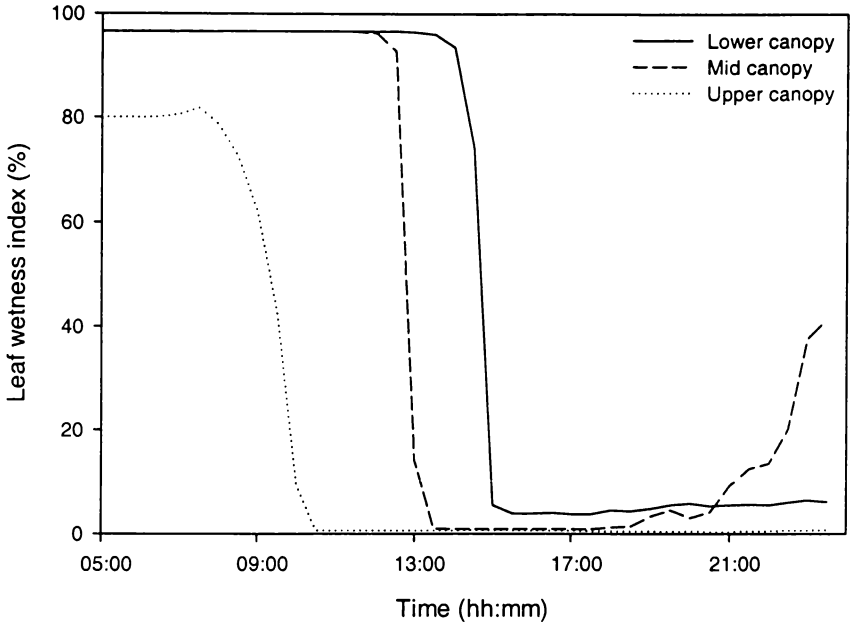

Figure 6.10 Leaf wetness index for 23 March, 2000. Sensors were placed at upper, mid and lower canopy with 100% wetness index defining a totally wet sensor and less than 10% (indicated by solid grey line) arbitrarily identifying a dry sensor.

A non-linear power law relationship becomes more conspicuous when dry canopy data are separated (WUE_{dry} is dry canopy water use efficiency, plotted in Figure 6.11). Under wet canopy conditions, precipitation that is intercepted and retained in the canopy fails to reach the soil and is evaporated directly. Intercepted rainwater is therefore unavailable to assist plant physiological processes and WUE is retarded. Intercepted water may also affect WUE by impeding photosynthesis through blockage of stomatal openings (Lee et al., 1999).

While the power law relationship appears more reasonable when dry canopy data are separated, there is still some scatter in the data at low D and $r^2 = 0.29$ indicates a poor fit. The best power law relationship is achieved for dry canopy data collected during Mar–Apr 2000 (Figure 6.12). While $r^2 = 0.63$ indicates a reasonable fit of the non-linear model in Figure 6.12, models of this kind failed to adequately explain the variance of WUE for dry canopy data collected throughout the rest of the study period. Apart from March–April 2000, half-hourly periods with low D were sometimes associated with only modest WUE.

The lowest depth to water table for the entire study period also occurred during March–April 2000 (Figure 3.7) and this suggests that WUE is also sensitive to water table depth.

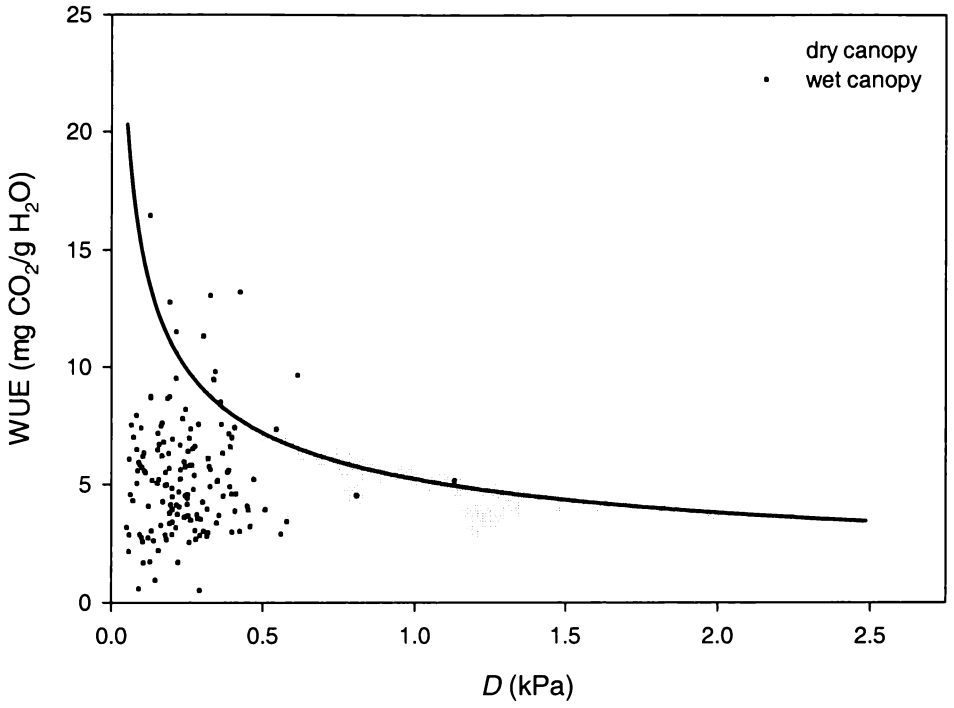

Figure 6.11 Relationship between half-hourly water use efficiency WUE and vapour pressure deficit *D* under dry-canopy and wet-canopy conditions between December 1998 and December 2000. Periods with a partially wet canopy are excluded. The plotted curve is fitted to dry canopy data and described by $WUE_{dry} = 5.234 \times D^{-0.459}$, $r^2 = 0.29$.

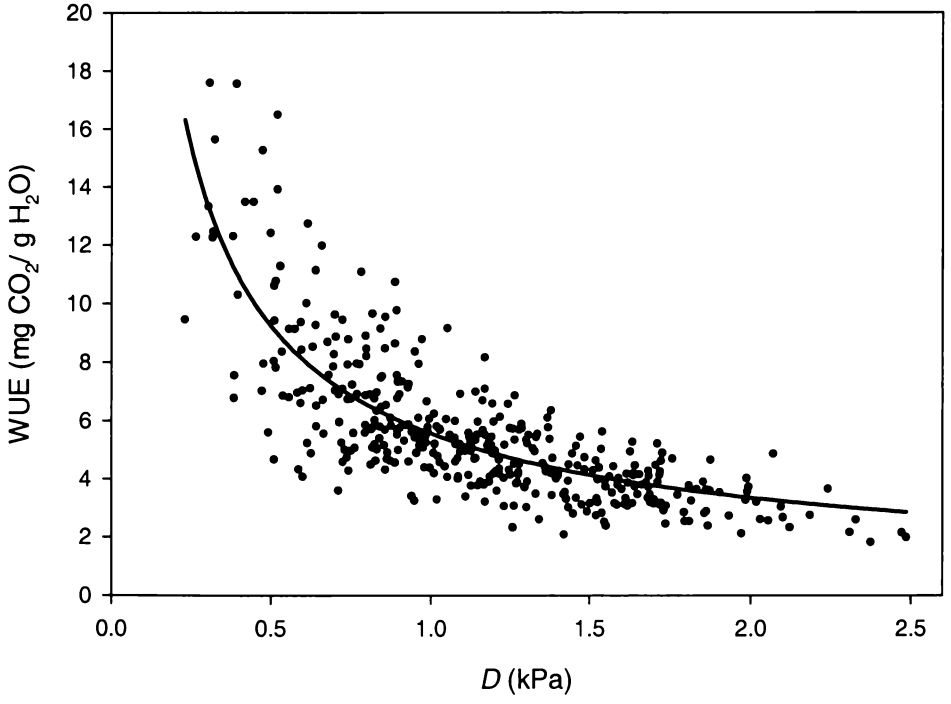

Figure 6.12 Relationship between dry-canopy water use efficiency (WUE_{dry}) and vapour pressure deficit (*D*) for March and April 2000. The plotted curve is described by $WUE_{dry} = 5.562 \times D^{-0.733}$, $r^2 = 0.63$.

While the trend of seasonal WUE is similar to seasonal variation of depth to water table, hysteresis is apparent (Figure 6.13). For the transition from summer to winter the trend of WUE imitates the ascent of the water table but between winter and summer the decline of WUE lags the water table descent.

This may be an artifact of canopy wetness. Figure 6.11 and 6.12 have shown that intercepted water has a significant influence on ecosystem WUE. When the water table is ascending, meteoric water is being added to the bog and, by inference, there would be an abundance of intercepted water available for evaporation. The increase of evaporation under wet canopy conditions would reduce the ecosystem WUE. Conversely, water table descent is a consequence of rainfall deficit and is a proxy indicator of the prevalence of dry canopy conditions. With less intercepted water available for evaporation, ecosystem WUE would be improved when the canopy is drier. This could explain the hysteresis in Figure 6.13.

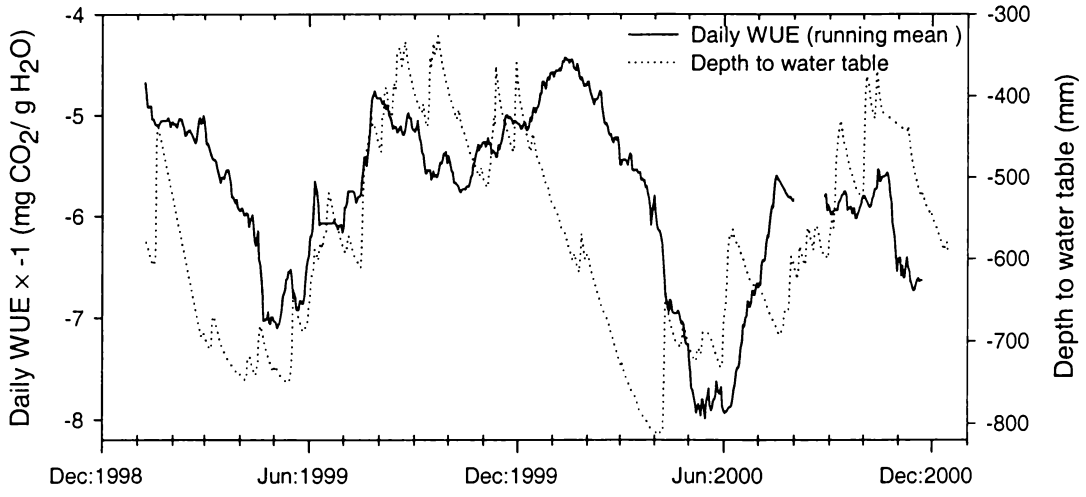

Figure 6.13 Time series of running mean of WUE plotted with depth to water table. Note that: (i) averaging period for WUE running mean is 45 days, and (ii) the sign of WUE is reversed for ease of comparison with other data; in this case increasingly negative numbers indicate more efficient water use.

While this is a speculative hypothesis, support is provided by the analysis in Chapter 4 that showed variability of canopy wetness has a profound influence on evaporation. A conclusion of Chapter 4 was that frequent rainfall events at Moanatuatua ensure the canopy is most frequently wet and plant physiological controls of evaporation are less

important due to the presence of intercepted water. Therefore ecosystem WUE is a reflection of bulk response and merely serves to demonstrate the importance of intercepted water. It is suggested that similarity of seasonal trends of WUE and depth to water table are both being driven by other variables, rather than being intrinsically linked. Because of the sensitivity of ecosystem WUE to intercepted water, a more pertinent analysis may be to investigate the sensitivity of carbon sequestration *per se* to water table variation.

6.3.2 Sensitivity to water table depth

IPCC predictions of global climate change suggest a 5% increase in rainfall for the Waikato by year 2080 (IPCC, 2001a) and at Moanatuatua the consequences would include a shallower water table. Table 6.2 shows that precipitation from 15 December 1998 – 15 December 1999 (referred to as 1999) was 8.4% (82 mm) greater than the following twelve month period (2000) and this is useful for investigating the IPCC prediction of climate change. The mean water table elevation was 70 mm shallower, yet 13% less carbon was sequestered in the wetter 1999 (Table 5.4). By inference, the magnitude of peat accumulation was not adversely affected by the deeper water table in 2000.

Table 6.2 Annual precipitation and depth to water table for consecutive twelve month periods. Precipitation data are from Moanatuatua meteorological station because of suspicions that EC rain gauge data were spurious at the beginning of the study.

	Precipitation (mm)	Mean depth to water table (mm)	Mean T_s at 8 cm depth (°C)
15/12/1998–15/12/1999	1060	542	12.53
15/12/1999–15/12/2000	978	612	12.72
Difference 1999-2000	82	–70	
% difference	8.4%		

This finding is surprising because conventional wisdom holds that raising the water table in bogs stimulates peat accumulation by decreasing respiration losses (Ingram, 1983). While Hodge's (2002) laboratory experiments suggested that water table variation is an important parameter for modelling respiration in Moanatuatua peat cores, Moore & Dalva (1993) note that water table position may have limited influence on respiration in field

conditions. This is probably due to the influence of root respiration and vertical temperature stratification at field sites (Moore and Dalva, 1993). Figure 5.4 and Table 5.2 indicate that a temperature driven respiration function (Equation 5.1) is valid on its own for long term modelling of respiration at Moanatuatua peat bog.

The positive annual carbon balances measured over 1999–2000 are also at odds with Shearer's (1997) suggestion that lowered water tables at Moanatuatua are causing peat degradation. Conflict between Shearer's (1997) hypothesis and positive carbon sequestration measured during 1999 and 2000 may also be explained by augmented GEP associated with deeper water tables. Crawford (1983) notes that many bog plants may exist in wetlands, but grow better in drained soils. Some wetland species go into survival mode when roots are in wet soil. Increased photosynthetic activity by restiad vegetation may be responsible for offsetting increased respiration losses under conditions of a deeper water table.

While direct measurements of photosynthesis were not conducted during this project, GEP estimates are an approximation of photosynthesis. Figure 6.14 suggests that GEP is reduced when the water table is closer to the peat surface. During autumn, for given inputs of solar radiation, more individual data points tend to be greater than the model used for reference in both plots of Figure 6.14. The converse is true during spring. The mean depth to water table was 452 mm and 723 mm for spring and autumn respectively, suggesting that photosynthesis is retarded by a shallow water table in spring.

Mitigation of increased respiration losses by GEP stimulation following water table lowering may explain the disparity of measured NEE with Shearer's (1997) presumption of peat degradation. Stimulation of photosynthesis as a consequence of recent water table lowering may also partly explain why the measured NEE of this research greatly exceeds the apparent average peat accumulation since the Taupo eruption 1800 years BP (Schipper and McLeod, 2002).

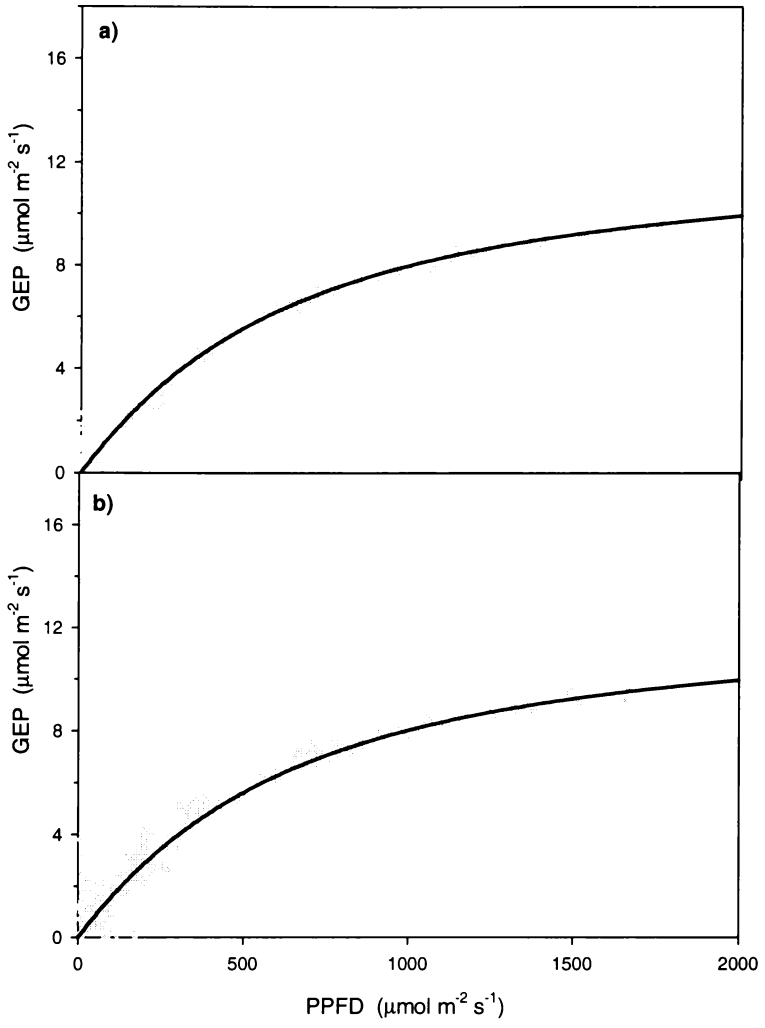

Figure 6.14 GEP vs PPFD for: (a) spring data (September–November inclusive) and (b) autumn data (March–May inclusive) measured September1999–May 2000. Solid lines are the same non-rectangular hyperbolic model determined with Equation 5.2, used here as a reference for both.

In this research the role of fire in releasing carbon to the atmosphere is not considered, however fires have occurred at Moanatuatua since the Taupo eruption (Clarkson, 1997). The most recent event was a fire in 1972 that destroyed vegetation over 75% of the surface area of Moanatuatua bog. Loss of carbon through burning would contribute to peat degradation and this also offers a partial explanation for the disagreement with Schipper and McLeod's (2002) calculations. Turetsky and Wieder (2001) quantified the carbon consumed from the peat profile of a Canadian boreal wetland during a single fire event to be 22(±5) tC ha^{-1}. At rates of carbon accumulation measured in 1999 and 2000, this represents ten years of sequestration at Moanatuatua. This estimate of carbon loss by fire

excludes consumption of canopy material, which makes the recovery estimate of ten years a conservative one.

Another assumption of this research is that peat accumulation occurs as a consequence of carbon sequestration. This assumption may not be met if carbon is being accumulated into canopy biomass rather than peat *per se*. The roots of *E. minus* are the dominant peat forming material at restiad bogs (Agnew et al., 1993) yet not all sequestered atmospheric carbon may be stored in *E. minus* roots. Clarkson et al. (1999) note an increase of height and extent of *E. minus* and *S. ferrugineus* from 1973 to 1994 as the vegetation recovered from the fire in 1972. The canopy may have still been in late successional stage of recovery in 1999–2000, which implies that some NEP was partitioned into above ground restiad biomass.

The relatively deep water table may also be modifying the ecological succession at Moanatuatua. At a Finnish peat bog, Laine and Minkkinen (1996) observed an increase of carbon accumulation following drainage. Augmentation of carbon sequestration by a tree stand exceeded the decrease in carbon accumulation rate of the peat, so that most of the increased NEP was stored as above-ground biomass. Modified ecosystem succession followed drainage of the Finnish bog, so that species composition changed towards forest vegetation (Laine and Minkkinen, 1996).

A low water table may likewise modify succession at Moanatuatua and partitioning of NEP could be favouring shrub species such as *Epacris pauciflora* and *Leptospermum scoparium*. An implication of this is that sequestered carbon would be stored in above-ground shrub mass rather than accumulating as peat-forming restiad biomass.

While the explanation of photosynthetic stimulation offers a rationalisation of disagreement with other research, it remains a speculative hypothesis due to assumptions and limitations of the approach. Further research is required to resolve the influence of the water table on field measurements of respiration. The derivation of GEP includes an estimate of the respiration component based on a temperature driven model and this requires validation. At least part of GEP variation between spring and autumn may be a consequence of increased LAI in autumn after summer growth and this requires measurement also.

Cuvette measurements of photosynthesis and LAI measurements in the field would help to verify the GEP component and its contribution to NEE. Measurement of incremental biomass and partitioning of NEP into canopy and peat stores is also required to test the assumption that sequestered carbon is being accumulated as peat.

Applying the principle of parsimony, the simplest approach for long term modelling of NEE for this research is to use a temperature driven Lloyd and Taylor model of field respiration and PPFD driven model of GEP. However additional field research into respiration and photosynthesis dynamics is required to resolve the issue of water table influence on carbon sequestration at Moanatuatua. Contemporaneous eddy covariance measurements at Moanatuatua and Kopouatai may be profitable, with the latter site having a perennially shallower water table than the former.

6.4 IPCC predictions of temperature increase

IPCC scenarios of climate change by 2080 include an increase in air temperature for the Waikato of 1.6°C in summer and 2.0°C in winter (IPCC, 2001a). Assuming soil temperature increases by the same magnitude as air temperature, these predictions are used for model simulations of change in respiration following global warming. Another assumption used here is that temperature increase during autumn and spring will be 1.8 °C : midway between summer and winter increases.

With these assumptions, IPCC predictions of temperature increase were applied to the model used in Figure 5.20 covering four years 1997–2000. Modelled respiration increased by 32% when the soil temperature increase was added, yet because R_e is such a large fraction of GEP the modelled NEE was reduced by 50% (Figure 6.15). This analysis shows that modelled respiration is highly sensitive to sustained warming of only a few degrees Celsius.

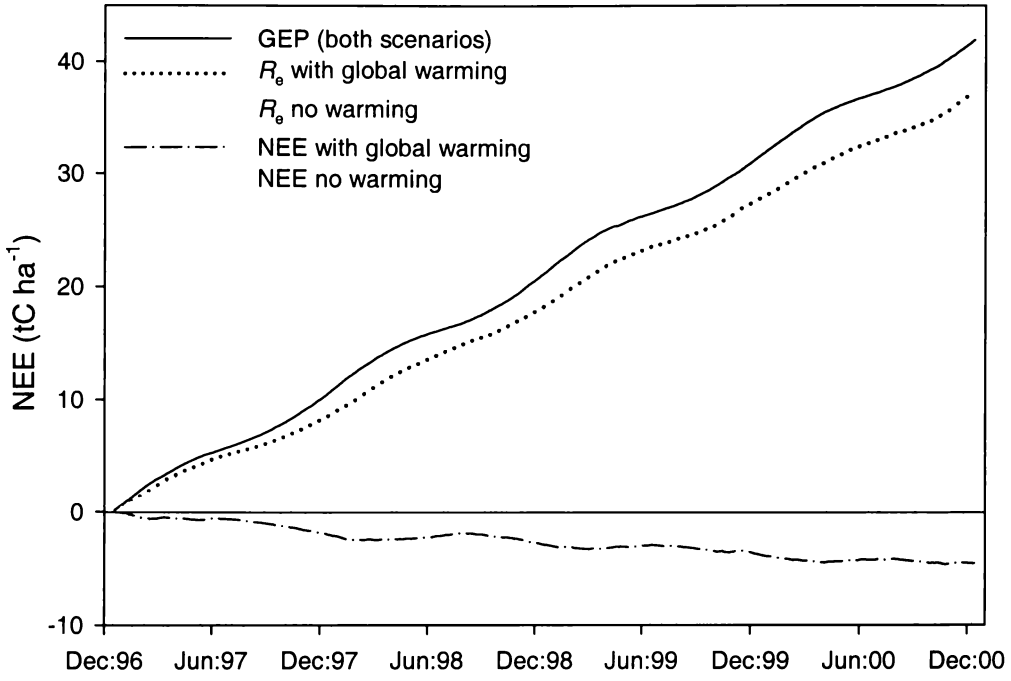

Figure 6.15 Modelled GEP, R_e and NEE simulated with and without IPCC climate warming scenarios (see text for details). Model inputs are the same meteorological data used in Figure 5.20 covering four years 15 December 1996 – 15 December 2000, aside from increased peat temperature.

Once again the effect of climate change on photosynthesis has not been examined. Photosynthetic production may be stimulated by temperature increase thus mitigating respiration losses to some extent. (Melillo et al., 1993). Plants tend to have an optimum temperature for photosynthesis, usually around 25°C (Lawlor and Mitchell, 2000; Nieveen, 1998), and increased temperatures associated with global warming may augment photosynthesis at Moanatuatua especially in winter when temperature increase is predicted to be greatest.

Analysis of a relationship between GEP and air temperature using the data from this research was inconclusive due to extreme scatter and is also not considered useful here because:

1. Variation in other variables such as *D* and PPFD are associated with temperature variability during the period of this research and have a confounding effect on the relationship of GEP with air temperature;

2. GEP includes a modelled respiration component and is as much an index as a measurement of photosynthetic production. To be useful for this analysis, a direct measurement of photosynthesis should be utilised (such as cuvette measurements).

Photosynthesis may also be increased via elevated atmospheric CO_2 associated with the global warming phenomenon. Van der Heijden et al. (2000) showed that experimental doubling of ambient CO_2 concentration (from 360 parts per million) increased dry mass of *Sphagnum spp.* by 17%. This level of atmospheric CO_2 concentration is anticipated by the year 2100 and may increase leaf photosynthetic production of C_3 species as much as 58% (Young and Long, 2000). The implications for GEP at Moanatuatua are substantial and warrant investigation of restiad photosynthesis under scenarios of elevated CO_2 concentrations.

Using a simple temperature driven model, peat respiration increases considerably under IPCC predictions of climate warming for the Waikato. While Figure 6.15 also suggests an associated decline of peat accumulation rate, further investigation of the impact that climate change will exert on photosynthesis at Moanatuatua is required to test this hypothesis. The conclusions here are tentative for this reason.

6.5 Summary

The objective of this chapter was to identify and investigate environmental variables that control carbon exchange at Moanatuatua.

Marginal quantum yield was relatively small– probably a consequence of the oligotrophic environment. Radiation use efficiency was improved under cloudy conditions due to more abundant diffuse radiation. Rates of carbon accumulation are therefore unlikely to be affected by reduced magnitude of PPFD under increasingly cloudy conditions at Moanatuatua caused by climate change scenarios.

Ecosystem water use efficiency varied according to the state of canopy wetness due to the sensitivity of evaporation to water stored on the surface of the canopy. The magnitude of annual NEP was not adversely affected by a deeper water table in 2000 compared with

1999. Photosynthetic production may be stimulated by a deeper water table, which would mitigate respiration losses under these conditions.

This research is unable to partition measurements of NEP into above-ground biomass and peat accumulation. An assumption is that sequestered carbon is stored as peat. This assumption may be tested by measurement of incremental biomass and direct measurement of photosynthesis, along with contemporaneous eddy covariance measurements of NEP and nocturnal R_e, at both Moanatuatua and Kopouatai peat bogs. Direct measurement of photosynthesis would also be useful to test the hypothesis that temperature variation has no significant effect on photosynthesis at restiad bogs.

Models developed during this research suggest that NEE is highly sensitive to temperature variation of only a few degrees due to variation of R_e. However photosynthesis may also be sensitive to changes of temperature and ambient CO_2 concentrations which could mitigate respiration losses caused by greenhouse gas induced global warming.

7 Conclusions

7.1 Summary

The following list is a summary of the results of this research.

- The dominant convective fluxes at Moanatuatua were H and λE, with β in excess of 2 sometimes observed during summer when the plant canopy was dry. In winter, the proportion of available energy used for evaporation was increased and the role of stomatal regulation of transpiration was less important than during summer. On an annual basis, periods with β >2 were rare and mean β was approximately unity, indicating that on average λE equals H.

- Evaporative demand is generally insufficient to force plant physiological restriction of transpiration and λE is controlled more by availability of energy than by stomatal controls observed over short periods during summer.

- Equilibrium-based models were superior to the Penman-Monteith equation for gap filling measurements of evaporation. For evaluating the annual water balance at Moanatuatua the evaporation component may be reliably estimated using equilibrium–based models exclusively, with α=0.80 and α=0.58 for wet– and dry–canopy periods respectively.

- For both years of this research, 64% of annual precipitation was removed as evaporation. Water was added to and released from storage during the first and second years respectively and the residual component, groundwater discharge (Q_w), was 34% and 40% for the first and second year of the study respectively.

- At the diurnal scale, carbon uptake is greatest during summer mornings. The bog was a sink of carbon for almost all of 1999 and 2000, apart from 2–3 months during winter when the wetland was a source of CO_2. Annual sequestration of carbon was 1.85 and 2.10 tC ha^{-1} for 1999 and 2000 respectively: greater than reported for other wetlands around the world.

- Models were developed for gap filling, with respiration driven by temperature and GEP modelled from inputs of PPFD. The seasonal trend of carbon exchange was different between 1999 and 2000 and this was probably because the seasonal pattern of peat temperature differed between the two years. Modelled annual NEE for 1997 was greater than for 1998. Increased carbon sequestration during the former year was a consequence of cooler peat temperatures that reduced respiration losses.

- Radiation use efficiency was improved under cloudy conditions due to diffuse radiation being absorbed more efficiently than direct radiation. Rates of carbon accumulation are unlikely to be adversely affected by reduced magnitude of PPFD under increasingly cloudy conditions at Moanatuatua caused by climate change scenarios.

- Compared with annual sequestration for 1999, the magnitude of annual NEP was not reduced in 2000 despite a deeper water table during the latter year. Photosynthetic production may be stimulated by a deeper water table, which would offset increased respiration losses under these conditions.

- Models developed during this research suggest that NEE is highly sensitive to peat temperature variation of only a few degrees due to variation of R_e. However photosynthesis may also be sensitive to changes of temperature and ambient CO_2 concentrations, which could mitigate increased respiration losses caused by greenhouse gas induced global warming.

7.2 Limitations and assumptions

Several limitations of the eddy covariance technique are acknowledged. A large unresolved energy balance closure error of at least 17% exists, suggesting there are problems with the eddy covariance system or assumptions. This closure error is within generally accepted standards for eddy covariance measurements so the lack of closure is acknowledged but unable to be completely explained. Another issue with the eddy covariance measurements is the high percentage of missing or spurious data that were replaced using models (55% of CO_2 data were modelled). This also is not uncommon for long-term eddy covariance measurements and is accepted as reasonable for this study.

Respiration models are based on nocturnal measurements, however there is an assumption that daytime respiration processes at Moanatuatua are not different to nocturnal respiration and this assumption remains untested by measurement.

The conclusions regarding interannual variation of carbon exchange are limited by estimates for a maximum four years. The frequency and role of fire are therefore not quantified in this research, yet this may represent a significant loss of peat over the long term. For example, Turetsky & Weider (2001) estimated a carbon loss of 22(±5) tC ha^{-1} from peat during one fire at a Canadian peatland.

A further assumption of this research is that sequestered carbon is stored as peat, but it may be accumulating as aboveground plant biomass. There is a need for further research to partition carbon storage into canopy and belowground components.

The influence of water table position on respiration was found to be negligible in this research although laboratory measurements suggest otherwise (Hodge, 2002). There is a need for further research to resolve this issue.

In this research photosynthesis is indexed by GEP, which has a respiration component modelled using temperature as the input. It is therefore unwise to use estimates of GEP to test the hypothesis that temperature is a control of photosynthesis. There is a need for

contemporaneous measurements of photosynthesis to verify the utility of eddy covariance research as a tool for investigating controls of photosynthesis at Moanatuatua.
Models of carbon and energy flux exchange processes in this thesis are suitable for long term utility (e.g. gap filling), but are inappropriate for more detailed, short term applications.

Along with magnitude of annual rainfall, the precipitation regime may be important when considering the impact of global climate change scenarios on fluxes of carbon dioxide and water vapour at Moanatuatua. This research discusses change of annual rainfall, but assumes no variation of precipitation regime under global climate change scenarios.

7.3 The good oil

Moanatuatua Scientific Reserve is a threatened ecosystem and requires appropriate management to ensure sustainability of habitat for the biota it supports. While a deep water table is believed to have resulted in a high degree of peat degradation at Moanatuatua (Shearer, 1997), the bog was a strong sink of carbon during 1999 and 2000. Also, a deeper water table during 2000 was not associated with decreased carbon sequestration.

These results show that net carbon loss has not occurred as a consequence of a lowered water table at Moanatuatua. Coupled with the assumption that sequestered carbon is stored as peat at Moanatuatua, this result falsifies the hypothesis that peat formation has been adversely affected by a lowered water table. This is encouraging for the sustainability of the wetland habitat, however a prerequisite to effective management of the ecosystem is further research to test the hypothesis that sequestered carbon is being stored as peat and not merely as aboveground biomass. There is also a risk that a lowered water table at Moanatuatua will promote growth of unwanted species at the expense of peat-forming restiads (Clarkson et al., 1999) and ongoing ecological research is required to monitor and manage this problem.

Climate change scenarios under greenhouse gas–induced global warming may not represent a catastrophic threat to the ecosystem. Reduced PPFD under increasingly cloudy conditions caused by climate change scenarios will have negligible effect on carbon sequestration due to improved radiation use efficiency under these conditions.

Respiration rates are highly sensitive to change in peat temperature and greenhouse gas induced global warming will therefore magnify respiration losses from Moanatuatua wetland. However to quantify the impact of temperature increase on the carbon budget *per se*, further investigation of the sensitivity of photosynthesis to changes of temperature and ambient CO_2 concentration is required.

The implications of Hodge's (2002) research suggests that reduction of respiration losses may occur following water table rise caused by increased precipitation under climate change scenarios. However this may be at least partly offset by a decrease in photosynthetic production resulting from the higher water table. The impact at Moanatuatua of increased precipitation caused by global climate change also depends on the nature of change to precipitation regime. Increased precipitation generated by a greater frequency of high magnitude rainfall events may have more impact on the water table than an increase in small magnitude rainfall events. This is because the dense canopy at Moanatuatua intercepts a large proportion of precipitation from low magnitude rain events and this rainfall exits the bog as evaporation. The percentage of precipitation appearing as throughfall may be larger during high magnitude events and these storms would have a greater impact on the water table.

The present precipitation regime is dominated by low magnitude, high frequency events and this ensures that moisture is generally available in the plant canopy so that about 60% of precipitation is removed as evaporation. While the dense plant canopy restricts evaporation from the moist peat surface, plant physiological regulation of transpiration is relatively less important and λE is controlled more by availability of radiation than by stomatal controls observed over short periods during summer.

7.4 Recommendations for future research

Ecological monitoring of unwanted plant species is required to measure and manage any relative decline of restiad species at Moanatuatua. Further eddy covariance research coupled with measurements of long-term incremental change of biomass is also required to partition measurements of NEP into peat accumulation and above-ground storage of carbon.

Laboratory measurements of respiration from peat cores suggest that water table position is an important variable (Hodge, 2002), however field measurements indicate that temperature alone is an adequate predictor of respiration. Contemporaneous research at both Moanatuatua and the relatively pristine Kopouatai bog would improve knowledge on the impact of water table position on respiration in the field.

Direct measurement of photosynthesis (e.g. using the LICOR LI-6400 cuvette system) at the two bogs would be useful to determine the effect of water table variation on photosynthesis. To predict the consequence of climate change scenarios on the carbon budget, there is also a need to determine the impact of temperature on photosynthesis.

Measurements of dark respiration during daylight periods would be useful to verify the assumption that nocturnal respiration is an adequate proxy for daytime respiration.

The frequency of fire and its role towards peat loss at Moanatuatua needs to be quantified. Determining the frequency of fire events may be achieved by counting ash layers in the peat profile. Estimating loss of carbon during fire events may be possible following (for example) the procedure of Turetsky and Wieder (2001).

Coupled with micrometeorological measurements, long term lysimeter measurements of evaporation from the peat surface would allow the partitioning of evaporation sources. Lysimeters could be positioned under representative canopy cover and at a cleared bare peat surface. This would be useful to quantify the modification of evaporation caused by the dense canopy that both increases interception of precipitation and restricts solar energy reaching the peat surface dense canopy. This would be particularly useful to estimate the consequences of change to the canopy structure, for example through burning.

References

Aerts, R. and Ludwig, F., 1997. Water-table changes and nutritional status affect trace gas emissions from laboratory columns of peatland soils. Soil Biology and Biochemistry, 29: 1691-1698.

Agnew, A.D.Q., Rapson, G.L., Sykes, M.T. and Wilson, J.B., 1993. The functional ecology of *Empodisma minus* (Hook. f.) Johnson & Cutler in New Zealand ombrotrophic mires. New Phytologist, 124: 703-710.

Allen, M.T. and Pearcy, R.W., 2000. Stomatal versus biochemical limitations to dynamic photosynthetic performance in four tropical rainforest shrub species. Oecologia, 122: 479-486.

Alm, J., Schulman, L., Walden, J., Nykänen, H., Martikainen, P.J. and Silvola, J., 1999. Carbon balance of a boreal bog during a year with an exceptionally dry summer. Ecology, 80(1): 161-174.

Armentano, T.V. and Menges, E.S., 1986. Patterns of change in the carbon balance of organic soils of the temperate zone. Journal of Ecology, 74: 755-774.

Asdak, C., Jarvis, P.G. and Gardingen, P.V., 1998. Evaporation of intercepted precipitation based on an energy balance in unlogged and logged forest areas of central Kalimantan, Indonesia. Agricultural and Forest Meteorology, 92: 173-180.

Aubinet, M., Grelle, A., Ibrom, A., Moncrieff, J., Foken, T., Kowalski, A.S., Martin, P.H., Berbigier, P., Bernhofer, C., Clement, R., Elbers, J., Granier, A., Grünwald, K., Morgenstern, K., Pilegaard, K., Rebmann, C., Snijders, W., Valentini, R. and Vesala, T., 2000. Estimates of the annual net carbon and water exchanges of forests: the Euroflux methodology. Advances in Ecological Research, 30: 113-175.

Aurela, M., Tuovinen, J.-P. and Laurila, T., 1998. Carbon dioxide exchange in a subarctic peatland ecosystem in northern Europe measured by the eddy covariance technique. Journal of Geophysical Research, 103(D10): 11289-11301.

Baldocchi, D., 1994. A comparative study of mass and energy exchange rates over a closed C_3 (wheat) and an open C_4 (corn) crop: II. CO_2 exchange and water use efficiency. Agricultural and Forest Meteorology, 67: 291-321.

Baldocchi, D., Falge, E., Gu, L., Olson, R., Hollinger, D., Running, S., Anthoni, P., Bernhofer, C., Davis, K., Evans, R., Fuentes, J., Goldstein, A., Katul, G., Law, B.,

Lee, X., Malhi, Y., Meyers, T., Munger, W., Oechel, W., Paw U, K.T., Pilegaard, K., Schmid, H.P., Valentini, R., Verma, S., Vesala, T., Wilson, K. and Wofsy, S., 2001. FLUXNET: A new tool to study the temporal and spatial variability of ecosystem-scale carbon dioxide and energy flux densities. Bulletin of the American Meteorological Society, 82(11): 2415-2434.

Baldocchi, D. and Meyers, T., 1998. On using eco-physiological, micrometeorological and biogeochemical theory to evaluate carbon dioxide, water vapor and trace gas fluxes over vegetation: a perspective. Agricultural and Forest Meteorology, 90: 1-25.

Baldocchi, D., Valentini, R., Running, S., Oechel, W. and Dahlman, R., 1996. Strategies for measuring and modelling carbon dioxide and water vapour fluxes over terrestrial ecosystems. Global Change Biology, 2: 159-168.

Baldocchi, D.D., Hicks, B.B. and Meyers, T.P., 1988. Measuring biosphere-atmosphere exchanges of biologically related gases with micrometeorological methods. Ecology, 69(5): 1331-1340.

Baldocchi, D.D., Kelliher, F.M., Black, T.A. and Jarvis, P., 2000. Climate and vegetation controls on boreal zone energy exchange. Global Change Biology, 6(Suppl. 1): 69-83.

Baldocchi, D.D., Verma, S.B. and Anderson, D.E., 1987. Canopy photosynthesis and water-use efficiency in a deciduous forest. Journal of Applied Ecology, 24: 251-260.

Baldocchi, D.D., Verma, S.B. and Rosenberg, N.J., 1985. Water use efficiency in a soybean field: influence of plant water stress. Agricultural and Forest Meteorology, 34: 53-65.

Baldocchi, D.D. and Vogel, C.A., 1996. Energy and CO_2 flux densities above and below a temperate broad-leaved forest and a boreal pine forest. Tree Physiology, 16: 5-16.

Black, T.A., den Hartog, G., Neumann, H.H., Blanken, P.D., Yang, P.C., Russell, C., Nesic, Z., Lee, X., Chen, S.G., Staebler, R. and Novak, M.D., 1996. Annual cycles of water vapour and carbon dioxide fluxes in and above a boreal aspen forest. Global Change Biology, 2: 219-229.

Blanken, P.D., Black, T.A., Neumann, H.H., den Hartog, G., Yang, P.C., Nesic, Z. and Lee, X., 2001. The seasonal water and energy exchange above and within a boreal aspen forest. Journal of Hydrology, 245: 118-136.

Bridgham, S.D., Pastor, J., Updegraff, K., Malterer, T., J,, Johnson, K., Harth, C. and Chen, J., 1999. Ecosystem control over temperature and energy flux in northern peatlands. Ecological Applications, 9(4): 1345-1358.

Burba, G.G., Verma, S.B. and Kim, J., 1999. Surface energy fluxes of *Phragmites australis* in a prairie wetland. Agricultural and Forest Meteorology, 94: 31-51.

Campbell, D.I., Laybourne, C.E. and Blair, I.J., 2002. Measuring peat moisture content using the dual-probe heat pulse technique. Australian Journal of Soil Research, 40: 177-190.

Campbell, D.I. and Williamson, J.L., 1997. Evaporation from a raised peat bog. Journal of Hydrology, 193: 142-160.

Chen, J.M. and Black, T.A., 1992. Defining leaf area index for non-flat leaves. Plant, Cell and Environment, 15: 421-429.

Clark, K.L., Gholz, H.L., Moncrieff, J.B., Cropley, F. and Loescher, H.W., 1999. Environmental controls over net exchanges of carbon dioxide from contrasting Florida ecosystems. Ecological Applications, 9(3): 936-948.

Clarkson, B.R., 1997. Vegetation recovery following fire in two Waikato peatlands at Whangamarino and Moanatuatua, New Zealand. New Zealand Journal of Botany, 35: 176-179.

Clarkson, B.R., Thompson, K., Schipper, L.A. and McLeod, M., 1999. Moanatuatua bog - proposed restoration of a New Zealand restiad peat bog system. In: W. Streever (Editor), An International Perspective on Wetland Rehabilitation. Kluwer Academic Publishers, Dordrecht, pp. 127-137.

Clymo, R.S., 1983. Peat. In: A.J.P. Gore (Editor), Mires: swamp, bog, fen and moor. Ecosystems of the world 4A. Elsevier, Amsterdam, pp. 159-224.

Clymo, R.S., Turunen, J. and Tolonen, K., 1998. Carbon accumulation in peatland. Oikos, 81: 368-388.

Crawford, R.M.M., 1983. Root survival in flooded soils. In: A.J.P. Gore (Editor), Mires: swamp, bog, fen and moor. Ecosystems of the world 4A. Elsevier, Amsterdam, pp. 257-283.

CSI, 1996. Q-7.1 Net radiometer manual. Campbell Scientific Inc., Logan, Utah, USA.

Davidson, E.A., Belk, E. and Boone, R.D., 1998. Soil water content and temperature as independent or confounded factors controlling soil respiration in a temperate mixed hardwood forest. Global Change Biology, 4: 217-227.

de Lange, P.J., Heenan, P.B., Clarkson, B.D. and Clarkson, B.R., 1999. Taxonomy, ecology, and conservation of *Sporodanthus* (Restionaceae) in New Zealand. New Zealand Journal of Botany, 37: 413-431.

Environment Waikato, 1999. For Peat's Sake: Good management practices for Waikato peat farmers, Environment Waikato Regional Council, Hamilton.

Falge, E., Baldocchi, D., Olson, R., Anthoni, P., Aubinet, M., Bernhofer, C., Burba, G., Ceulemans, R., Clement, R., Dolman, H., Granier, A., Gross, P., Grünwald, T., Hollinger, D., Jensen, N.-O., Katul, G., Keronen, P., Kowalski, A., Ta Lai, C., Law, B.E., Meyers, T., Moncrieff, J., Moors, E., Munger, J.W., Pilegaard, K., Rannik, Ü., Rebmann, C., Suyker, A., Tenhunen, J., Tu, K., Verma, S., Vesala, T., Wilson, K. and Wofsy, S., 2001a. Gap filling strategies for defensible annual sums of net ecosystem exchange. Agricultural and Forest Meteorology, 107: 43-69.

Falge, E., Baldocchi, D., Olson, R., Anthoni, P., Aubinet, M., Bernhofer, C., Burba, G., Ceulemans, R., Clement, R., Dolman, H., Granier, A., Gross, P., Grünwald, T., Hollinger, D., Jensen, N.-O., Katul, G., Keronen, P., Kowalski, A., Ta Lai, C., Law, B.E., Meyers, T., Moncrieff, J., Moors, E., Munger, J.W., Pilegaard, K., Rannik, Ü., Rebmann, C., Suyker, A., Tenhunen, J., Tu, K., Verma, S., Vesala, T., Wilson, K. and Wofsy, S., 2001b. Gap filling strategies for long term energy flux data sets. Agricultural and Forest Meteorology, 107: 71-77.

Fan, S.M., Goulden, M.L., Munger, J.W., Daube, B.C., Bakwin, P.S., Wofsy, S.C., Amthor, J.S., Fitzjarrald, D.R., Moore, K.E. and Moore, T.R., 1995. Environmental controls on the photosynthesis and respiration of a boreal lichen woodland: a growing season of whole-ecosystem exchange measurements by eddy correlation. Oecologia, 102: 443-452.

Fan, S.M., Wofsy, S.C., Bakwin, P.S. and Jacob, D.J., 1990. Atmosphere-biosphere exchange of CO_2 and O_3 in the central Amazon forest. Journal of Geophysical Research, 95(D10): 16851-16864.

Fang, C. and Moncrieff, J.B., 1999. A model for soil CO_2 production and transport 1: Model development. Agricultural and Forest Meteorology, 95: 225-236.

Farquhar, G.D., von Caemmerer, S. and Berry, J.A., 1980. A biochemical model of photosynthetic CO2 assimilation in leaves of C3 species. Planta, 149: 78-90.

Farquhar, G.D. and Wong, S.C., 1984. An empirical model of stomatal conductance. Australian Journal of Plant Physiology, 11: 191-210.

Freeman, C., Ostle, N. and Kang, H., 2001. An enzymatic 'latch' on a global carbon store. Nature, 409: 149.

Frolking, S.E., Bubier, J.L., Moore, T.R., Ball, T., Bellisario, L.M., Bhardwaj, A., Carroll, P., Crill, P.M., Lafleur, P.M., McCaughey, J.H., Roulet, N.T., Suyker, A.E., Verma, S.B., Waddington, J.M. and Whiting, G.J., 1998. Relationship between ecosystem productivity and photosynthetically active radiation for northern peatlands. Global Biogeochemical Cycles, 12(1): 115-126.

Gorham, E., 1991. Northern peatlands: Role in the global carbon cycle and probable responses to global warming. Ecological applications, 1: 182-195.

Goulden, M., Munger, J., Fan, S.-M., Daube, B. and Wofsy, S., 1996. Exchange of carbon dioxide by a deciduous forest: response to interannual climate variability. Science, 271: 1576-1578.

Goulden, M., Wofsy, S., Harden, J.W., Trumbore, S.E., Crill, P.M., Gower, S.T., Fries, T., Daube, B., Fan, S.-M., Sutton, D.J., Bazzaz, A. and Munger, J., 1998. Sensitivity of boreal forest carbon balance to soil thaw. Science, 279: 214-216.

Goulden, M.L., Daube, B.C., Fan, S.-M., Sutton, D.J., Bazzaz, A., Munger, J.W. and Wofsy, S.C., 1997. Physiological responses of a black spruce forest to weather. Journal of geophysical research, 102(D24): 28987-28996.

Grace, J., Malhi, Y., Lloyd, J., Mcintyre, J., Miranda, A.C., Meir, P. and Miranda, H.S., 1996. The use of eddy covariance to infer the net carbon dioxide uptake of Brazilian rain forest. Global Change Biology, 2: 209-217.

Greco, S. and Baldocchi, D.D., 1996. Seasonal variations of CO_2 and water vapour exchange rates over a temperate deciduous forest. Global Change Biology, 2: 183-197.

Grelle, A. and Lindroth, A., 1996. Eddy-correlation system for long-term monitoring of fluxes of heat, water vapour and CO_2. Global Change Biology, 2: 297-307.

Griffis, T.J., Rouse, W.R. and Waddington, J.M., 2000. Interannual variability of net ecosystem CO_2 exchange at a subarctic fen. Global Biogeochemical Cycles, 14(4): 1109-1121.

Grimshaw, D.A., 2000. Groundwater dynamics in a restiad peat bog: Moanatuatua Scientific Reserve, Waikato, New Zealand. Unpublished MSc(Tech) Thesis, The University of Waikato, Hamilton, New Zealand, 128 pp.

Grulke, N., Riechers, G.H., Oechel, W.C., Hjelm, U. and Jaeger, C., 1990. Carbon balance in tussock tundra under ambient and elevated atmospheric CO_2. Oecologia, 83: 485-494.

Gu, L., Fuentes, J.D., Shugart, H.H., Staebler, R.M. and Black, T.A., 1999. Responses of net ecosystem exchanges of carbon dioxide to changes in cloudiness: results from two North American deciduous forests. Journal of Geophysical Research, 104: 31421-31434.

Hilbert, D.W., Roulet, N. and Moore, T., 2000. Modelling and analysis of peatlands as dynamical systems. Journal of Ecology, 88: 230-242.

Hodge, P.W., 2002. Respiration Processes in Waikato Peat Bogs. MSc Thesis, The University of Waikato, Hamilton, 137 pp.

Hogg, E.H., Lieffers, V.J. and Wein, R.W., 1992. Potential carbon losses from peat profiles: effects of temperature, drought cycles and fire. Ecological Applications, 2(3): 298-306.

Hollinger, D.Y., Goltz, S.M., Davidson, E.A., Lee, J.T., Tu, K. and Valentine, H.T., 1999. Seasonal patterns and environmental control of carbon dioxide and water vapour exchange in an ecotonal boreal forest. Global Change Biology, 5: 891-902.

Hollinger, D.Y., Kelliher, F.M., Byers, J.N., Hunt, J.E., McSeveny, T.M. and Weir, P.L., 1994. Carbon dioxide exchange between an undisturbed old-growth temperate forest and the atmosphere. Ecology, 75(1): 134-150.

Hunt, J.E., Kellher, F.M., McSeveny, T.M. and Byers, J.N., 2002. Evaporation and Carbon Dioxide Exchange Between the Atmosphere and a Tussock Grassland During a Summer Drought. Agricultural and Forest Meteorology, 111: 65-82.

Ingram, H.A.P., 1983. Hydrology. In: A.J.P. Gore (Editor), Mires: Swamp, Bog, Fen and Moor. Ecosystems of the World 4A. Elsevier, Amsterdam, pp. 67-158.

IPCC, 2001a. Climate Change 2001: Impacts, Adaptation, and Vulnerability. Contribution of Working Group II to the Third Assessment of the Intergovernmental Panel on Climate Change. Cambridge University Press, Cambridge, United Kingdom, 1032 pp.

IPCC, 2001b. Working Group II: Impacts, adaptation and vulnerability. In: R.T. Watson and the Core Writing Team (Editors), Climate Change 2001: Synthesis Report. A Contribution of Working Groups I, II and III to the Third Assessment of the

Intergovernmental Panel on Climate Change. Cambridge University Press, Cambridge, United Kingdom, pp. 219-289.

Joiner, D.W., Lafleur, P.M., McCaughey, J.H. and Bartlett, P.A., 1999. Interannual variability in carbon dioxide exchanges at a boreal wetland in the BOREAS northern study area. Journal of Geophysical Research, 104(D22): 27663-27672.

Kaimal, J.C. and Finnigan, J.J., 1994. Atmospheric Boundary Layer Flows: their structure and measurement. Oxford University Press, NY.

Kelliher, F., Leuning, R. and Schulze, E.-D., 1993. Evaporation and canopy characteristics of coniferous forests and grasslands. Oecologia, 95: 153-163.

Kelliher, F.M., Hollinger, D.Y., Schulze, E.-D., Vgodskaya, N.N., Byers, J.N., Hunt, J.E., McSeveny, T., Milukova, I., Sogatchev, A., Varlargin, A., Ziegler, W., Arneth, A. and Bauer, G., 1997. Evaporation from an eastern Siberian larch forest. Agricultural and Forest Meteorology, 85: 135-147.

Kelliher, F.M., Lloyd, J., Arneth, A., Byers, J.N., McSeveny, T., Milukova, I., Grigoriev, S., Panfyorov, M., Sogatchev, A., Varlargin, A., Ziegler, W., Bauer, G. and Schulze, E.-D., 1998. Evaporation from a central Siberian pine forest. Journal of Hydrology, 205: 279-296.

Kim, J. and Verma, S.B., 1996. Surface exchange of water vapour between an open *Sphagnum* fen and the atmosphere. Boundary Layer Meteorology, 79: 243-264.

Klinger, L.F., Zimmerman, P.R., Greenberg, J.P., Heidt, L.E. and Guenther, A.B., 1994. Carbon trace gas fluxes along a successional gradient in the Hudson Bay lowland. Journal of Geophysical Research, 99(D1): 1469-1494.

Kustas, W.P., 1990. Estimates of evapotranspiration with a one- and two-layer model of heat transfer over a partial canopy cover. Journal of Applied Meteorology, 29: 704-715.

Kustas, W.P., Goodrich, D.C., Moran, M.S., Amer, S.A., Bach, L.B., Blanford, J.H., Chenbouni, A., Claasen, H., Clements, W.E., Doraiswamy, P.C., Dubois, P., Clarke, T.R., Daughtry, C.S.T., Gellman, D.I., Grant, T.A., Hipps, L.E., Huete, A.R., Humes, K.S., Jackson, T.J., Keefer, T.O., Nichols, W.D., Parry, R., Perry, E.M., Pinker, R.T., Pinter, T.P.J., Qi, J., Riggs, A.C., Schmugge, T.J., Shutko, A.M., Stannard, D.I., Swiatek, E., van Leeuwin, J.D., van Zyl, J., Vidal, A., Washburne, J. and Weltz, M.A., 1991. An interdisciplinary field study of the energy and water fluxes in the atmosphere-biosphere over semi-arid rangelands:

description and some preliminary results. Bulletin of the American Meteorological Society, 72(11): 1683-1705.

Lafleur, P.M., 1990a. Evaporation from wetlands. In: N. Roulet (Editor), Focus: aspects of the physical geography of wetlands. The Canadian Geographer, pp. 79-88.

Lafleur, P.M., 1990b. Evapotranspiration from sedge-dominated wetland surfaces. Aquatic Botany, 37: 341-353.

Lafleur, P.M., McCaughey, J.H., Joiner, D.W., Bartlett, P.A. and Jelinski, D.E., 1997. Seasonal trends in energy, water and carbon dioxide fluxes at a northern boreal wetland. Journal of Geophysical Research, 102(D24): 29009-29020.

Lafleur, P.M. and Roulet, N.T., 1992. A comparison of evaporation rates from two fens of the Hudson Bay Lowland. Aquatic Botany, 44: 59-69.

Lafleur, P.M., Roulet, N.T. and Admiral, S.W., 2001. Annual cycle of CO_2 exchange at a bog peatland. Journal of Geophysical Research, 106(D3): 3071-3081.

Laine, J. and Minkkinen, K., 1996. Effect of forest drainage on the carbon balance of a mire. Scandinavian Journal of Forest Research, 11: 307-312.

Lappalainen, E., 1996. General review on world peatland and peat resources. In: E. Lappalainen (Editor), Global Peat Resources. International Peat Society, Jyskä, Finland, pp. 53-56.

Laubach, J.M., Raschendorfer, H.K. and Gravenhorst, G., 1994. Determination of heat and water vapour fluxes above a spruce forest by eddy correlation. Agricultural and Forest Meteorology, 71: 373-401.

Lawlor, D.W. and Mitchell, R.A.C., 2000. Crop ecosystem responses to climate change: wheat. In: K.R. Reddy and H.F. Hodges (Editors), Climate Change and Global Crop Productivity. CABI publishing, New York, pp. 488.

Laybourne, C.E., 2000. Measuring peat water content. MSc(Tech) Thesis, The University of Waikato, Hamilton.

Lee, X., 1998. On micrometeorological observations of surface-air exchange over tall vegetation. Agricultural and Forest Meteorology, 91: 39-49.

Lee, X., Black, T.A., den Hartog, G., Neumann, H.H., Nesic, Z. and Olejnik, J., 1996. Carbon dioxide exchange and nocturnal processes over a mixed deciduous forest. Agricultural and Forest Meteorology, 81: 13-29.

Lee, X., Fuentes, J.D., Staebler, R.M. and Neumann, H.H., 1999. Long-term observation of the atmospheric exchange of CO_2 with a temperate deciduous forest in southern Ontario, Canada. Journal of Geophysical Research, 104(D13): 15975-15984.

LiCor, 1996. Li-6262 CO /H2O analyzer operating and service manual. Publication number 9003-59. LiCor Inc., Lincoln, NB, USA.

Lloyd, C., 1998. Global change: Arctic hydrology. Institute of Hydrology Scientific Report, 1997-1998: 27-29.

Lloyd, J. and Taylor, J.A., 1994. On the temperature dependence of soil respiration. Functional Ecology, 8: 315-323.

Maltby, E. and Proctor, M.C.F., 1996. Peatlands: their nature and role in the biosphere. In: E. Lappalainen (Editor), Global Peat Resources. International Peat Society, Jyskä, Finland, pp. 11-19.

Martikainen, P.J., 1996. The fluxes of greehouse gases CO_2, CH_4 and N_2O in northern peatlands. In: E. Lappalainen (Editor), Global Peat Resources. International Peat Society, Jyskä, Finland, pp. 29-36.

Massman, W.J., Fox, D.G., Zeller, K.F. and Lukens, D., 1990. Verifying eddy correlation measurements of dry deposition: a study of the energy balance of the Pawnee grasslands. Research Paper RM-288, Rocky Mountain Forest and Range Experiment Station, Forest Service. United States Department of Agriculture, Fort Collins, Colorado, 14 pp.

Massman, W.J. and Ham, J.M., 1994. An evaluation of a surface energy balance method for partitioning ET data into plant and soil components for a surface with partial canopy cover. Agricultural and Forest Meteorology, 67: 253-267.

McGlone, M.S., Moar, N.T. and Meurk, C.D., 1997. Growth and vegetation history of alpine mires on the Old Man Range, Central Otago, New Zealand. Arctic and Alpine Research, 26: 32-34.

Melillo, J.M., McGuire, A.D., Kicklighter, D.W., Moore III, B., Vorosmarty, C.J. and Schloss, A.L., 1993. Global climate change and terrestrial net primary productivity. Nature, 363: 234-240.

Mitsch, W.J. and Gosselink, J.G., 1993. Wetlands. Van Nostrand Reinhold, New York, 722 pp.

Moncrieff, J., Valentini, R., Greco, S., Seufert, G. and Ciccioli, P., 1997a. Trace gas exchange over terrestrial ecosystems: methods and perspectives in micrometeorology. Journal of Experimental Botany, 48(310): 1133-1142.

Moncrieff, J.B., Massheder, J.M., de Bruin, H., Elbers, J., Friborg, T., Heusinkveld, B., Kabat, P., Scott, S., Soegaard, H. and Verhoef, A., 1997b. A system to measure surface fluxes of momentum, sensible heat, water vapour and carbon dioxide. Journal of Hydrology, 188-189: 589-611.

Moncrieff, J.B., Monteny, B., Verhoef, A., Friborg, T., Elbers, J., Kabat, P., de Bruin, H., Soegaard, H., Jarvis, P.G. and Taupin, J.D., 1997c. Spatial and temporal variations in net carbon flux during HAPEX-Sahel. Journal of Hydrology, 188-189: 563-588.

Monteith, J.L., 1965. Evaporation and environment, The State and Movement of Water in Living Organisms. Proceedings of the 19th Symposium of the Society for Experimental Biology. Cambridge University Press, NY, pp. 205-234.

Monteith, J.L. and Unsworth, M.H., 1990. Principles of Environmental Physics. Edward Arnold, Auckland, 291 pp.

Moore, C.J., 1986. Frequency response corrections for eddy correlation systems. Boundary Layer Meteorology, 37: 17-35.

Moore, T.R. and Dalva, M., 1993. The influence of temperature and water table position on carbon dioxide and methane emissions from laboratory columns of peatland soils. Journal of Soil Science, 44: 651-664.

Neumann, H.H., den Hartog, G., King, K.M. and Chipanshi, A.C., 1994. Carbon dioxide fluxes over a raised open bog at the Kinosheo Lake tower site during the Northern Wetlands Study (NOWES). Journal of Geophysical Research, 99(D1): 1529-1538.

Newnham, R.M., de Lange, P.J. and Lowe, D.J., 1995. Holocene vegetation, climate and history of a raised bog complex, northern New Zealand based on palynology, plant macrofossils and tephrochronology. The Holocene, 5(3): 267-282.

Nieveen, J.P., 1998. Eddy covariance and scintillation measurements of atmospheric exchange processes over different types of vegetation. PhD Thesis, Wageningen Agricultural University, Wageningen, 121 pp.

Nieveen, J.P., Jacobs, C.M.J. and Jacobs, A.F.G., 1998. Diurnal and seasonal variation of carbon dioxide exchange from a former true raised bog. Global Change Biology, 4: 823-833.

Norman, J.M., Kucharik, C.J., Gower, S.T., Baldocchi, D.D., Crill, P.M., Striegl, R.G., Savage, K. and Rayment, M., 1997. A comparison of six methods for measuring

soil-surface carbon dioxide fluxes. Journal of Geophysical Research, 102(D24): 28771-28777.

Nykänen, H., Alm, J., Silvola, J., Tolonen, K. and Martikainen, P.J., 1998. Methane fluxes on boreal peatlands of different fertility and the effect of long-term experimental lowering of the water table on flux rates. Global Biogeochemical Cycles, 12(1): 53-69.

Oechel, W.C., Hastings, S.J., Vourlitis, G., Jenkins, M., Riechers, G. and Grulke, N., 1993. Recent changes of Arctic tundra ecosystems from a net carbon dioxide sink to a source. Nature, 361: 520-526.

Oechel, W.C., Vourlitis, G.L., Hastings, S.J., Ault Jr, R.P. and Bryant, P., 1998. The effects of water table manipulation and elevated temperature on the net CO_2 flux of wet sedge tundra ecosystems. Global Change Biology, 4: 77-90.

Oke, T.R., 1990. Boundary Layer Climates. Routledge, London and NY, 435 pp.

Penman, H.L., 1948. Natural evaporation from open water, bare soil and grass. Proceedings of the Royal Society (London), A193: 120-145.

Petrone, R.M., Waddington, J.M. and Price, J.S., 2001. Ecosystem scale evapotranspiration and net CO_2 exchange from a restored peatland. Hydrological Processes, 15: 2839-2845.

Priestley, C.H.B. and Taylor, R.J., 1972. On the assessment of surface heat flux and evaporation using large-scale parameters. Monthly Weather Review, 100: 81-92.

Qiu, G.Y., Momii, K., Yano, T. and Lascano, R.J., 1999. Experimental verification of a mechanistic model to partition evapotranspiration into soil water and plant evaporation. Agricultural and Forest Meteorology, 93: 79-93.

Roderick, M., Farquhar, G.D., Berry, S.L. and Noble, I.R., 2001. On the direct effect of clouds and atmospheric particles on the productivity and structure of vegetation. Oecologia, 129: 21-30.

Roulet, N.T., Munro, D.S. and Mortsch, L., 1998. Wetlands. In: W.G. Bailey, T.R. Oke and W.R. Rouse (Editors), The Surface Climates of Canada. McGill-Queen's University Press, Montreal & Kingston, pp. 150-171.

Rouse, W.R., Bello, R.L., D'Souza, A., Griffis, T.J. and Lafleur, P.M., 2002. The annual carbon budget for fen and forest in a wetland at Arctic treeline. Arctic, 55(3): 229-237.

Ruimy, A., Jarvis, P.G., Baldocchi, D.D. and Saugier, B., 1995. CO_2 fluxes over plant canopies and solar radiation: a review. Advances in Ecological Research, 26: 1-69.

Ruimy, A., Saugier, B. and Dedieu, G., 1994. Methodology for the estimation of terrestrial net primary production from remotely sensed data. Journal of Geophysical Research, 99(D3): 5263-5283.

Scheidegger, Y., Saurer, M., Bahn, M. and Siegwolf, R., 2000. Linking stable oxygen and carbon isotopes with stomatal conductance and photosynthetic capacity: a conceptual model. Oecologia, 125: 350-357.

Schipper, L.A. and McLeod, M., 2002. Subsidence rates and carbon loss in peat soils following conversion to pasture in the Waikato region, New Zealand. Soil Use and Management, 18: 91-93.

Schmid, H.P., 1994. Source areas for scalars and scalar fluxes. Boundary Layer Meteorology, 67: 293-318.

Schmid, H.P., Grimmond, C.S.B., Cropley, F., Offerle, B. and Su, H.-B., 2000. Measurements of CO_2 and energy fluxes over a mixed hardwood forest in the mid-western United States. Agricultural and Forest Meteorology, 103: 357-374.

Schuepp, P.H., Leclerc, M.Y., Macpherson, J.I. and Desjardins, R.L., 1990. Footprint prediction of scalar fluxes from analytical solutions of the diffusion equation. Boundary Layer Meteorology, 50: 355-373.

Sharp, L.M., 1995. Aspects of the growth of the wire rush *Empodisma minus* (Hook. f.) Johnson and Cutler in raised bogs of Northern New Zealand, and some implications for ecological management. Unpublished MSc(hons.) Thesis, The University of Waikato, Hamilton.

Shearer, J.C., 1997. Natural and anthropogenic influences on peat development in Waikato/Hauraki Plains restiad bogs. Journal of the Royal Society of New Zealand, 27(3): 295-313.

Shurpali, N.J., Verma, S.B. and Kim, J., 1995. Carbon dioxide exchange in a peatland ecosystem. Journal of Geophysical Research, 100(D7): 14319-14326.

Shuttleworth, W.J. and Wallace, J.S., 1985. Evaporation from sparse crops - an energy combination theory. Quarterly Journal of the Royal Meteorological Society, 111: 839-855.

Sundh, I., Mikkelä, C., Nilsson, M. and Svensson, B.H., 1995. Potential aerobic methane oxidation in a Sphagnum-dominated peatland: controlling factors and relation to methane emission. Soil Biology and Biochemistry, 27(6): 829-837.

Tanner, B.D., Swiatek, E. and Greene, J.P., 1993. Density fluctuations and the use of the krypton hygrometer in surface flux measurements. In: R.G. Allen (Editor), Management of Irrigation and Drainage Systems. American Society of Civil Engineers, Utah.

Taylor, R., Smith, I., Cochrane, P., Stephenson, B. and Gibbs, N., 1997. The State of New Zealand's Environment 1997. The Ministry for the Environment, Wellington, New Zealand.

Thom, A.S., 1975. Momentum, mass and heat exchanges of plant communities. In: J.L. Monteith (Editor), Vegetation and the Atmosphere. Academic Press, London, pp. 57-109.

Thompson, M.A., 1997. Evaporation regimes in two restiad peat bogs. North Island, New Zealand. Unpublished MSc(Tech) Thesis, The University of Waikato, Hamilton, 125 pp.

Thompson, M.A., Campbell, D.I. and Spronken-Smith, R.A., 1999. Evaporation from natural and modified raised peat bogs in New Zealand. Agricultural and Forest Meteorology, 95: 85-98.

Turetsky, M.R. and Wieder, R.K., 2001. A direct approach to quantifying organic matter lost as a result of peatland fire. Canadian Journal of Forest Research, 31: 363-366.

Turunen, J. and Tolonen, K., 1996. Rate of carbon accumulation in boreal peatlands and climate change. In: E. Lappalainen (Editor), Global Peat Resources. International Peat Society, Jyskä, Finland, pp. 21-28.

Twine, T.E., Kustas, W.P., Norman, J.M., Cook, D.R., Houser, P.R., Meyers, T.P., Prueger, J.H., Starks, P.J. and Wesely, M.L., 2000. Correcting eddy-covariance flux underestimates over a grassland. Agricultural and Forest Meteorology, 103: 279-300.

Urban, N.R., Bayley, S. and Eisenreich, S.J., 1989. Export of dissolved organic carbon and acidity from peatlands. Water Resources Research, 25(7): 1619-1628.

Valentini, R., Gamon, J.A. and Field, C.B., 1995. Ecosystem gas exchange in a Californian grassland: seasonal patterns and implications for scaling. Ecology, 76(6): 1940-1952.

van Breemen, N., 1995. How *Sphagnum* bogs down other plants. Trends in Ecology and Evolution, 10(7): 270-275.

van der Heijden, E., Verbeek, S.K. and Kuiper, P.J.C., 2000. Elevated atmospheric CO2 and increased nitrogen deposition: effects on C and N metabolism and growth of the peat moss *Sphagnum recurvum* P. Beauv. var. *mucronatum* (Russ.) Warnst. Global Change Biology, 6: 201-212.

Vourlitis, G.L. and Oechel, W.C., 1999. Eddy covariance measurements of CO_2 and energy fluxes of an Alaskan tussock tundra ecosystem. Ecology, 80(2): 686-701.

Waddington, J.M. and Roulet, N.T., 2000. Carbon balance of a boreal patterned wetland. Global Change Biology, 6: 87-97.

Waddington, J.M., Roulet, N.T. and Swanson, R.V., 1996. Water table control of CH_4 emission enhancement by vascular plants in boreal peatlands. Journal of Geophysical Research, 101(D17): 22775-22785.

Webb, E.K., Pearman, G.J. and Leuning, R., 1980. Correction of flux measurements for density effects due to heat and water vapour transfer. Quarterly Journal of the Royal Meteorological Society, 106: 85-100.

Wilson, K.B. and Baldocchi, D.D., 2000. Seasonal and interannual variability of energy fluxes over a broadleaved temperate deciduous forest in North America. Agricultural and Forest Meteorology, 100: 1-18.

Wofsy, S., Goulden, M., Munger, J., Fan, S.-M., Bakwin, P., Daube, B., Bassow, S. and Bazzaz, F., 1993. Net exchange of CO_2 in a mid-latitude forest. Science, 260: 1314-1317.

Woods, R. and Rowe, L., 1996. The changing spatial variability of subsurface flow across a hillslope. Journal of Hydrology (NZ), 35: 51-86.

Xu, L.-K., Matista, A.A. and Hsiao, T.C., 1999. A technique for measuring CO_2 and water vapor profiles within and above plant canopies over short periods. Agricultural and Forest Meteorology, 94: 1-12.

Young, K.J. and Long, S.P., 2000. Crop ecosystem responses to climate change: maize and sorghum. In: K.R. Reddy and H.F. Hodges (Editors), Climate Change and Global Crop Productivity. CABI publishing, New York, pp. 107-131.

APPENDIX

The attached CD-ROM contains information relevant to this research (assuming your CD-ROM drive is mapped as d:\ ...) –

Location	Description
d:\readme.txt	soft copy of this appendix (also saved as d:\readme.doc)
d:\binary\...	Binary files containing half-hourly fluxes, calibrations, profile measurements and meteorological data. See readme.txt files in database directories for details of data stored in individual files.
d:\manual\...	Manual describing setting up, operation and servicing of the UW eddy covariance system
d:\matlab\...	Matlab m-files used for data processing and analysis
d:\plots\...	Sigmaplot files with plots from each chapter stored in appropriately named files. Some plots are used in more than one chapter: e.g. some climate data stored in Thesis_2002_Ch3_1.JNB are plotted in Chapters 3 & 5 of the thesis
d:\programs\...	Final versions of CR10X programs used for: i) acquiring eddy covariance data (eddy.csi); ii) controlling the eddy covariance functions such as sample tube heating and calibrations (control.csi); iii) logging meteorological data (met.csi); iv) logging peat temperature (m_aux.csi)
d:\thesis\...	Soft copy of this thesis as MS Word documents. To view entire thesis, open d:\thesis\master.doc and expand subdocuments
d:\website\...	html files describing the project design, operation and preliminary results. Open file index.shtml to begin. At 23 January 2003, this website was also hosted online at: http://erth.waikato.ac.nz/research.campbell/carbon.flux/index.htm